Delft University of Technology
Department of Electrical Engineering
Telecommunications and Traffic Control Systems Group

Eurofix and GNSS:
The possibility of integrating GLONASS into Eurofix

Author: Remco Vroeijenstijn

Thesis Report
175 + xii pages
June 1995

Professor:	Prof. Dr. Ir. D. van Willigen
Mentor:	Ir. E.J. Breeuwer
Period:	March 1994 - June 1995
Contents:	Provision of differential GLONASS corrections through Eurofix should be possible. Based on published differential GNSS standards, an asynchronous differential GNSS message format is proposed. A DGLONASS update rate is determined. As the ionosphere is the largest and most varying error source in GLONASS, a model is used to represent the ionosphere and its influence on GLONASS signals. This report is concluded with the consequences of integrating GLONASS into Eurofix concerning the DGPS/DGLONASS accuracy and the system differences.

Preface

This report concludes my study of Electrical Engineering at the Delft University of Technology. It discusses the possibility of integrating the Russian GLONASS into Eurofix. Eurofix is part of the Beek program "Integrated Navigation for Traffic and Transportation". Perhaps this report might be the start of the development of an integrated GNSS-Eurofix system.

I would like to express my gratitude and thanks to a number of persons. First of all, I would like to thank prof. dr. ir. D. van Willigen and Edward Breeuwer for their help and support. Furthermore, I also would like to thank Gerard Offermans and Sandor van Goor for their help and suggestions. Finally, I would like to thank all the students of the P&N-group for making my presence at the group very pleasant.

Remco Vroeijenstijn,
June 30th 1995.

Summary

Currently, two independent Global Navigation Satellite Systems (GNSS) are under development: the Global Positioning System (GPS) and Global Orbiting Navigation Satellite System (GLONASS). For harbour approaches a 95% horizontal position accuracy of 8-20m is required. Due to several error sources, this accuracy can not be met by stand alone GNSS. Differential GNSS is a technique to improve the GNSS accuracy. Eurofix is an integrated navigation system consisting of DGPS and Loran-C, in which differential GPS corrections are transmitted to the GPS-users by additionally modulating the Loran signals. Loran-C is a terrestrial positioning system. GLONASS is to be expected to reach full constellation status at the end of 1995. Therefore, the provision of differential GLONASS corrections through the Eurofix datalink is opportune. This report discusses the possibility of integrating GLONASS into Eurofix.

In this report a comparison between GLONASS and GPS is made. The consequences of distinctive differences on the integration of GLONASS into Eurofix are discussed.

Several differential GNSS standards supporting DGPS/DGLONASS have been proposed. Special Committee No. 104 of the Radio Technical Commission for Maritime services (RTCM SC-104) proposed to add message types to the RTCM DGPS standards to support differential GLONASS. Based on these proposals an asynchronous GNSS-Eurofix message format is developed in this report.

The accuracy of GLONASS is not intentionally degraded by Selective Availability as GPS is. The ionosphere causes the largest and most varying range errors in GLONASS positioning. By using an existing model of the ionosphere, the Bent Ionospheric Model, the effects of the ionosphere are investigated. Using this model, GLONASS range errors and the temporal decorrelation of these errors are determined. The temporal decorrelation of the range error is one of the most important factors determining the update rate of DGLONASS messages to obtain the required 95% horizontal position accuracy for harbour approaches.

Transmission of differential GLONASS messages together with differential GPS corrections will affect the final DGPS accuracy. The influence of different sequences of DGLONASS and DGPS messages (at different data rates) are being investigated. It is shown that it should be possible to meet the requirement of 8-20m when transmitting differential GLONASS corrections at a low data rate through the same datalink, which is also used for the differential GPS messages.

Table of contents

Abbreviations

C/A	Coarse-Acquisition
CDMA	Code Division Multiple Access
CIS	Commonwealth of Independent States
CSIC	Coordinated Scientific Information Center
DGNSS	Differential GNSS
DGLONASS	Differential GLONASS
DGPS	Differential GPS
DoD	Department of Defense
ECEF	Earth-Centered-Earth-Fixed
FDMA	Frequency Division Multiple Access
FRP	Federal Radionavigation Plan
GLONASS	Global Orbiting Navigation Satellite System Globalnaya Navigatsionnaya Sputnikovaya Sistema
GNSS	Global Navigation Satellite System
GPS	Global Positioning System
GRI	Group Repetition Interval
ICAO	International Civil Aviation Organization
IMO	International Maritime Organization
IOD	Issue of Data
Loran	Long Range Navigation
P	Precision

PPS	Precise Positioning Service
PR	Pseudo Range
PRC	Pseudo Range Correction
PRM	Pseudo Range Measured
PRN	Pseudo-Random-Noise
PZ-90	Parametry Zemli 1990
RIRT	Russian Institute of Radionavigation and Time
RRC	Range Rate Correction
RSTF	Russian State Time and Frequency
RTCM	Radio Technical Commission for Maritime services
SA	Selective Availability
SC-104	Special Committee No. 104
SGS-85/90	Soviet Geocentric System 1985/1990
SPS	Standard Positioning Service
SSN	Sunspot Number
TEC	Total Electron Content
TOA	Time Of Arrival
TOT	Time Of Transmission
UDRE	User Differential Range Error
USA	United States of America
UTC(SU)	Universal Time Coordinated-Soviet Union
UTC(USNO)	Universal Time Coordinated-United States Naval Observatory
WGS-84	World Geodetic System 1984

1. Introduction

Global Navigation Satellite Systems make navigation on a world-wide basis possible. Currently, two independent GNSS are under development: the Global Positioning System and the Global Orbiting Navigation Satellite System. While GPS already has reached the full constellation, GLONASS will reach the full constellation at the end of 1995. Compared to stand alone GPS and GLONASS, integrated use of GPS and GLONASS introduces advantages concerning availability, accuracy, reliability and integrity.

GNSS suffer from error sources which cause a degradation of the accuracy. Differential GNSS is a technique to correct for these errors to a great extent. One of the proposed differential navigation systems is Eurofix: a radionavigation system consisting of the existing satellite-based GPS and the terrestrial Loran-C. Differential GPS corrections are transmitted by additionally modulating the Loran signals. Until now, Eurofix only supports differential GPS.

If Eurofix is to support differential GLONASS too, differential GLONASS corrections are to be transmitted through the same datalink. Several differential GNSS standards supporting DGPS/DGLONASS are published in the Commonwealth of Independent States and in the United States of America. Based on DGNSS standards of the Radio Technical Commission for Maritime services a GNSS-Eurofix message format is proposed in which the differential use of GPS and GLONASS is supported.

As GLONASS does not suffer from Selective Availability, the ionosphere is the largest error source influencing the GLONASS accuracy. The temporal decorrelation of the ionospheric range errors is one of the most important factors determining the GLONASS correction update rate. The temporal decorrelation of the ionospheric range error is investigated by using a model for the ionosphere: the Bent Ionospheric Model. From the temporal decorrelation the update rate is derived.

Transmission of GLONASS together with GPS corrections through the same datalink will reduce the effective GPS correction update rate and thus the DGPS positioning accuracy. The influence of adding GLONASS corrections on DGPS accuracy is investigated.

GLONASS and GPS apply different coordinate and timing reference systems. The differences in these systems will have its consequences on providing differential corrections for both systems via Eurofix. These differences and the effects are discussed.

In chapter 2 GNSS, and more specific GPS and GLONASS, are described. Both systems are compared. This chapter is followed by a discussion of differential GNSS (chapter 3). A short description of Eurofix is given in chapter 4. Chapters 5 and 6 deal with differential GNSS standards. In chapter 7 the ionospheric problem is introduced followed by chapter 8 giving a description of the Bent Ionospheric Model used in the simulation model, described in chapter 9. Chapter 10 discusses the simulations and results. In this chapter the GLONASS correction update rate is determined. In chapter 11 the consequences of integrating GLONASS into Eurofix are discussed. This report is concluded with a chapter giving conclusions and recommendations.

2. Global Navigation Satellite Systems

2.1 Introduction

In today's world, transportation of people and goods through the air, over water and land is constantly increasing. Safe and economic transportation requires accurate navigation all over the world. As a result, radionavigation systems have become very important. The best way to make navigation on a world-wide basis possible is by using satellites. Therefore, several navigation systems based on satellites are being developed. Such systems are called Global Navigation Satellite Systems (GNSS). In section 2.2 the general design of GNSS is discussed, followed by a section on positioning with GNSS.

Currently, two independent GNSS are under development: the Global Positioning System (GPS) developed by the United States of America (USA) and the Global Orbiting Navigation Satellite System or Globalnaya Navigatsionnaya Sputnikovaya Sistema (GLONASS) developed by the former Soviet Union (now Commonwealth of Independent States (CIS)). Both systems are described in section 2.4.

2.2 The design of GNSS

A Global Navigation Satellite System can be subdivided into three segments (figure 2.1):

1. *The space segment:*

   This segment is formed by the satellites. The satellites transmit signals modulated with navigational data, to be used for positioning.

2. *The control and monitoring segment:*

   This segment consists of *(a)* a master control station, *(b)* monitor and *(c)* uplink stations. The purpose of this segment is to control and monitor the satellites in their orbits. In addition, satellite orbital parameters, satellite clock

error and navigational messages are determined and uploaded into the space segment.

3. *The user segment:*

This segment is formed by different types of users (land, marine and air). By means of a receiver, the users are able to determine their position on a world-wide basis.

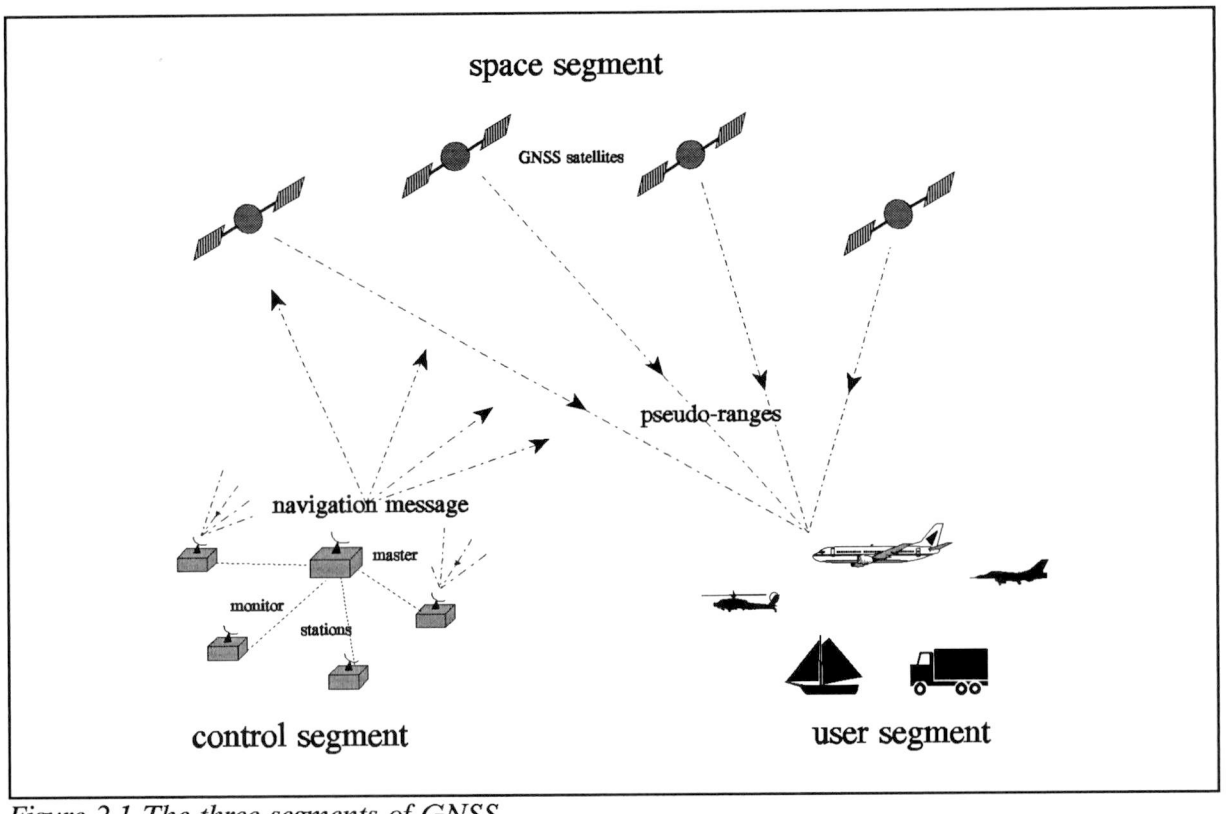

Figure 2.1 The three segments of GNSS

2.3 Positioning with GNSS

The principle of positioning with GNSS is based on measuring time differences. A satellite transmits a radiosignal, which is received by a receiver. The time of arrival (TOA) of this signal is determined. This signal is modulated with data concerning the position and velocity of the satellite. The time of transmission (TOT) is also modulated onto the signal. The time difference ΔT (= TOA - TOT) is decisive for the distance of the user to the satellite.

Multiplying the time difference by the velocity of light (c) gives the distance (R) from the receiver to the satellite:

$$R = c \times \Delta t \tag{2.1}$$

These distances are called pseudoranges: the measured distances are not the actual distances as the measurements suffer from several errors (see chapter 3).

Positioning with GNSS is based on the so called range-range method. A user (the receiver) receives a signal transmitted by a satellite. If the user and satellite clocks are synchronized, the user has to be on a sphere with a radius equal to the distance from the user to the satellite. If a second satellite is included, the user has to be on two spheres. There remains a circle, being the intersection of the two spheres, on which the user is located. Including a third satellite introduces a third sphere. The intersection of the three spheres is formed by two points. One of these points is the position of the user.

In principle, range measurements to three satellites are sufficient to determine a position (in three dimensions). This is only the case when the receiver is equipped with an accurate time reference, such as an atomic clock. However, the user receiver is usually not equipped with such an accurate time reference: in most receivers crystal oscillators are used. As a result, the transmitter and receiver clock are not exactly synchronized. To solve this problem a fourth measurement must be used. By solving a system of four equations with four unknowns the position can be determined:

$$R_i = [(X_{si} - X)^2 + (Y_{si} - Y)^2 + (Z_{si} - Z)^2]^{\frac{1}{2}} + T + \delta_i \tag{2.2}$$

where:

	R	=	pseudorange
	i	=	1, 2, 3, 4
	X_{si}, Y_{si}, Z_{si}	=	coordinates of the i^{th} satellite
	X, Y, Z	=	user's coordinates (to be determined)
	T	=	difference receiver clock and GNSS system time (expressed in meters)
	δ_i	=	error in pseudorange determination

2.4 Two GNSS: GPS and GLONASS

2.4.1 GPS

In 1973 the Department of Defense (DoD) of the USA started the development of GPS [1]. Although GPS is primarily a military system, the civil community is allowed to use the system as well. Authorized users are provided with the Precise Positioning Service (PPS). For security reasons, the civilian users are provided with the less accurate Standard Positioning Service (SPS). As the intended SPS appeared to be more accurate than expected, the SPS accuracy is degraded intentionally. This is called Selective Availability (SA).

The satellite segment consists of 24 satellites, divided over 6 orbital planes. The planes have a separation of 60° at the equator and an inclination of 55°. The satellites orbit at a height of 20200 km above the earth's surface. The orbital period of a GPS satellite is approximately 12 hours.

GPS satellites transmit on two carrier frequencies (f_{L1} and f_{L2}) in the L-band : f_{L1} = 1575.42 MHz and f_{L2} = 1227.60 MHz. The carrier waves are modulated with Pseudo-Random-Noise (PRN) codes and navigational data (Appendix A). Two kinds of PRN-codes are being used: a 1.023 MHz Coarse-Acquisition (C/A) code for SPS and a 10.23 MHz Precision (P) code for PPS. The L1-frequency contains both codes, the L2-frequency only the P-code. Each satellite uses a unique PRN-code. The satellites are distinguished by this code. GPS is a Code Division Multiple Access (CDMA) system.

The control and monitoring subsystem consists of a Master Control Station in Colorado and Uplink and Monitor Stations in Ascension, Diego Garcia, Kwajalein and Hawaii.

2.4.2 GLONASS

In the early 1970s, the former Soviet Ministry of Defense started the development of GLONASS, a satellite based navigation system similar to GPS. GLONASS is now the centrepiece of the CIS's Intergovernmental Radionavigation Program, which has close ties with the International Civil Aviation Organization (ICAO) and the International Maritime

Organization (IMO). By presidential decree on September 24, 1993, the GLONASS program was officially placed under auspices of the Russian Military Space Forces [2, 3]. Fourteen years after the launch of the first test space craft, the Russian GLONASS program remains viable and essentially on schedule despite the economic and political turmoil surrounding the final years of the Soviet Union and the emergence of the Commonwealth of Independent States. By the spring of 1995, a total of 73 GLONASS spacecraft (8 "dummy" satellites launched on the first 7 launches included) had been launched by Proton launchers[1]. Of the 65 "real" satellites, only 16 had been normally operational since the establishment of the Phase I constellation in 1990. With the commissioning of a third orbital plane in August 1994, the 1988 goal of a complete 24-spacecraft constellation by the year 1995 is within reach, and support for the high-precision, real-time navigation network has expanded from its national military origins to the international civil sector.

GLONASS provides (like GPS) services for authorized users (PPS) and civilian users (SPS) [4, 5]. The SPS is less accurate than PPS. There is, however, an important difference between GPS and GLONASS concerning the SPS: GLONASS makes no use of SA to degrade the accuracy of the SPS.

The satellite segment consists (when fully operational) of 24 satellites. These satellites are equally divided over three orbital planes, having a separation of 120° at the equator and an inclination of 64.8°. As there will be 8 satellites in 3 planes, the spacing between the satellites will be 45°. To improve coverage uniformity, satellites in one plane will be phased 15° from satellites in adjacent planes. The satellites orbit at a height of 19100 km above the earth's surface. The orbital period of a satellite is approximately 11 hours and 15 minutes.

GLONASS satellites transmit on two carrier frequencies (f_{L1} and f_{L2}) in the L-band, given by:

$$\begin{aligned} f_{L1} &= f_{01} + c\,\Delta f_{c1} \\ f_{L2} &= f_{02} + c\,\Delta f_{c2} \end{aligned} \tag{2.3}$$

[1] Data from P. Daly (CAA Institute of Satellite Navigation, Department of Electrical Engineering, University of Leeds, United Kingdom) and M. G. Lebedev (Coordinational Scientific Information Center, Russian Space Forces, Moscow, Russia) coordinated by R. Langley (Geodetic Research Laboratory, Department of Geodesy and Geomatics Engineering, University of New Brunswick, Canada).

where:

f_{01} = 1602 MHz

f_{02} = 1246 MHz

c = 1, 2,..., 24 (= carrier frequency number or channel number)

Δf_{c1} = 0.5625 MHz

Δf_{c2} = 0.4375 MHz

The CIS authorities had the intention that each satellite would transmit at two unique frequencies. However, it turned out to be that some of the frequencies were interfering with signals of radio and mobile satellite service systems in the frequency range 1610-1626.5 MHz and with radioastronomical measurements in the frequency range 1610.6-1613.8 MHz. Therefore, the frequency plan has been changed recently. It is planned to transit to 12 frequencies (c ranging from -7 to +6, 5th and 6th are technological). Antipodal satellites will transmit on the same frequency [6].

Each carrier wave is modulated with a PRN code and navigational data (Appendix A). Two kinds of PRN codes are being used: a C/A-code, for civil use, and a P-code, for authorized use. On the L1-frequency each satellite transmits the same C/A and the same P-code. The L2-frequency only contains the P-code. Each satellite is distinguished by its own carrier frequency: GLONASS is a Frequency Division Multiple Access (FDMA) system.

The different elements of the control and monitoring segment are entirely placed on former Soviet ground.

2.4.3 GPS and GLONASS: A comparison

In GPS and GLONASS some distinctive differences can be distinguished. These differences concern the satellite orbits as well as the satellite signal characteristics.

Satellite orbits

After full implementation, both systems will consist of 24 satellites. However, the orbital arrangement of the satellites is not the same. The differences are summarized in table 2.1.

The orbital height is related to the orbital period by Kepler's third law. The GPS orbital period is exactly one half of a sidereal day (= the rotation period of the earth, equal to a calendar day minus four minutes). Therefore, after one sidereal day the geometric relationship between fixed spots on the earth and the satellites repeats. For an observer on the earth, all GPS satellites reappear in the same part of the sky day after day, always four minutes earlier each day. In GLONASS, the orbital height is about 1,100 kilometres lower than that of the GPS satellites. Accordingly, the shorter orbital radius yields a shorter orbital period of 8/17 of a sidereal day such that, after eight sidereal days, the GLONASS satellites have completed exactly 17 orbital revolutions. For an observer on the earth, a particular satellite will reappear at the same place in the sky after eight sidereal days. Because each orbital plane contains eight equally spaced satellites, one of the satellites will be at the same spot in the sky at the same sidereal time each day.

Table 2.1 Differences in satellite orbits

	GPS	**GLONASS**
Orbital planes	6, spaced by 60°	3, spaced by 120°
Satellites per orbital plane	4, unevenly spaced	8, evenly spaced
Orbital plane inclination	55°	64.8°
Orbital height above earth's surface	20,200 km	19,100 km
Orbital period	1/2 of a sidereal day ≈ 11 hours 58 minutes	8/17 of a sidereal day ≈ 11 hours 16 minutes
Repeat ground track	every sidereal day	every 8 sidereal days

Satellite signal characteristics

As already mentioned, one of the differences between GLONASS and GPS is the method of distinguishing the different satellites in the system: GLONASS uses FDMA, GPS applies CDMA. Further differences can be distinguished in the information contained in the navigational messages.

In GLONASS and GPS, navigational data are transmitted at a rate of 50 bits per second. Important in positioning are the satellite clock data and the ephemeris. The GPS clock data

transmitted contain terms of clock offset, clock frequency offset, and clock frequency rate, and allow the calculation of the difference between the individual GPS satellite's time and the GPS system time. The latter is related to Universal Time Coordinated as kept by the United States Naval Observatory, UTC(USNO). In contrast, the broadcast GLONASS clock and clock frequency offset yield the difference between the individual GLONASS satellite's time and the GLONASS system time, which is related to UTC(SU) as kept in the CIS.

Table 2.2 Satellite signal characteristics

	GPS	**GLONASS**
Carrier signals	L1: 1575.42 MHz L2: 1227.60 MHz	L1: (1602+c×0.5625) MHz L2: (1246+c×0.4375) MHz c = channel number
Codes	different for each satellite C/A-code on L1 P-code on L1 and L2	same for all satellites C/A-code on L1 P-code on L1 and L2
Code frequency	C/A-code: 1023 MHz P-code: 10.23 MHz	C/A-code: 0.511 MHz P-code: 5.11 MHz
Clock data	- clock offset - frequency offset - frequency rate	- clock offset - frequency offset
Ephemeris data	modified Keplerian orbital elements every hour	satellite position, velocity and acceleration every half hour

The satellite ephemerides broadcast by the GPS satellites contain the parameters of the satellite orbit in terms of a linearly varying ellipse and small correction terms accounting for irregularities in the orbit (Keplerian orbital parameters). The ephemeris data are updated every hour. From the parameters, the user can compute the Earth-Centered-Earth-Fixed (ECEF) coordinates of the satellite for a particular measurement time using published equations [1]. The resulting ECEF-coordinates are referenced to the World Geodetic System 1984 (WGS-84). In GLONASS, each satellite directly broadcasts its three-dimensional ECEF position, velocity, and acceleration valid for every half-hour epoch. For a measurement time somewhere between these half-hour epochs, the user interpolates the satellite's coordinates

using position, velocity, and acceleration data from the half-hour marks before and after the measurement time. The resulting ECEF coordinates are referenced to the Soviet Geocentric System 1985 (SGS-85). SGS-85 will be followed by PZ-90 (Parametry Zemli = Parameters of Earth). The GPS and GLONASS signal characteristics are summarized in table 2.2.

3. Differential GNSS

3.1 Introduction

The position accuracy of GNSS is degraded by several error sources. A technique to improve the accuracy is differential GNSS (DGNSS). In DGNSS, differential GNSS corrections determined at a reference station are transmitted to the users through a data communication link. In section 3.2 the concept of DGNSS is being discussed followed by a section dealing with the need for DGNSS. Although it is a powerful concept, there is a limit to the final accuracy of DGNSS. Errors, which are corrected for, are not the same with time and place. This problem of temporal and spatial decorrelation is discussed in section 3.4.

3.2 The concept of differential GNSS

The principle of differential GNSS is quite simple (figure 3.1). A reference station is placed at an exactly known location. As this position and the satellite position are exactly known, the ranges to the satellites are also known. A receiver at the reference station measures pseudoranges to the GNSS satellites. These measured pseudoranges are compared to the known ranges and a range correction (the difference between measured and known range) can be determined. This range correction is broadcast to the GNSS user who is able to correct his measured range with this correction.

As discussed in [7], one of the distinctions which can be made in differential GPS (DGPS) is synchronous and asynchronous DGPS. As the synchronous or asynchronous technique is not bounded to DGPS only, the distinction can be made more general: i.e. synchronous and asynchronous DGNSS. In synchronous DGNSS, the user is not allowed to use corrections generated at different moments in time: range errors computed at different moments in time contain a different reference station clock error, due to clock drift, etc. In asynchronous DGNSS, the user can apply range corrections generated at different moments in time. The user is allowed to do this, because the reference station has a very stable clock reference to its

disposal (e.g. an atomic clock). In asynchronous DGNSS it is allowed to apply a correction as soon as it is received; in synchronous DGNSS a correction cannot be applied until all the corrections have been received. For low bit rate channels, the aging of the asynchronous DGNSS corrections is much less than the aging of the synchronous DGNSS corrections.

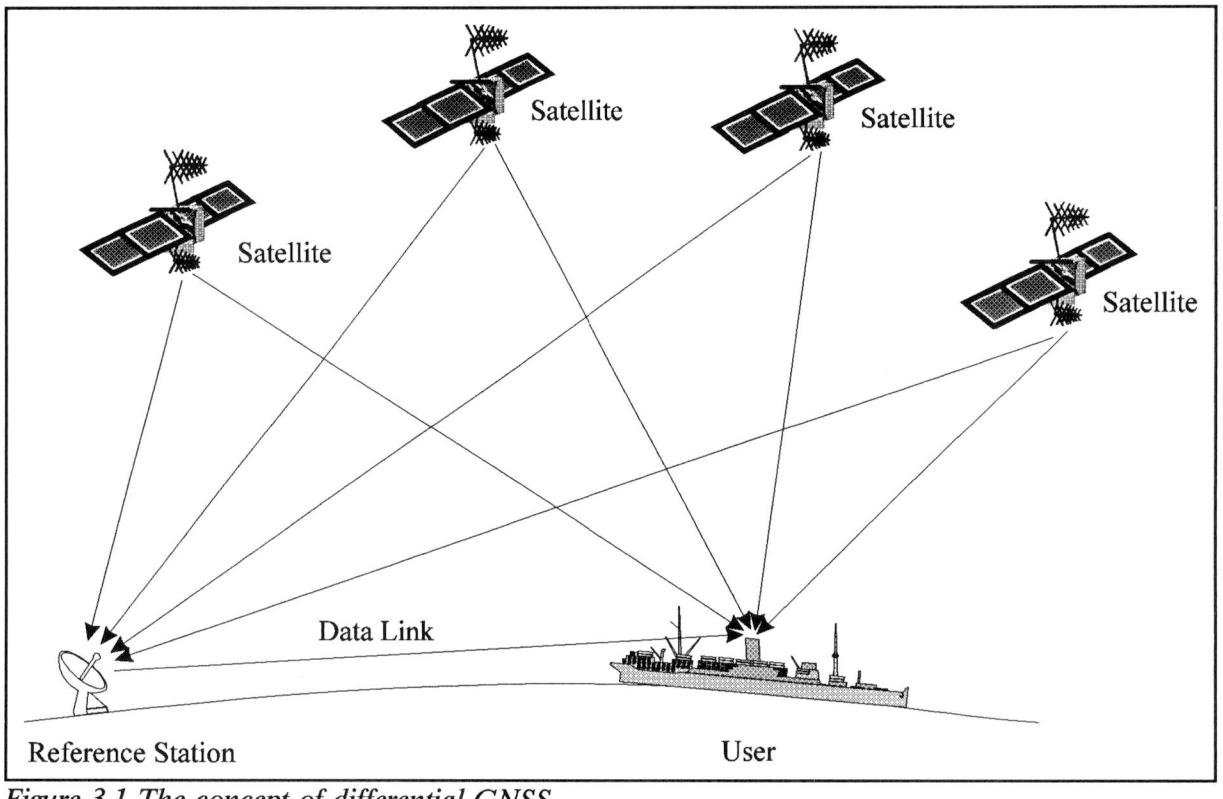

Figure 3.1 The concept of differential GNSS

3.3 The need for differential GNSS

GNSS provides global, 24-hour-a-day, highly accurate navigation and positioning service over the entire world. Due to several error sources the accuracy of GNSS is reduced. GPS (with Selective Availability) has a horizontal accuracy of 100m (95%). For GLONASS, which is not affected by Selective Availability, different values for the horizontal accuracy (95%) are given. According to [7], the horizontal accuracy is 100m (95%). In the Russian Radionavigation Plan [8] a value of 60m (95%) is given. For some applications, for example, harbour approaches, these accuracies are not sufficient. The Federal Radionavigation Plan (FRP) [9] specifies a

positioning accuracy of 8-20m (95%) for the harbour approach phase. Differential GNSS is a technique which is able to improve the accuracy of stand alone GNSS.

The error sources influencing the accuracy of stand alone GNSS are the following:

- multipath
- measurement noise
- ionospheric delay
- tropospheric delay
- satellite clock errors
- satellite position errors (ephemeris prediction errors)
- Selective Availability (GPS only)

These errors can be classified as correlated and non-correlated errors. If these errors are approximately the same for users separated over a certain distance, the errors are said to be correlated. If not, the errors are non-correlated. Error correlation again can be subdivided into temporal and spatial correlation. Errors which do not change with time are said to be temporally correlated. Spatial correlated errors are errors which do not change with distance. Differential GNSS is capable of correcting for correlated errors. From the above mentioned errors, multipath and measurement noise are non-correlated errors. The other error sources are correlated.

multipath

Multipath is caused by reflections from the earth's surface and nearby obstacles. The reflected signals are a distortion to the direct signals. Multipath depends on the local area and therefore changes with increasing distance between separated users.

measurement noise

Measurement noise is receiver dependent and is caused amongst others by thermal noise in the receiver. The measurement noise varies with the receiver used.

ionospheric delay

The ionospheric delay is proportional to the number of free electrons (Total Electron Content, TEC), along the signal path. This delay is also wavelength dependent. The TEC

varies in time and place and depends on the solar activity. The ionosphere can cause a propagation group delay of a satellite signal by as much as 100 meters during peak solar cycle conditions, and more typically causes delays of 20-30 meters (for low-elevation angle satellites). The signal propagation paths to two receivers at different positions will not be the same. Along these paths the signals will suffer different delays. Only receivers located not far from each other will meet similar ionospheric delay.

By modelling the ionosphere much of the group delay can be removed. GPS transmits ionospheric model coefficients in the navigational messages [1] which can be used to model approximately 50 per cent of the delay. In GLONASS, however, no such model is provided. Therefore the ionosphere has a larger impact on GLONASS than on GPS accuracy. In GLONASS (and GPS without SA), the ionospheric delay is the largest error source.

tropospheric delay

The troposphere is the lower part of the atmosphere. The index of refraction in the troposphere is almost, but not quite, unity. It approaches unity at the top of the troposphere. Its value (typically 1.0030) depends on the temperature, pressure, and the partial pressure of water vapour. While the time delay caused by the troposphere is typically 3 meters overhead to 50 meters at 3 degrees elevation, a simple model, i.e. one not involving any temperature or pressure measurements, can predict this quite well. Above 5 degrees elevation the unmodelled error is usually less than a meter. The model can be improved somewhat by a local measurement of the meteorological parameters.

satellite clock errors

Each satellite is provided with an atomic clock. The GNSS satellites should be exactly synchronized to the system time. However, this is not possible. In the navigation message, clock correction parameters are included. These parameters make a reduction of the clock error possible. Finally, there will remain a residual clock error. This clock error is the same for every user in the coverage area. So, the satellite clock error is completely spatial correlated.

satellite position errors

Satellite positions are calculated from the ephemeris parameters transmitted by the satellites. These parameters are predicted in the Control and Monitoring segment and uploaded to the

satellites. Errors in these predictions lead to errors in the satellite position. The satellite position error consists of three components: along-track, cross-track and radial error vectors. Depending on the user's location, different components of these errors will subtend into the range from the user to the satellite. Therefore, the satellite position errors will not cancel completely unless the user and reference station are close to each other.

Selective Availability

GPS suffers, in contrast to GLONASS, from an additional error: Selective Availability. Selective Availability is an intentional degradation of the accuracy of SPS GPS. It is an artificial error introduced at the satellite's signals for security reasons. SA is a combination of satellite clock dithering and ephemeris data manipulation. In GPS positioning, it is the largest error source.

3.4 The problem of decorrelation

The above mentioned error sources in GNSS are not fully correlated. The errors change with place (spatial decorrelation) and time (temporal decorrelation). As a result the final accuracy of DGNSS can be limited by this decorrelation.

Spatial decorrelation

As already mentioned, the errors influencing the accuracy of GNSS will be different for users at different locations. This spatial decorrelation is a function of the distance between two receivers. In DGNSS, spatial decorrelation limits the distance between user and reference station at which the differential corrections should be applied.

Temporal decorrelation

When a differential correction is received, this correction is aged. This aging is caused by the limited channel capacity. Furthermore, the correction is used until the next correction is received. Temporal decorrelation results: the measured pseudorange (with a certain error) and the correction (correction for an earlier error) do not fully correlate.

In GPS, the largest variation of the corrections is caused by SA. The relatively fast changing clock error results in a correction which decorrelates fast. The range error caused by the time decorrelation effect for small time delays (up to 50 seconds) can be approximated by [7]:

$$\sigma_{range} = \frac{1}{2} a t^2 \tag{3.1}$$

with a the rms value of the SA clock error acceleration, approximately 0.004 m/s^2.

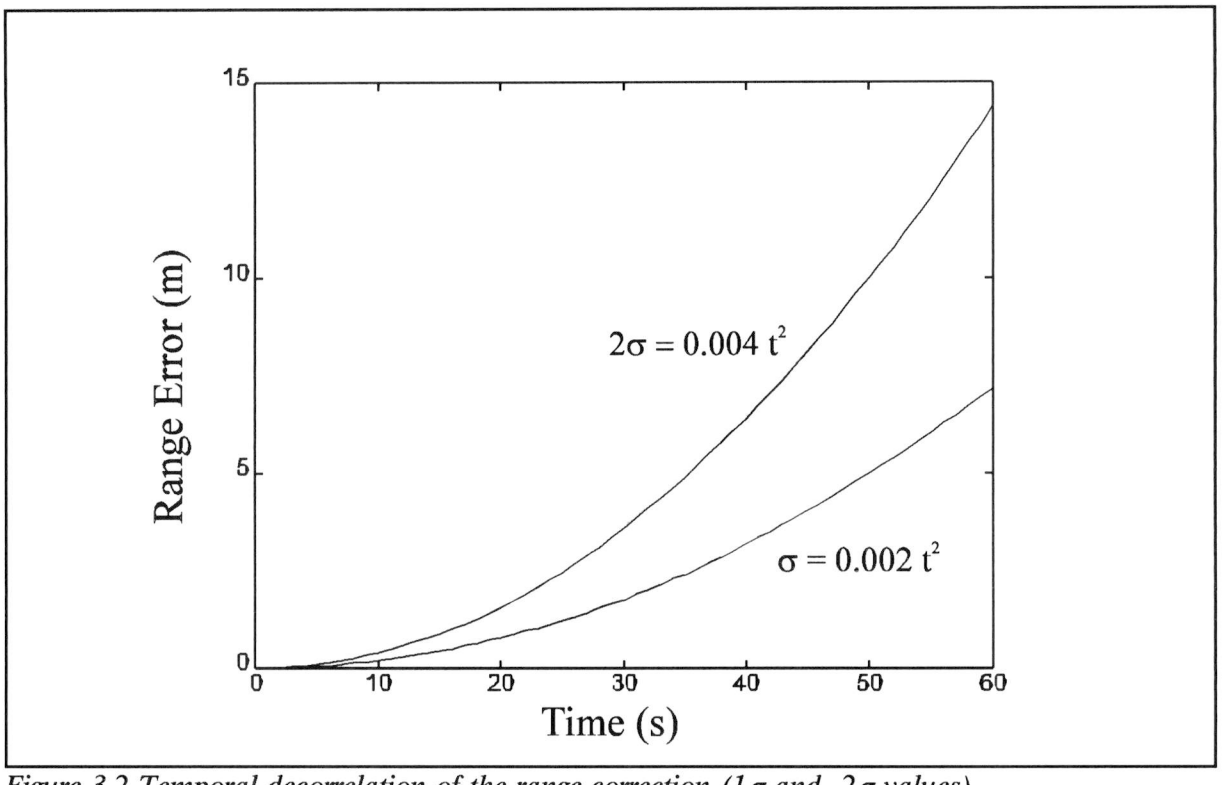

Figure 3.2 Temporal decorrelation of the range correction (1 σ and 2 σ-values)

If the final position error distribution is assumed to be normal, the 95% interval is given by the 2σ value. Apparently, this temporal decorrelation term has great influence on the final accuracy when DGPS corrections are transmitted using a low data rate channel.

GLONASS does not suffer from SA. The error source with the largest impact on differential GLONASS (DGLONASS) will be the ionospheric delay. The ionospheric errors can be seen as spatially correlated errors as already mentioned. But when it is realized that a satellite position changes in time, the ionospheric errors can also be seen as temporally correlated errors. In this report (see chapters 7, 8, 9 and 10), this temporal decorrelation will be discussed. The spatial decorrelation has been left out of consideration. However, as the

temporal decorrelation appears to be little the spatial decorrelation will have to be taken into account in future research.

4. The Eurofix concept

4.1 Introduction

As mentioned in chapter 3, the FRP requires an accuracy of 8-20m (95%) in the harbour approach phase. Therefore Eurofix has been proposed [10]. Eurofix is a navigation system consisting of two existing navigation systems: GPS, a satellite based navigation system and the terrestrial Loran-C (Long Range Navigation) [11]. In Eurofix, Loran-C is used as a datalink to transmit DGPS corrections from reference station to users. In section 4.2 the Eurofix data format is described in which the corrections are transmitted. This transmission is done by additionally modulating the Loran-C pulses. In the following section this modulation is briefly described. This chapter is concluded with a section on the major advantages of Eurofix.

4.2 The Eurofix asynchronous data format

The differential GPS corrections have to be transmitted to the GPS users in some format. The Radio Technical Commission for Maritime Services Special Committee 104 (RTCM SC-104) has developed a standard for differential GPS services [12]. In this standard synchronous DGPS is applied. It can be shown that the RTCM SC-104 type 1 synchronous DGPS message is not suitable for low bit rate data channels like Eurofix [7]. Due to the long transmission time the temporal decorrelation becomes too large. Therefore, an asynchronous DGPS format has been proposed. This format requires less bits than the RTCM SC-104 format type 9. Transforming the Eurofix format to the synchronous RTCM type 1 message should give no difficulties. The reason behind this: it is to be assured that the asynchronous Eurofix format is compatible with existing standard GPS receivers. Therefore, the Eurofix format contains more or less the same information as the RTCM type 1 message. In order to keep the total number of bits as small as possible some parameters were omitted or shortened. An example of the Eurofix asynchronous pseudorange correction format is given in table 4.1.

Table 4.1 Eurofix asynchronous DGPS correction [7]

Function	**Number of bits**	**Range**	**Resolution**
Message Type	2	4 messages	-
Satellite ID	5	32 satellites	-
Issue of Data (IOD)	8		-
Time Reference	10	1 hour	3.6 seconds
Range	12	-655.32..+655.32 m	0.32 m
Range Rate	7	-2.048..2.048 m/s	0.032 m/s
UDRE	1	2 states	-
Total number of bits	45		

The compatibility with standard GPS receivers is assured by repacking the asynchronous corrections into a synchronous RTCM type 1 message at the receiving end. Every time a new asynchronous correction is received, the old corrections have to be recalculated to match the new time reference. The new correction and the recalculated ones fit into one synchronous message which is used by the GPS receiver to upgrade its position calculation. The validity of the recalculated corrections, however, is still related to the time reference in which they were generated. So, each repacked RTCM type 1 message contains only one updated satellite, the rest of the corrections are recalculated ones.

From table 4.1 it can be seen that 4 types of messages are possible, for example:

1. Asynchronous pseudorange correction
2. Delta Asynchronous pseudorange correction (like RTCM SC-104 message type 2: old navigation data)
3. Integrity message
4. Can be defined

Also can be seen from table 4.1 that the Eurofix message consists of 45 bits, using no parity bits. As the performance of the Eurofix data channel is influenced by all kinds of error

sources, error correcting techniques need to be designed. As this is not the scope of this report, the reader is referred to [13, 14] for more information on this subject.

4.3 Loran-C as the Eurofix datalink

Loran-C is a hyperbolic, terrestrial navigation system [11]. Loran-C consists of several so called chains. Each chain is formed by one primary station (the master) and two (or more) secondary stations (the slaves). Each Loran-C station transmits a group of 8 pulses at 1 ms intervals. In Eurofix, the DGPS corrections are transmitted to the users by additionally modulating these Loran-C pulses.

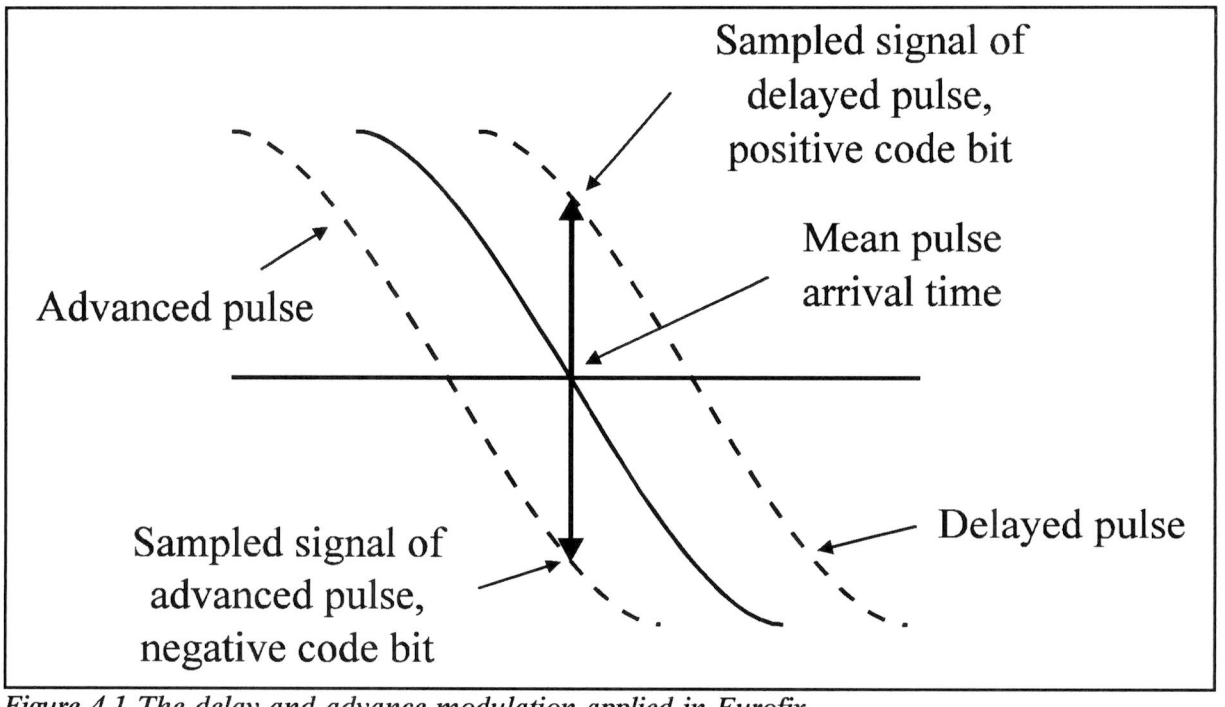

Figure 4.1 The delay and advance modulation applied in Eurofix

The modulation applied consists of advancing or delaying the Loran pulses by 1 μs (Figure 4.1). A delayed pulse agrees with a positive code bit; an advanced pulse with a negative code bit.

Each bit (a '1' or a '0') of the DGPS corrections is formed by a combination of a number of advances and delays [7, 13, 14, 15]. An example is given in table 4.2.

Table 4.2 Possible modulation pattern of the bursts in one group of bursts [7]

Binary databit	Modulation pattern
1	0 0 + - + - + -
0	0 0 - + - + - +

0 = no time shift

\+ = positive code bit = 1 μs delay

\- = negative code bit = 1 μs advance

In order to ensure normal navigation with Loran-C is still possible, some restrictions are imposed on the applied modulation:

1. The Eurofix modulation has to be balanced. Normal Loran-C performance requires that the mean value of the time shifts should not change from the original unmodulated signal.
2. The first two pulses of each GRI (Group Repetition Interval [11]) are used by the Loran-C stations to signal a malfunction of the system (blinking). Therefore these pulses cannot be modulated.

For extensive information concerning the Eurofix datalink, see references [13, 14, 15, 16, 17].

4.4 Advantages of Eurofix

The use of Loran-C as a datalink for the transmission of the DGPS corrections has two major advantages. First of all, Loran-C is an already existing navigation system. Therefore an infrastructure for the DGPS reference stations does not have to be set up. As a result Eurofix is a DGPS solution with relatively low costs. The second advantage concerns frequency allocation. Transmission of corrections through a new datalink requires bandwidth. As the radio spectrum is limited and most of it is already in use, bandwidth is hard to get. By using an already existing system, this problem is solved.

5. RTCM Recommended Standards for Differential GPS

5.1 Introduction

The Radio Technical Commission for Maritime Services established Special Committee No. 104 "Differential Navstar/GPS Service". This committee is concerned with the development of the "RTCM Recommended Standards for Differential Navstar GPS Service". In January 1994, version 2.1 of this RTCM SC-104 standard was published [12]. This recommended standards document replaces version 2.0.

The RTCM SC-104, Differential GPS Service, has examined the technical and institutional issues, and has formulated recommendations in the following areas:

1. *Data Message and Format*
   The message elements that make up the corrections, the status messages, the station parameters, and ancillary data are defined in some detail. They are structured into a data format similar to that of the GPS satellite signals, but a variable-length format is employed.
2. *User Interface*
   A standard interface is defined which enables a receiver to be used in concert with a variety of different datalinks. For example, using the standard, a receiver can be used with a satellite link or a radiobeacon datalink.

A number of different messages have been defined in the *Data Message and Format* area, with different levels of finality. Some message types have been "fixed", i.e., they will not be subject to change. If, for some reason that emerges in the future, they prove inadequate, new messages will be defined to accommodate the new situations; however, the message structure is considered fixed for Version 2. Some message types are considered tentative, and may be fixed (in their current or altered form) at some future time, if field experience with them justifies it. Still other message types have been reserved for specific use, but their content has

not been defined or proposed. The other types are available for future definition, and can be used by service providers who want to provide specially tailored messages. As the RTCM recommended standards is used as a basis for developing a differential standard supporting both GPS and GLONASS (chapter 6), the *Data Message and Format* will be discussed in short in this chapter.

5.2 General message format

Each RTCM SC-104 message type has the same general format. The messages consist of N+2 30-bit words (N words contain the data of the message). The number of words containing the data varies with the message type as well as within a message type. The minimum length of a message is 2 words; the maximum is 33 words.

The header (figure 5.1), which precedes each RTCM SC-104 message, is identical for each message type. This header consists of two words, containing data that is pertinent to any type of message: Reference Station information, reference time and information required for user's frame synchronization. Their contents are summarized in table 5.1.

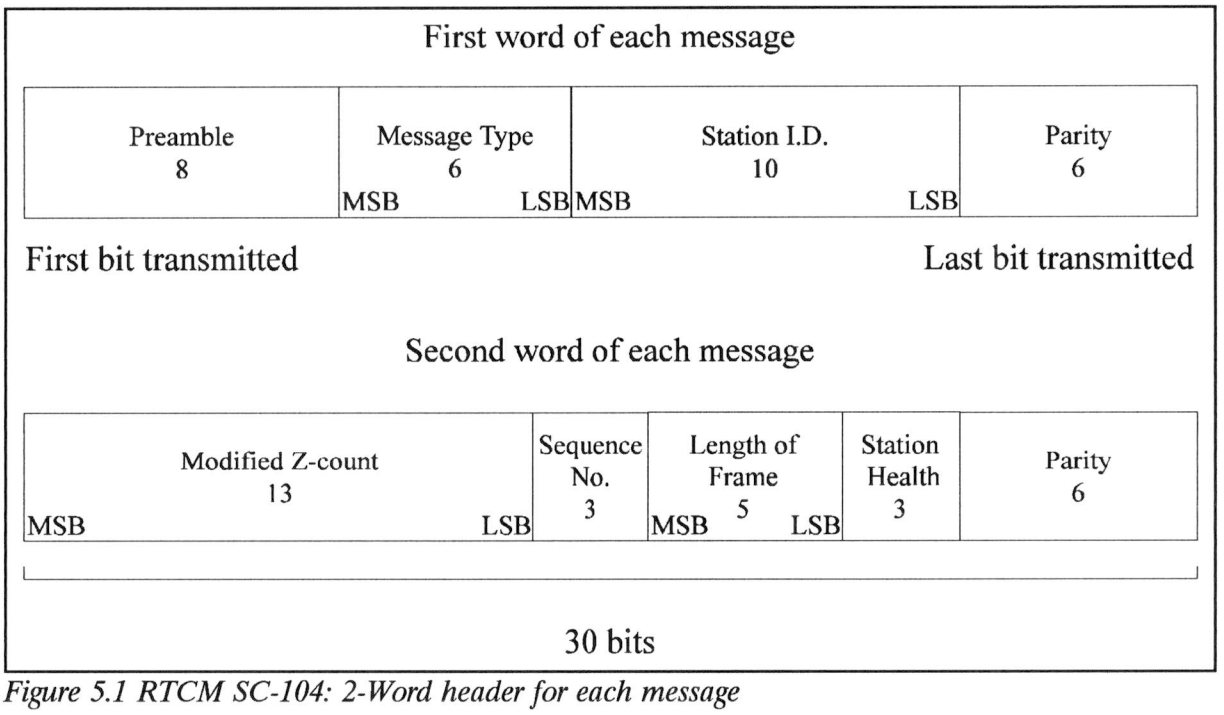

Figure 5.1 RTCM SC-104: 2-Word header for each message

Table 5.1 RTCM SC-104: Content of first and second words

Word	Content	Number of bits	Scale factor and units	Range
First	Preamble	8	-	-
	Frame ID/Message Type	6	1	1-64
	Station ID	10	1	0-1023
	Parity	6	See ICD-GPS-200 [1]	
Second	Modified Z-count	13	0.6 sec	0-3599.4 sec
	Sequence No.	3	1	0-7
	Length of frame	5	1 Word	2-33 Words
	Station Health	3	-	8 States
	Parity	6	See ICD-GPS-200 [1]	-

The beginning of the first word is a *preamble,* a fixed sequence of 8 bits (01100110). This preamble is used for synchronization. Each type of message which is transmitted is indicated by the *message type number* (6 bits). In table 5.2, the message types are summarized. The message type number is followed by a *station ID* (10 bits), identifying the reference station.

The second word starts with the *modified Z-count* (13 bits). For pseudolite transmissions, the modified Z-count is the time of the start of the next frame as well as the reference time for the message parameters. In the case of non-pseudolite type transmission, it is only the reference time for the message parameters. The modified Z-count is different from the GPS Z-count in that the LSB has a scale factor of 0.6 seconds, instead of 6 seconds, to account for the variable length frames. This is required only for pseudolite transmissions. Also, the range of the Z-count is only one hour in order to conserve bits. The reasoning behind this is that all differential GPS users will have already initialized via the GPS system and will know what the time is. It should be noted that the DGPS Z-count is referenced to GPS time, not UTC. The *sequence number* (3 bits) aids in frame synchronization for non-pseudolite transmissions. It replaces the sequencing Z-count as an incrementing parameter. It will increment on each frame. The *frame length* (5 bits) indicates the total length of a message (in words) The frame length is two more than the number of words (N) following the header. Thus a zero in the

frame length field would mean that the frame length would be 2, and no words would follow the header. In comparison to version 2.0 the meaning of the three *station health* bits has been redefined: rather than requiring a fixed definition of the field, 6 states are made available to the system provider to define their meaning. However, '111' shall continue to indicate that the reference station is not working properly, and "110" shall indicate that the transmission is unmonitored.

5.3 Message types

In the RTCM DGPS standards 64 different messages are possible. In Version 2.1 26 messages are defined. Those can be tentative, fixed, retired or reserved (table 5.2).

As an example of a differential GPS message, Message Type 1 (figure 5.2, table 5.3) will be discussed. This is the primary message type which provides the pseudorange correction (PRC(t)) for any user GPS measurement time "t":

$$PRC(t) = PRC(t_0) + RRC \times [t - t_0] \tag{5.1}$$

where $PRC(t_0)$ is the 16 bit pseudorange correction, RRC is the 8-bit rate of change of the pseudorange correction (range rate correction), and t_0 is the 13-bit modified Z-count of the second word. These parameters are all associated with the satellite indicated by the 5-bit Satellite ID, which indicates its PRN number. The pseudorange measured by the user, PRM(t), is then corrected as follows:

$$PR(t) = PRM(t) + PRC(t) \tag{5.2}$$

Note that the correction is added to the measurement. PR(t) is the differentially corrected pseudorange measurement that should be processed by the User Equipment navigation filter.

Also provided is a 1-bit Scale Factor and 2-bit User Differential Range Error (UDRE). The UDRE is a one-sigma estimate of the uncertainty in the pseudorange correction as estimated by the reference station, and combines the estimated effects of multipath, signal-to-noise ratio, and other effects. It should be noted that the real-time kinematic messages use signal quality indicators which separate out multipath effects from other effects [12, Appendix II].

Table 5.2 Message types of the RTCM SC-104 Version 2.1

Message Type No.	Current Status	Title
1	Fixed	Differential GPS Corrections
2	Fixed	Delta Differential GPS Corrections
3	Fixed	Reference Station Parameters
4	Retired	Surveying
5	Fixed	Constellation Health
6	Fixed	Null Frame
7	Fixed	Beacon Almanacs
8	Tentative	Pseudolite Almanacs
9	Fixed	Partial Satellite Set Differential Corrections
10	Reserved	P-code Differential Corrections (all)
11	Reserved	C/A-Code L1, L2 Delta Corrections
12	Reserved	Pseudolite Station Parameters
13	Tentative	Ground Transmitter Parameters
14	Reserved	Surveying Auxiliary Message
15	Reserved	Ionosphere (Troposphere) Message
16	Fixed	Special Message
17	Tentative	Ephemeris Message
18	Tentative	Uncorrected Carrier Phase Measurements
19	Tentative	Uncorrected Pseudorange Measurements
20	Tentative	RTK Carrier Phase Corrections
21	Tentative	RTK Pseudorange Corrections
22-58	-	Undefined
59	Tentative	Proprietary Message
60-63	Reserved	Multipurpose Usage

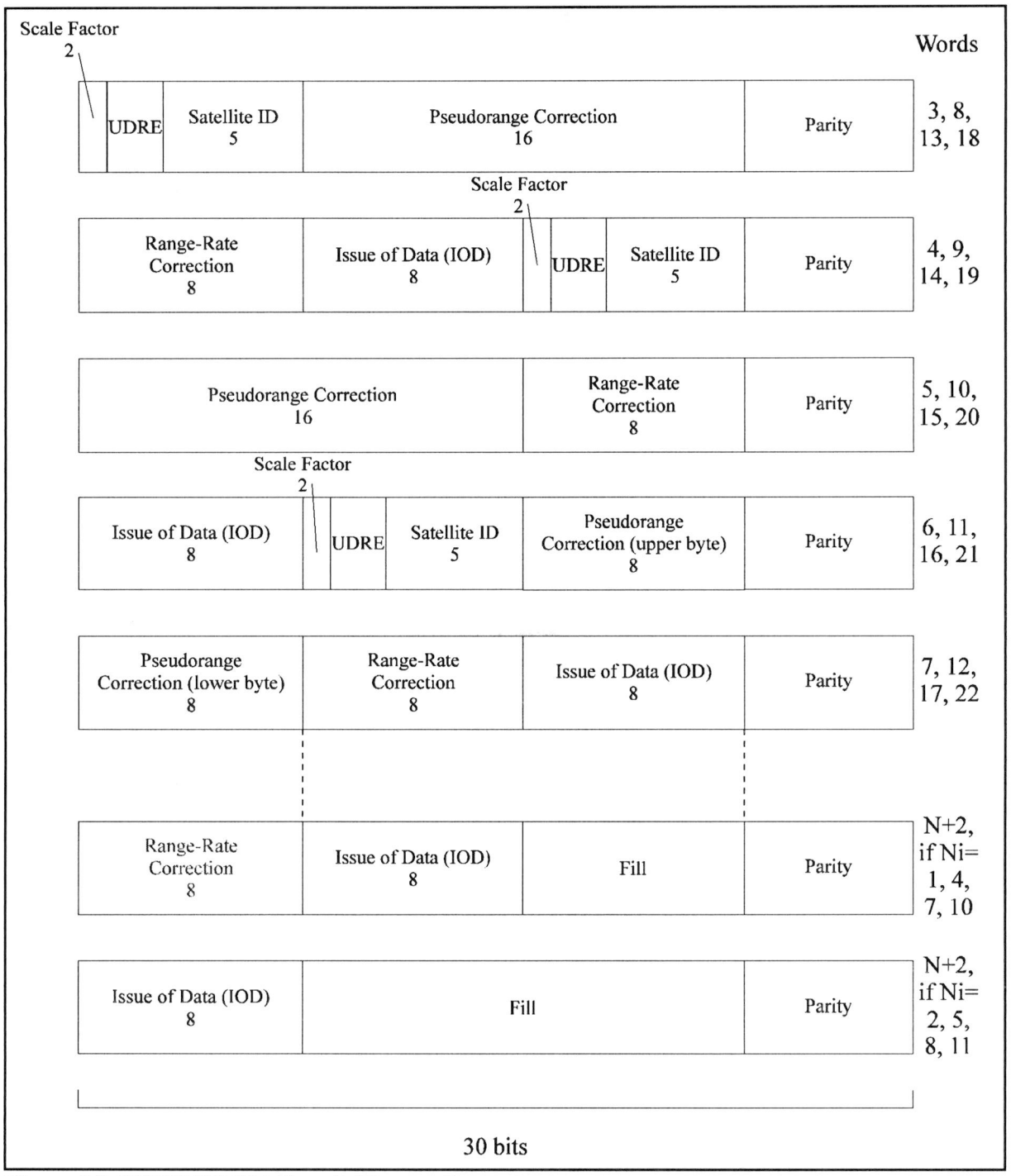

Figure 5.2 RTCM SC-104 Type 1 Message Format

Table 5.3 Contents of a RTCM SC-104 Type 1 Message

parameter	no. of bits	scale factor and units	range
scale factor	1	[5]	2 states
UDRE	2	[6]	4 states
Satellite ID	5	1	1-32[4]
$PRC(t_0)$[1]	16	0.02 or 0.32m	±655.34 or ±10485.44 m[2]
RRC[1]	8	0.002 or 0.032m/s	±0.254 or ±4.064 m/s[3]
Issue of Data	8	See ICD-GPS-200 [1]	
	$40 \times N_s$		
Fill	$8 \times [N_s \bmod 3]$	bits	0, 8, or 16
Parity	$N \times 6$	See ICD-GPS-200 [1]	

1) 2's complement

2) Binary 1000 0000 0000 0000 indicates a problem and the User Equipment should immediately stop using this satellite

3) Binary 1000 0000 indicates a problem and the User Equipment should immediately stop using this satellite

4) Satellite number 32 is indicated with all zeros (00000)

5) 0: Scale factor for pseudorange correction is 0.02 meter and for range rate correction is 0.002 meter/second

1: Scale factor for pseudorange correction is 0.32 meter and for range rate correction is 0.032 meter/second

6) 00: ≤ 1 meter

01: > 1 meter and ≤ 4 meters

10: > 4 meters and ≤ 8 meters

11: > 8 meters

N_s Number of satellite corrections contained in message

N Number of words in message containing data. Message length = N+2 words

The Type 1 Message contains data for all satellites in view of the reference station (N(s)). Since 40 bits are required for the corrections from each satellite, there will not always be an exact integer number of words required. There will be messages that require 8 or 16 bits of fill to finish the frame. The fill will be alternating 1's and 0's so as not to be confused with the "preamble" synchronization code. Each word has one of five formats unless it is the last word in the message. If N(s) is not a multiple of 3, the last word has one of two formats, containing either 8 or 16 fill bits.

The pseudorange correction $PRC(t_0)$ will diverge from the proper value as it "grows old". Because of this characteristic, it will be updated and transmitted as often as possible. The User Equipment should update the corrections accordingly.

The range rate correction (RRC) is designed to compensate for the predicted rate of change of the pseudorange correction. This is an attempt to "extend the life" of the pseudorange correction as it "grows old". The RRC can also be used to correct the user receiver's velocity.

The Issue of Data (IOD) is included in the message so that the User Equipment may compare it with the IOD of the GPS navigation data being used. The IOD is the key that ensures that the User Equipment calculations and reference station corrections are based on the same set of broadcast orbital and clock parameters. If they don't agree, it is the responsibility of the differential User Equipment to take the appropriate actions to acquire parameters that match the ones in use at the reference station. This can be done two ways: test the present IOD for a match to the IOD in a Type 1 or Type 2 messages, or acquire another navigation data message from the appropriate satellite. In general, the reference station attempts to use the present navigation data being broadcast by a satellite. Unless there is a major problem with the navigation data, the Type 1 Message will begin using new navigation data within a few minutes of a change.

Message Type 1 is the most important message of the RTCM recommended standards. For the contents of the other types of messages, see reference [12].

6. Differential GNSS Standards

6.1 Introduction

In chapter 5 of this report the RTCM recommended standards have been discussed. These standards only apply to differential GPS. Similar standards are under development at the Russian Institute of Radionavigation and Time (RIRT) in the CIS [18].

As the integrated use of GPS and GLONASS is becoming more and more important, a differential standard supporting both systems has to be developed. Both systems have some differences which have to be taken into account when creating a combined standard. Therefore, this chapter starts with a section on the principles of developing a differential GPS/GLONASS standard (section 6.2).

As the RTCM standard is widely accepted, most of the investigations carried out by the CIS and Western authorities are based on adapting the RTCM standard. In the CIS, a standard supporting the differential use of both GPS and GLONASS has been developed by the RIRT [18, 19]. In the USA, the RTCM SC-104 also came up with a proposal on expanding the RTCM DGPS recommended standards with messages supporting DGLONASS [20]. Both standards will be discussed briefly (sections 6.3 and 6.4).

6.2 A combined differential GPS and GLONASS standard

6.2.1 Differences in the contents of the GLONASS and GPS navigational messages

Most investigations carried out in the CIS and Western countries concerning a combined GLONASS/GPS differential standard are based on changing and enlarging the RTCM DGPS standard. Developing a combined differential GPS/GLONASS standard requires knowledge of the contents (and more important the differences in their contents) of the navigation

messages. In Appendix A, the GPS and GLONASS navigation message stuctures are discussed. From this appendix the following major differences can be extracted:

1. GLONASS: Transmission of the time mark by a 15-digit code
   GPS: Transmission of the Z-count and numbering of the Issue of Data (IOD)
2. GLONASS: Ephemeris in Earth-Centered-Earth-Fixed (ECEF) coordinates
   GPS: Ephemeris in modified Kepler parameters
3. GLONASS: There are no ionospheric parameters included in the messages
   GPS: Ionospheric correction parameters

6.2.2 Main principles of developing a DGNSS standard

Due to the differences in GLONASS and GPS it is not possible to take the RTCM standard and apply them to the differential use of GLONASS. Some changes have to be made. Moreover, a DGNSS standard should cover the integrated use of both navigation systems as well as the independent use of GLONASS and GPS.

Message type identification

Identification of differential messages for GPS and GLONASS can be done in two different ways:

a. Each message type supporting GLONASS should be given its own message number. This is the approach followed in the proposal of the RTCM.
b. Each message type which is the same for GLONASS and GPS should be given the same message number. To distinguish GPS and GLONASS differential messages, one bit has to be included as a kind of system identification: e.g. '1' indicating that the message is of the GLONASS type, '0' indicating that the message is of the GPS type. The provision of one bit for this purpose will give no problem in the GLONASS message frames. As the differential messages already have been defined, a slight change has to be made: the one bit required can be borrowed from the "Station Identificator", for which 10 bits are allocated. There still will remain 9 bits to indicate the reference stations, which should be sufficient (the number of reference stations is

not likely to exceed 512). This approach has been followed in the standards proposed by the RIRT.

New message types

In the combined differential GPS/GLONASS standard a number of message types should be reserved for new types of messages (GPS or GLONASS).

Contents of the messages

The contents of the differential messages should be coordinated with the contents of the GNSS navigational messages.

Message format of the DGLONASS corrections

There are two alternative formats in which the GLONASS differential messages can be transmitted:

- A format comparable to the GLONASS navigation message format.
- A format comparable to the GPS navigation message format. This format is used in the RTCM DGPS standards

6.3 The RIRT DGNSS proposal

In the CIS the RIRT has developed a DGNSS proposal [18, 19]. In this proposal the GPS as well as the GLONASS format is supported. The DGPS messages shall be transmitted in the format as recommended by the RTCM standard. The DGLONASS messages are transmitted in the format as applied in GLONASS [4]: a message consisting of a line comprising 100 bits transmitted during 2 seconds and having the last 15 bits used for the time mark (excluding the cases when the users need the lines shortened to the maximum possible extent and when the time mark is eliminated and the initial timing code is transferred into the first line and accommodated in the reserve field). The DGNSS standards developed by the RIRT are based on enlarging the RTCM DGPS standard version 2.0.

Any type of DGLONASS message shall start with the standard line which is equivalent to the two standard lines from the RTCM standard (table 6.1, figure 6.1).

Table 6.1 Contents of the header of a message in the RIRT proposal

Parameter	No. of bits	Scale Factor and Units	Range
Null Character, 0	1		
Line Number, m	4	1 line	0-15
GNSS Identifier, Π_{00} [1]	1		2 states
Message Type, Π_{01}	6	1	0-63
Reference Station Identifier, Π_{02}	10	1	0-1023
Time Numbering of Corrections, Δt_n [2]	12	1 s	0-±34,12 min
Number of Message Lines, n_c	5	1 line	0-31
Reference Station Working Ability, Π_{03}	3	[4]	8 states
Error of Coordinate Referencing, Π_{04}	3	[5]	8 states
Availability of Time Referencing, Π_{05} [3]	1		2 states
Reserve Field Bits, R	31		
Hamming Code, Hc	8		

[1] 0 ≙ GLONASS, 1 ≙ GPS (or other systems)

[2] MSB is a sign bit

[3] 0 ≙ reference station time is not referenced to GLONASS system time, 1≙ reference station time is referenced to GLONASS system time

[4]
111 : Reference Station is not working
110 : See message type 16-G [19]
101 : delay > 96 s
100 : delay < 96 s
011 : delay < 48 s
010 : delay < 24 s
001 : delay < 18 s
000 : delay < 12 s

[5]
111 : No reference
110 : error of referencing < 15 m
101 : error < 10 m
100 : error < 5 m
011 : error < 2 m
010 : error < 0.5 m
001 : error < 10 cm
000 : error ≤ 2 cm

The header of each message will consist of a *Null Character, 0* (1 bit), *Line Number, m* (4 bits), a *Hamming Code, Hc* (8 bits) and the *Time Mark, TM* (15 bits) like the GLONASS navigation messages. *GNSS Identifier,* Π_{00} (1 bit) indicates if the differential message is intended for GLONASS users or users of other systems. The type of messages transmitted is indicated by *Message Type,* Π_{01} (5 bits). In table 6.2, the message types supporting differential GLONASS are summarized. *Reference Station Identifier,* Π_{02} (10 bits) identifies the reference station. *Time Numbering of Corrections,* Δt_n (12 bits) is part of the time referencing of the message parameters. As the length of the message depends on the number of satellites in view, the parameter *Number of Message Lines,* n_c (5 bits) is provided. The *Reference Station Working Ability,* Π_{03} (3 bits) indicates the status of the reference station. An error in the coordinate referencing of the reference station is indicated by the *Error of Coordinate Referencing,* Π_{04} (3 bits). *Availability of Time Referencing,* Π_{05} (1 bit) indicates if the reference station time scale is referenced to the GLONASS system time. Each header consists of *Reserve Field Bits, R* (31 bits). When a selective availability mode (specified by a departmental user) is being realized a respective code is transmitted in this reserve field zone.

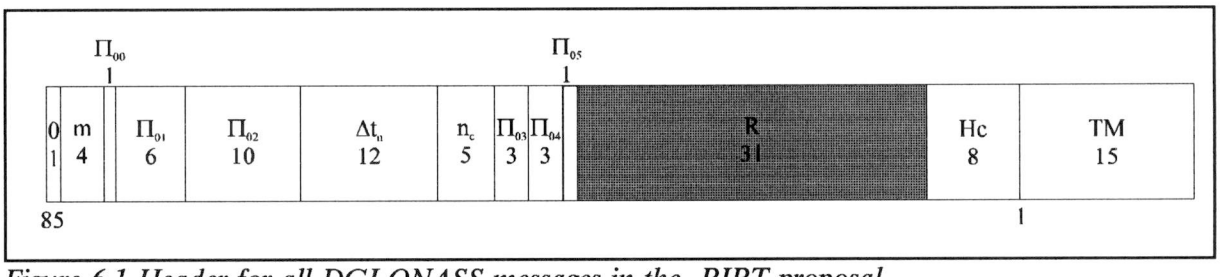

Figure 6.1 Header for all DGLONASS messages in the RIRT proposal

In table 6.2 the message types supporting DGLONASS in the RIRT proposal are summarized. The contents of the message types 1-G through 17-G (with the exception of 6-G and 13-G) are somewhat different from the message types of the RTCM message types supporting DGPS. Message Type 3-G consists of Reference Station Parameters (just like Message Type 3 of the RTCM standards) but also information concerning the offset of the system times (set by the Russian State Time and Frequency (RSTF) and the USNO). The RIRT also proposed some new messages not implemented in the DGPS standard. These are: "GLONASS Differential Corrections for Pseudorange Changing Rates" (18-G), "GLONASS High-Precision Delta Differential Corrections" (19-G), "Working Rules of the Reference Station" (20-G) and "Data for Aircraft Landing on Non-equipped Airfields" (21-G).

Table 6.2 Message Types in RIRT DGNSS proposal

Message Type	Title
1-G	Differential GLONASS Corrections
2-G	Delta Differential GLONASS Corrections
3-G	Reference Station Parameters+ difference system times set by RSTF and USNO
4-G	Surveying
5-G	Constellation Health
6-G	Null Frame
7-G	Beacon Almanacs
8-G	Pseudolite Almanacs
9-G	Partial Satellite Set Differential Corrections GLONASS
10-G	P-Code Differential Corrections GLONASS
11-G	C/A-Code L1, L2 Delta Corrections
12-G	Pseudolite Station Parameters
13-G	Ground Transmitter Parameters
14-G	Surveying Auxiliary Message
15-G	Ionosphere (Troposphere) Message
16-G	Special Message
17-G	Ephemeris Almanac
18-G	GLONASS Differential Corrections for Pseudorange Changing Rates
19-G	GLONASS High-Precision Delta Differential Corrections
20-G	Working Rules of the Reference Station
21-G	Data for Aircraft Landing on Non-Equipped Airfields

As an example message type 1-G will be described briefly. Message Type 1-G is the GLONASS counterpart of Message Type 1 of the RTCM SC-104 recommended standards (table 6.3) This message type provides the pseudorange corrections Δr and the pseudorange correction rates $\Delta r'$. Message Type 1-G also contains information indicating whether other message types (e.g. 2-G, 10-G , 11-g and 17-G) are to be used by the user or not. The information will be transmitted for all satellites in view. One line (as indicated in figure 6.2) contains the information concerning 2 satellites (1 satellite ≙ 36 bits, 2 spare bits included). If 10 satellites are in view, the message consists of 6 lines (1 for the header and 5 for the Differential Pseudorange Corrections).

Message type 1-G gives the pseudorange corrections $\Delta r(t)$ at moment t:

$$\Delta r(t) = \Delta r(t_b + \Delta t_n) + \Delta r' [t - (t_b + \Delta t_n)] \tag{6.1}$$

where $t_b + \Delta t_n$ the time moment for which the pseudorange correction transmitted in Message Type 1-G is valid, Δt_n is the time numbering of the corrections transmitted in the header, t_b is the time reference of the ephemeris and $\Delta r'$ is the pseudorange correction rate. The pseudorange measured by the user, r(t), is corrected as follows:

$$r_k(t) = r(t) + \Delta r(t) \tag{6.2}$$

$r_k(t)$ is the corrected pseudorange.

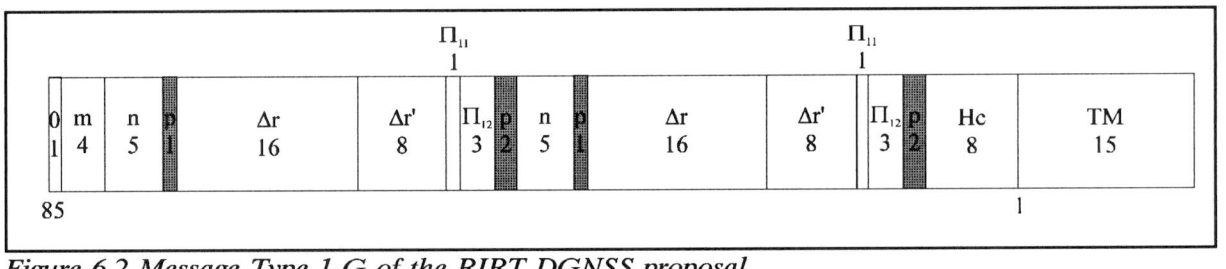

Figure 6.2 Message Type 1-G of the RIRT DGNSS proposal

In the GLONASS navigation message the parameter Π_2 is transmitted and is received by the user and the reference station (Appendix A). This parameter is repeated in message type 1-G (parameter Π_{11}). The parameter Π_2 received by the user should equal Π_{11}. If not, the user should use (next to message type 1-G) also message type 2-G.

Table 6.3 Contents of Message Type 1-G

Parameter	No. of bits	Scale Factor and Unit	Range
Null Character, 0	1		
Line Number, m	4	1 line	0-15
Satellite Number, n	5	1	0-23
Scale Factor, p [1)]	1		2 states
Pseudorange Correction, Δr [2)]	16	0.02m or 0.32 m	± 655.36 m or ± 10483.76 m
Range Rate Correction, $\Delta r'$ [2)]	8	0.002 m/s or 0.032 m/s	± 0.256 m/s or ± 4.096 m/s
Parity of the ephemeris data and time-and-frequency corrections, Π_{11} [3)]	1		2 states
Message type changing, Π_{12} [4)]	3		4 states
Reserve field bits, R	2		
Satellite Number, n	5	1	0-23
Scale Factor, p	1		2 states
Pseudorange Correction, Δr [2)]	16	0.02 m or 0.32 m	± 655.36 m or ± 10483.76 m
Range Rate Correction, $\Delta r'$ [2)]	8	0.002 m/s or 0.032 m/s	± 0.256 m/s or ± 4.096 m/s
Parity of the ephemeris data and time-and-frequency corrections, Π_{11} [3)]	1		2 states
Message type changing, Π_{12} [4)]	3		4 states
Reserve field bits, R	2		
Hamming Code, Hc	8		

1) 0: Δr = 0.02 m and $\Delta r'$ = 0.002 m/s; 1: Δr = 0.32 m and $\Delta r'$ = 0.032 m/s

2) MSB ≙ sign bit; 0 indicates '+', 1 indicates '-'

3) 0 if Π_2 in GLONASS message is 0; 1 if Π_2 is 1

4) 00 : 1-G; 01 : 10-G; 10 : 11-G; 11 : 17-G; MSB of Π_{12} is spare

6.4 Differential GLONASS messages in the RTCM SC-104 standards

In Version 2.1 of the RTCM DGPS standards, SC-104 stated [12, p.1-8]:

A differential GLONASS implementation for both the code and carrier phase is obviously both useful and feasible. It is the intent of this committee to issue DGLONASS standards in the near future.

In September 1994 the message structure for differential GLONASS corrections was discussed by the committee [20]. Attention in the meeting was focused on the issue of making sure that a dual GPS/GLONASS radiobeacon system would be able to provide information that clearly applies to one system or the other. In particular the header contains information on system health, so it was deemed important that the message must be system-specific. This led to the recommendation of separate GPS and GLONASS message types for station location, null frames, radiobeacon almanac, and text/ASCII messages. As a result of the discussions, the committee came up with a proposed set of differential GLONASS messages. These proposed messages will be incorporated in the next version of the RTCM SC-104 standard on differential GNSS, Version 2.2. The messages will be designated as "tentative" until some experience is gained in the field to ensure that they are adequate. In the following an overview of the proposal will be given.

Proposal overview

Concerning the differential GLONASS standard the following general objectives and assumptions were made:

1. Maximize commonality with DGPS Standard
2. Minimize new messages
3. Minimize data link requirements

All messages will be preceded with a two word header.

First word:

- 8 bit preamble: to be defined
- 6 bit message type: RTCM SC-104 Version 2.1

- 10 bit station ID: RTCM SC-104 Version 2.1
- 6 bit parity: RTCM SC-104 Version 2.1

Second word:

- RTCM SC-104 Version 2.1

The DGLONASS messages will be designated by new identification numbers. The DGLONASS identifiers will be 31, 32, 33, 34, 35 and 36. These messages correspond to the DGPS messages 1, 3, 5, 6, 9 and 16.

Message Type 31

Message Type 31 is a message describing the main corrections to be issued by a reference station. It is identical to Type 1, except that the 8-bit IOD is replaced by a 1-bit spare followed by a 7-bit T_b indicator, where T_b identifies the ephemeris message (Appendix A). Message Type 31 is displayed in figure 6.3.

Message Type 32

Message Type 32 is the GLONASS counterpart of the Reference Station Parameters Message Type 3. It is identical in form, except that the coordinates are in the Russian SGS-90[1] datum, rather than WGS-84, unless specified to be a third system by the service provider (the same comment applies to Message Type 3). Dual system stations will issue both Types 3 and 32.

Message Type 33

Message Type 33 is the GLONASS counterpart of the Constellation Health Message Type 5. Its primary purpose is to provide a mechanism for enabling a user to make use of a satellite which has been declared unhealthy by the satellite control segment by overriding its health indication. It also provides real-time specific information on the satellite performance not available from any other source. It is identical in form and content to Message Type 5, with one exception, namely that bit #7 will be declared a spare bit, since it would always be set to zero if it took on the same meaning as in a Type 5. For both Types 5 and 33, the first (reserved) bit of the message will be used to accommodate augmented GPS and GLONASS systems.

1 In the literature, the follow up on the SGS-85 coordinate reference system is indicated as SGS-90 or PZ-90.

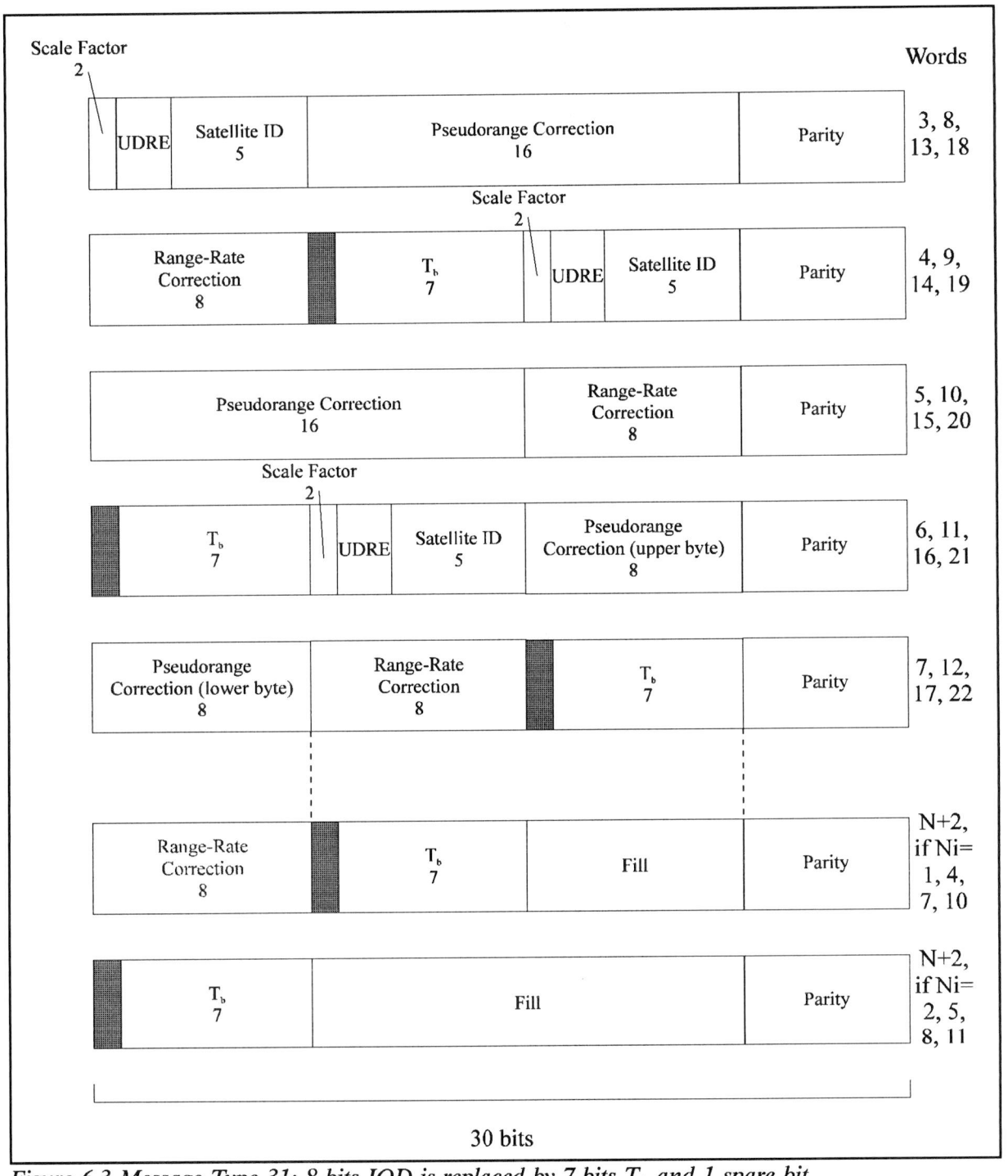

Figure 6.3 Message Type 31: 8 bits IOD is replaced by 7 bits T_b and 1 spare bit

Message Type 34

Message Type 34 is roughly the GLONASS counterpart of the Message Type 9 (Partial Satellite Set Differential Corrections), but also covers the function of Type 6 (Null Frame). It is identical in form and content to the Message Type 31, with two exceptions. One exception is that, like Message Type 9, there is no requirement to include the complete set of satellites in view in the message. The second exception is that if the number of data words N=0 or 1, the message is to be treated as a filler word, exactly as a Message Type 6. Note that N=0 or 1 can not indicate a valid number of satellites, because even if only one satellite is covered in the message, N must be set to 2. The reason for distinguishing Message Types 6 and 34 is to allow for the possibility that a dual-use system would have different system health information for the GPS and GLONASS.

Message Type 35

Message Type 35 is the GLONASS counterpart of the Radiobeacon Almanac Message Type 7. It is identical in form, except that it only includes beacon broadcast stations that support GLONASS. The reason for two message types here is to ensure there is no confusion caused to a GPS-only or GLONASS-only user who is listening to a dual-use broadcast. If only one message type were used, there would be no way of distinguishing whether a radiobeacon supported GPS, GLONASS or both.

Message Type 36

Message Type 36 is the GLONASS counterpart of Type 16 (Special Message). It is completely defined for 7-bit ASCII characters, because they are standardized internationally. However, the 8th bit can be set to 1, in order to support national broadcasts. The Russians, for example, plan to issue messages in Russian, using a set of definitions of ASCII characters 128-255 which support the Russian alphabet. It is up to the service provider to inform the users of the system of the meaning of the ASCII characters 128-255.

Other message types were discussed, notably the constellation message 17 and the real-time kinematic message types 18-21, but it was decided not to table any action on these until there has been a need expressed by the membership for their usage.

The differential GLONASS messages are summarized in table 6.4.

Table 6.4. The proposed differential GLONASS messages

Message Type	Content	Comment
31	DGLONASS Corrections	• As defined in RTCM SC-104 Ver. 2.1 • Replace IOD by T_b (7 bits needed, 8 available) • Satellite ID is GLONASS slot number
32	Reference Station Parameters	• As defined in RTCM SC-104 Ver. 2.1 • Default datum is SGS-90
33	Constellation Health	• As defined in RTCM SC-104 Ver. 2.1 • Only one GLONASS health bit used vs. 3 for GPS
34	Null frame	• As defined in RTCM SC-104 Ver. 2.1
35	Radiobeacon Almanac	• As defined in RTCM SC-104 Ver. 2.1 • Lat/Lon accuracy not affected by WGS-84 vs SGS-90 differences
36	Special Message	• As defined in RTCM SC-104 Ver. 2.1 • Provides GLONASS information • Transmits alternatively in Russian and English

7. The ionospheric problem

7.1 Introduction

The time delay introduced by the ionosphere is the largest source of accuracy degradation of GLONASS (and GPS without SA). In this chapter attention is paid to the ionospheric influence. Section 7.2 describes the general characteristics of the ionosphere: in this section the ionospheric production processes and the layer structure are discussed.

A radio signal which penetrates the ionosphere is modified by the medium due to the presence of electrons and the earth's magnetic field. The effects of the ionosphere are numerous and complex. An important effect is the ionospheric time delay. A modulated radio signal passing through the ionosphere will be slowed down by an amount that is directly proportional to the total (integrated) number of electrons (TEC) along the radio propagation path. In section 7.3 the TEC and its influence on signal propagation will be discussed.

7.2 The ionosphere

This section is an introduction to the ionospheric properties and follows from reference [21]. In this section a general description of the ionospheric properties is given. For an extensive and detailed discussion of all possible kinds of irregularities encountered in the ionospheric properties, see reference [21].

7.2.1 Ionospheric production processes

The ionosphere is the ionized region in the earth's atmosphere extending from about 50 km to roughly 2000 km above the surface. The principal source of ionization in the ionosphere is electromagnetic radiation from the sun extending over the ultra-violet and X-ray portions of the spectrum. Other sources of ionization are important however, such as energetic charged particles of solar and magnetospheric origin and galactic cosmic rays. The ionization rate at

various altitudes depends upon the intensity of the solar radiation as a function of wavelength, and the ionization efficiency of the neutral atmospheric gasses. Since the sun's radiation is progressively absorbed in passing through the atmosphere, its residual ionizing ability depends upon the length of the atmospheric path, and consequently upon the solar zenith angle χ. The maximum ionization rate occurs when the sun is overhead (χ=0), but geographic, diurnal and seasonal variations in the ionization density are found.

The production of free ionization by solar radiation (and charged particles) is counter-balanced by ionization loss processes, principally the collisional recombination of electrons and positive ions, and the attachment of electrons to neutral gas atoms and molecules. It is possible to determine, from physical principles, a reasonably realistic mathematical description of the altitude distribution of ionization, based on estimates of the solar ionizing flux, the vertical distribution of neutral atmospheric constituents and their absorption efficiency, and the solar zenith angle.

In the lowest part of the ionosphere, below about 65 km altitude, the dominant source of ionization is galactic cosmic rays. Consequently the variation of electron density at these altitudes is not dominated by the solar zenith angle dependence.

7.2.2 The ionospheric layer structure

The ionosphere is divided into three layers designated as D, E and F, respectively, in order of increasing altitude (Figure 7.1). Subdivisions of these layers may exist under certain conditions, for example F1 and F2 layers. From the viewpoint of HF propagation, the E and F layers act principally as radio wave reflectors, and permit long range propagation between terrestrial terminals. The D region acts principally as an absorber, causing signal attenuation in the HF range, although VLF and ELF waves are reflected at D-region altitudes. The transition between reflection at D-region altitudes and E-region altitudes occurs in the medium frequency range. The ionosphere is also an important factor in space communications at VHF and higher frequencies, since the signal is modified and degraded to varying degrees in passing through the ionosphere.

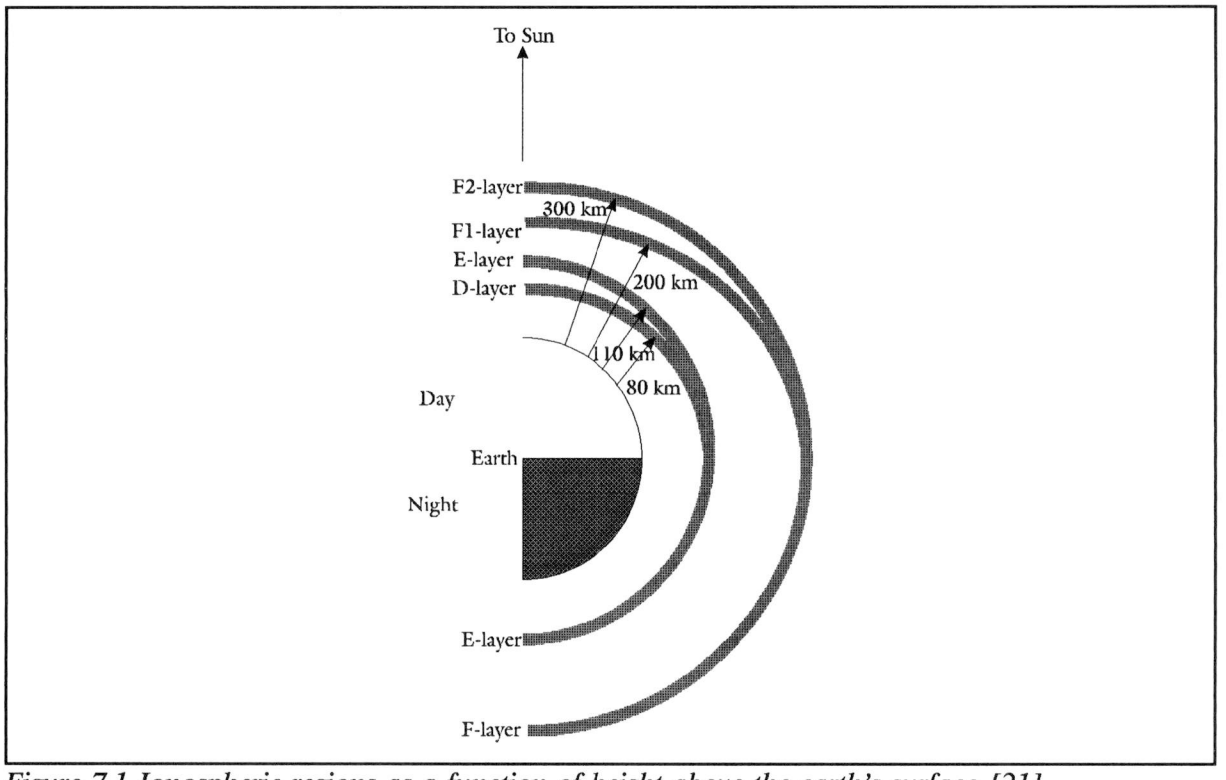

Figure 7.1 Ionospheric regions as a function of height above the earth's surface [21]

D region

The D region spans the approximate altitude range 50 to 90 km with the electron density increasing rapidly with altitude. The D-region electron density exhibits large diurnal variations with maximum density shortly after solar noon, and small values at night. This diurnal variation is greatest in the altitude interval 70 to 90 km, with typical noon values of 10^8 to 10^9 electrons/m^3. There is a pronounced seasonal variation in D-region electron densities with a maximum in summer. In winter, although the solar zenith angle is greater, there often appears anomalously high electron density in the 70 to 90 km range, probably resulting from neutral atmosphere composition changes. The solar-cycle variation in D-region electron density is different at different altitudes. In the 70 to 90 km range, where solar X-rays are the dominant source, ionization is maximum at the peak of the solar cycle. Below 70 km, where production by cosmic rays dominates, maximum densities are found at solar minimum, because of reduced interplanetary scattering of galactic cosmic rays. For undisturbed days following a geomagnetic storm and associated with its recovery phase, the electron density in the 75 to 90 km range is

enhanced in sub-auroral latitudes and mid-latitudes due to precipitation of energetic electrons from the outer radiation belt.

E region

The altitude range from 90 to 130 km constitutes the E region and encompasses the so-called "normal" and "sporadic"-E layers. The former is a regular layer displaying a strong solar zenith angle dependence with maximum density near noon and a seasonal maximum in summer. The altitude of maximum density is about 110 km, with a value of approximately 10^{11} electrons/m^3, corresponding to a maximum plasma frequency[1] of about 3 MHz. At night, only a small residual level of ionization remains in the E region, with typical plasma frequency of 0.4 to 0.6 MHz. The solar cycle dependence exhibits a maximum layer density at solar maximum, with a variation in daytime E-layer plasma frequency of about 30% over the solar cycle at a given location.

F region

The F region extends upward from about 130 km. The lower F region displays a different variation from the upper F region, which has resulted in a further subdivision into F1 and F2 layers, although the vertical electron density profile may display no clear stratification. The distinction between the F1 and F2 layers is not maintained at night.

The F1 layer is the region between 130-210 km altitude, in which the maximum electron density is about $2\times10^{11}/m^3$. The F1 layer has a solar zenith angle dependence which is different from that of the E layer.

The F2 layer is the highest ionospheric layer, and usually exhibits the greatest electron density, which may range typically from $10^{12}/m^3$ in daytime to about $5\times10^{10}/m^3$ at night. The F2 layer is strongly influenced by winds, diffusion and other dynamic effects.

1 The ionosphere is an ionized medium or plasma. The motion of an ion in an electric field can be described by a harmonic motion with an angular frequency ω_p. ω_p is called the angular plasma frequency. If ω_p is divided by 2π, the plasma frequency f_p is obtained.

7.3 Ionospheric effects on earth-space propagation

A radio signal which penetrates the ionosphere is modified by the medium due to the presence of electrons and the earth's magnetic field [22]. Both large scale changes due to the variation of electron density as well as smaller scale irregularities affect the signal. The effects include scintillation (= variations of amplitude, phase, polarization and angle-of-arrival produced when radio waves pass through electron density irregularities in the ionosphere), absorption, variation in the direction of arrival, propagation delay, dispersion, frequency change, and polarization rotation.

A single parameter of the ionization distribution which is very significant in determining ionospheric effects on communication and navigation systems is the integral $\int n_e ds$, which is the integrated or Total Electron Content (TEC) along the ray path from transmitter to receiver. A number of these effects, such as refraction, dispersion and group delay, are in magnitude directly proportional to the TEC; Faraday rotation is also approximately proportional to TEC, with the contributions from different parts of the ray path weighted by the longitudinal component of the magnetic field. Knowledge of the TEC thus enables many important ionospheric effects to be estimated quantitatively. When used without qualification TEC is usually taken to mean the content of a vertical column of unit cross-section, but for practical applications it is generally the content along a slant path from the receiver to the satellite which. As in GLONASS, the accuracy of navigation is determined to a great extend by the ionospheric time delay, only this effect will be described. For all other aforementioned effects, see reference [22].

For radiowave propagation along a station-satellite link, the presence of free electrons along the ray path causes the radiowave to travel with a group velocity less than the in-vacuo speed of light, thereby increasing the travel time over that expected from a free space geometry. This retardation suffered by the radiowave is commonly called the "group delay" which affects the accuracy of satellite navigation systems. For high-precision, delay must be compensated for either by prediction techniques or by direct measurement. The problem can nonetheless be solved in real time by exploiting the dispersive effect of the ionosphere by combining the ionospheric effects on several carefully chosen frequencies.

The motion of ions in electric and magnetic fields is described by the magneto-ionic theory [23]. From this theory, when neglecting higher order effects, such as the geomagnetic field and collisions, it can be shown that the ionospheric group delay depends inversely on the square of the frequency used and directly upon the integral of the number of electrons along the ray path.

In the absence of a geomagnetic field and of collisions the refractive index μ of the ionosphere is given by:

$$\mu^2 = 1 - \frac{f_p^2}{f^2} \tag{7.1}$$

where f is the transmission frequency and f_p is the plasma frequency given by:

$$f_p^2 = \frac{Ne^2}{4\pi^2 \epsilon_0 m} = 80.5N \tag{7.2}$$

where N the local electron concentration, ϵ_0 the permittivity of free space (8.85×10^{-12} F/m), e the charge of an electron (1.6×10^{-19} C) and m the mass of an electron (9.1×10^{-31} kg).

For transmission frequencies above 100 MHz $f^2 \gg f_p^2$ and formula 7.1 can be approximated by:

$$\mu \approx 1 - \frac{f_p^2}{2f^2} \tag{7.3}$$

The group velocity v_{gr} of a signal is approximated by:

$$v_{gr} = c_0 \mu = c_0 \left(1 - \frac{f_p^2}{2f^2} \right) \tag{7.4}$$

with c_0 the velocity of light (3×10^8 m/s). The time delay of a signal travelling along a path s extending from a satellite to a receiver is given by:

$$t = \int_0^s \frac{1}{v_{gr}} ds \tag{7.5}$$

Using equation 7.4, the time delay can be written as:

$$t \approx \frac{1}{c_0}\int_0^s ds + \frac{1}{2c_0 f^2}\int_0^s f_p^2 ds \qquad (7.6)$$

For signal propagation along a straight path, the first integral in equation 7.6 is the actual distance R from the satellite to the receiver. If the pseudo distance is defined as $R'=c_0 \times t$, the range error δR (in meters) is given by:

$$\delta R = R' - R = \frac{1}{2f^2}\int_0^s f_p^2 ds = \frac{40.25}{f^2}\int_0^s N ds = \frac{40.25}{f^2}TEC \qquad (7.7)$$

where f is the transmission frequency in Hz and $\int_0^s Nds$ is the integrated electron concentration (TEC) expressed in electrons/m^2 along the slant ray path.

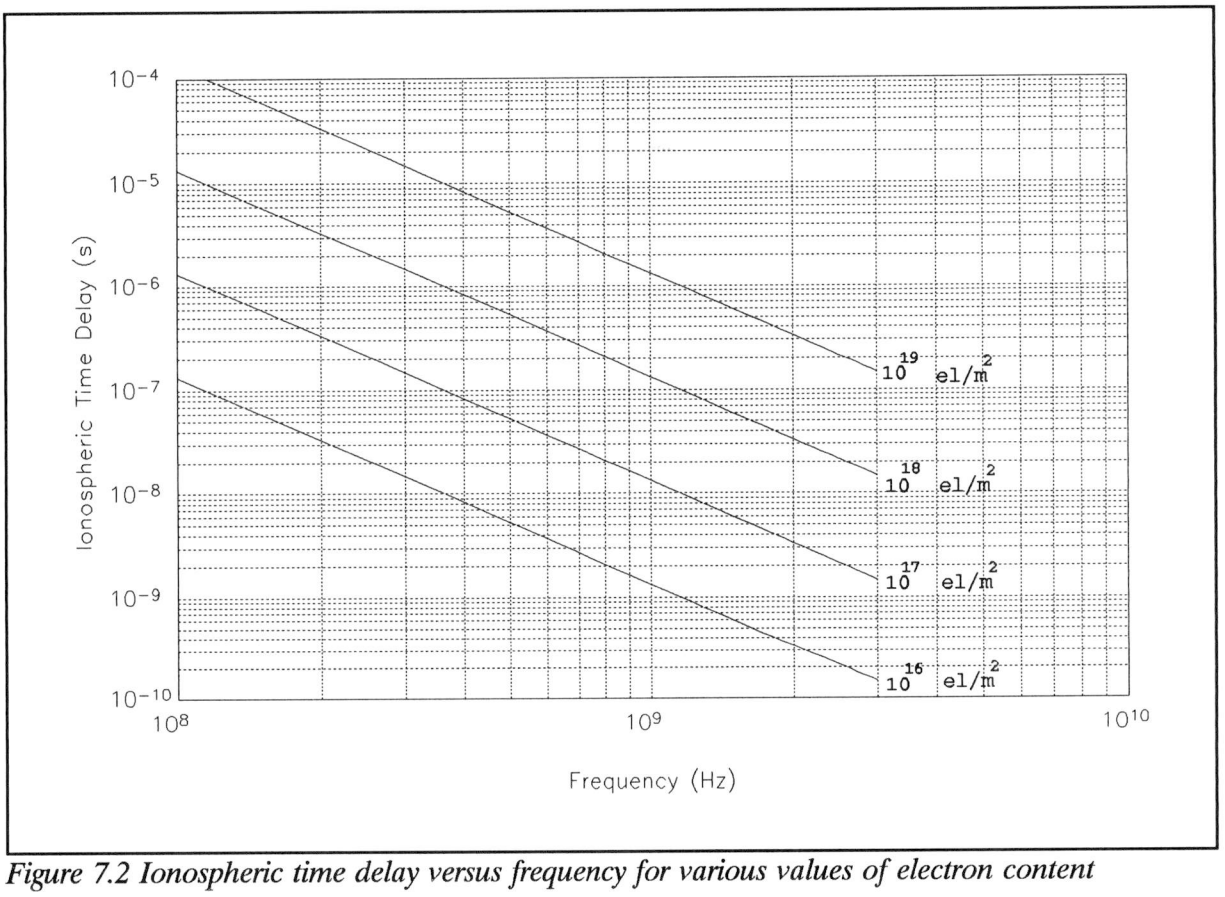

Figure 7.2 Ionospheric time delay versus frequency for various values of electron content

In figure 7.2 the ionospheric time delay ($\Delta\tau=\delta R/c_0$) versus the frequency for several TEC values is displayed. For a band of frequencies around 1600 MHz the signal group delay varies from approximately 0.5 to 500 ns, for TEC from 10^{16} to 10^{19} electrons/m^2.

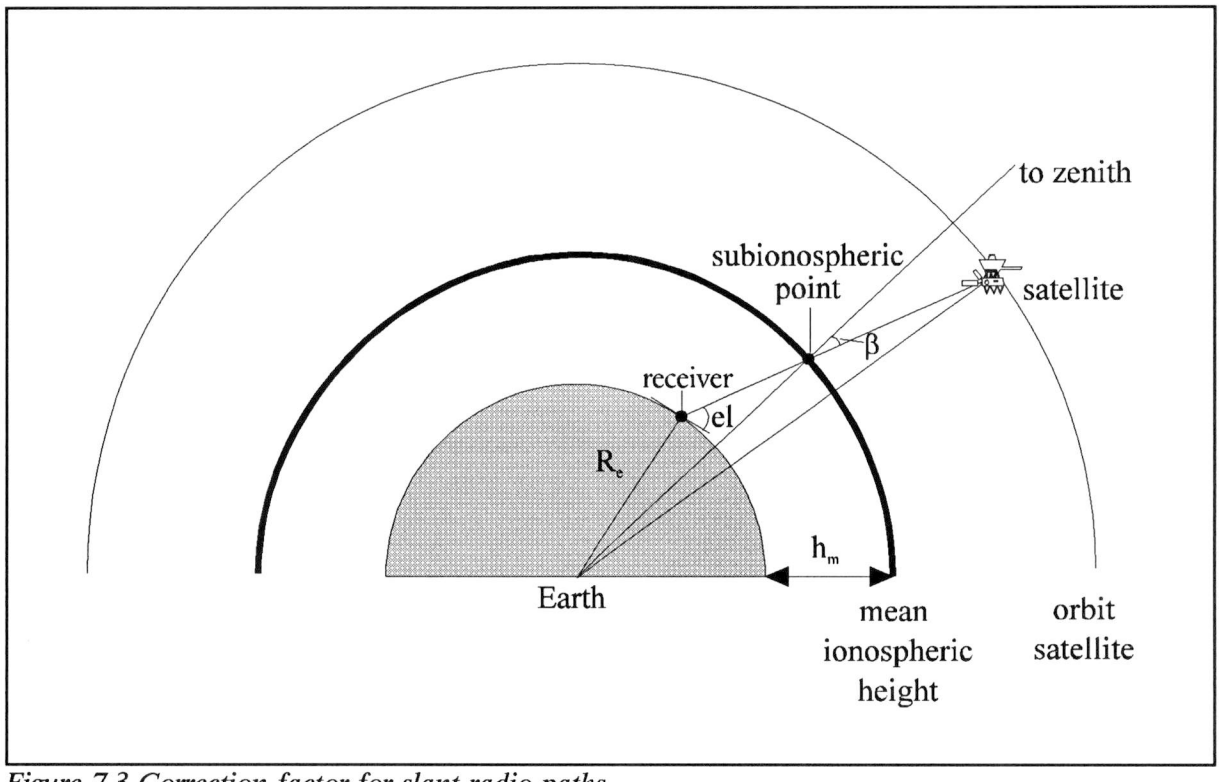

Figure 7.3 Correction factor for slant radio paths

In equation 7.7, the TEC was taken to be the total electron content along a slant path (from satellite to receiver). As already mentioned, the TEC is usually defined as being the total electron content of a vertical column of unit cross-section. This column intersects the subionospheric point (the point of intersection of the transmitted signal and the mean ionospheric height h_m, figure 7.3)[2]. If vertical TEC is assumed, this TEC value has to be corrected to obtain the TEC along the signal propagation path.

The zenith angle β (the angle between the line through subionospheric point to the zenith[3] and the line from the satellite through the subionospheric point) is given by:

---

2 subionospheric point: also known as ionospheric point
mean ionospheric height: also known as height of maximum electron density

3 zenith: point in infinity on the line through the subionospheric point perpendicular to the surface of the earth

$$\beta = \text{asin}\left(\frac{R_e \cos(el)}{R_e + h_m}\right) \tag{7.8}$$

where R_e the earth's radius (km), el the elevation angle (radians or degrees) and h_m the mean ionospheric height (km). Typical mean ionospheric heights range from 300 to 450 km.

The correction factor z for a slant path by which the vertical total electron content has to be multiplied is given by:

$$z = \frac{1}{\cos\beta} \tag{7.9}$$

An ionospheric model from which TEC can be easily obtained is the Bent Ionospheric Model [24]. In chapter 8, this model will be described.

8. The Bent Ionospheric Model

8.1 Introduction

The Bent Ionospheric Model [24] is an empirical world-wide algorithm capable of accurate estimating the electron density profile and the associated delay and directional changes of a wave due to refraction. The model computes the electron density versus height profile from which the range, range rate, and the angular refraction corrections for the wave are obtained as well as the vertical and angular total electron content.

The only required inputs to the model are satellite and station position and time information and a limited amount of solar data. The ionospheric predictions can be improved by use of actual ionospheric observations: measured values of electron content or the critical frequency of the F2 layer (f_0F2) can be incorporated along with the observation station and time information. By applying a weighted mean technique, several measurements from different stations separated in time and space from the time and location at which the ionosphere is to be evaluated can be used.

The updating process is used for predicting ionospheric conditions or refraction corrections after the fact, when observations are available. However, the model's prediction accuracy without update accounts for approximately 75 to 80 percent of the ionosphere which can improve with update to approximately 90 percent. The model, therefore, may be applied for predictions or after the fact calculations. Since the model has been developed on a world-wide basis, predictions are not limited to any particular land mass or segment of the world. The updating technique does, however, require that ionospheric observations are from stations within 2000 km radius of the evaluation site. The model is applicable for determining wave refraction and ionospheric characteristics up to 2000 km in height and for all radio wave frequencies as long as the vertical component is slightly higher than critical frequency.

Built into the model are the combined influences of geographical and geomagnetic effects,

solar activity, local time, and seasonal variations. These combined effects are the results of an extensive investigation of a vast ionospheric data base that included over 50,000 topside soundings, 6,000 satellite measurements of electron density and related f_0F2, and over 400,000 bottomside soundings. The data base, which formed the basis of the model, extended over the period of 1962 to 1969, covering the minimum to the maximum of a solar cycle.

The following description of the model is taken from [24].

8.2 Description of the Bent Ionospheric Model

8.2.1 The ionospheric electron density profile

The electron density profile forms the basis of the Bent Ionospheric Model. From this profile the range, range rate, and the angular refraction corrections for the wave as well as the vertical and angular total electron content are obtained. The electron density is modeled differently in five height layers (figure 8.1). Each layer is described by an electron density function. The five different electron density functions are given by:

$$N = N_m\left(1-\frac{b_2^2}{y_m^2}\right)^2 \quad , \text{for } h_m - y_m \le h < h_m \tag{8.1a}$$

$$N = N_m\left(1-\frac{b_1^2}{y_t^2}\right) \quad , \text{for } h_m \le h < h_0 = h_m + d \tag{8.1b}$$

$$N = N_0 e^{-k_1 a_1} \quad , \text{for } h_0 \le h < h_1 = h_0 + (1012\,\text{km} - h_0)/3 \tag{8.1c}$$

$$N = N_1 e^{-k_2 a_2} \quad , \text{for } h_1 \le h < h_2 = h_1 + (1012\,\text{km} - h_1)/3 \tag{8.1d}$$

$$N = N_2 e^{-k_3 a_3} \quad , \text{for } h_2 \le h \le 2000\,\text{km} \tag{8.1e}$$

where

$$
\begin{aligned}
N_m &= 1.24 \times 10^{10} f_0F2^2 \\
N_0 &= N_m\left(1 - \frac{d^2}{y_t^2}\right) \\
N_1 &= N_0 e^{-k_1(h_1 - h_0)} \\
N_2 &= N_1 e^{-k_2(h_2 - h_1)}
\end{aligned}
\tag{8.2}
$$

N_m, N_0, N_1 and N_2 are the values of the electron densities of the various layers at the starting point and a_1, a_2, a_3 and b_1, b_2 are height increments measured from the starting point of the layers. To determine the electron density profile the following ionospheric parameters are required:

f_0F2	:	critical frequency at vertical incidence of the F2-layer; f_0F2 is the minimum frequency required for a signal to penetrate the F2-layer
h_m	:	height of the maximum electron density
y_t	:	half thickness of the topside parabolic layer
y_m	:	half thickness of the bottomside bi-parabolic layer
d	:	distance above h_m at which the lower exponential layer starts
k_1, k_2, k_3	:	decay constants for the lower, middle and upper section of the exponential topside profile

The factor M(3000)F2 is also a very important ionospheric parameter from which h_m is determined. M(3000)F2 is a numerical factor which, when multiplied by the critical frequency f_0F2, gives the basic MUF (maximum usable frequency) for a distance of 3000 km. The basic MUF is the highest frequency at which a radio wave can propagate between given terminals, on a specified occasion, by ionospheric refraction alone.

Before the values of the above ionospheric parameters can be determined, the ionospheric point (see section 8.2.2) and the modified magnetic dip (see section 8.2.3) must be determined. Figure 8.2 displays the relations between the ionospheric point, the modified magnetic dip (and magnetic field components), electron density profile parameters and range, range rate, angular refraction corrections, the vertical and angular total electron content.

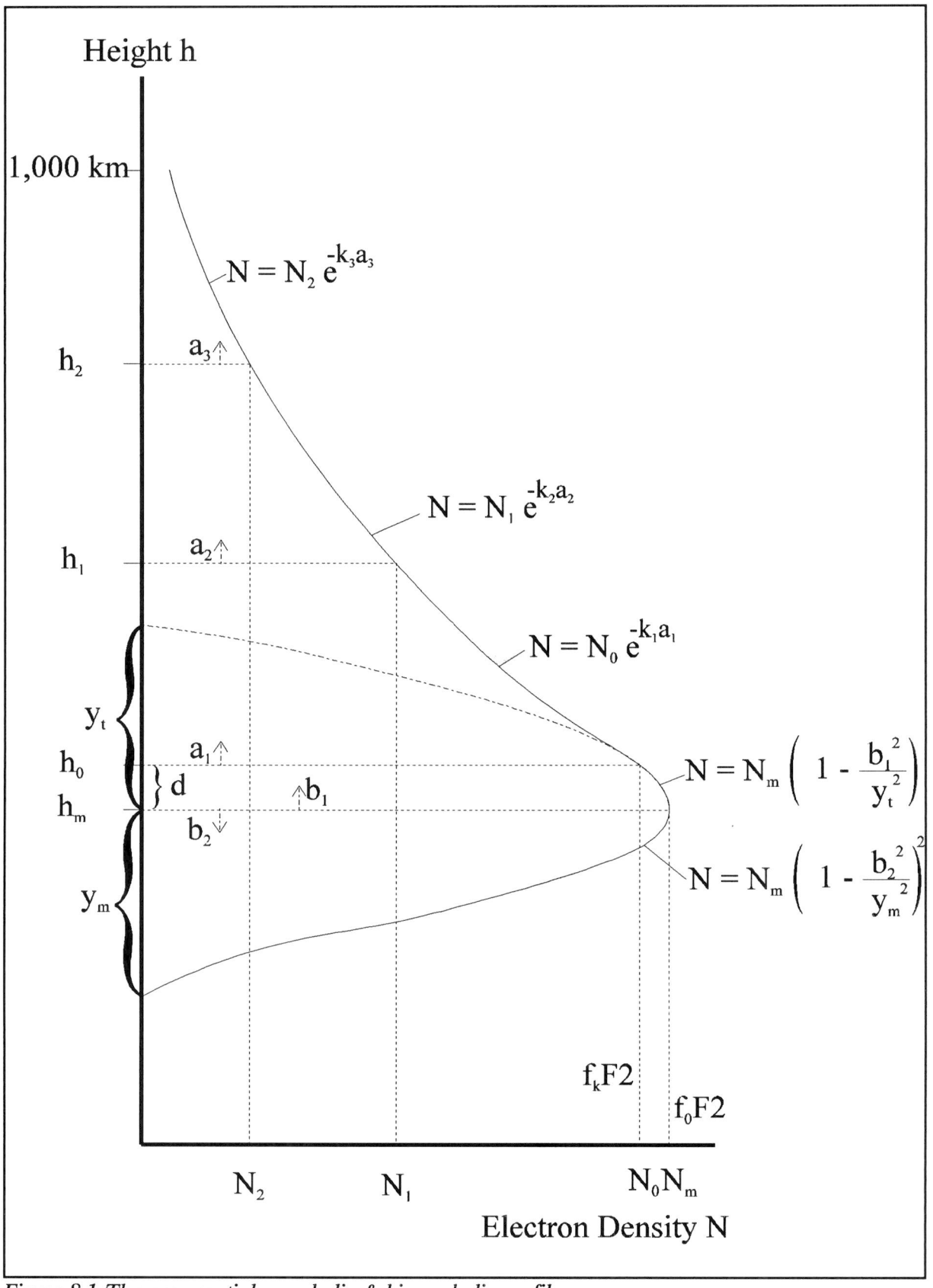

Figure 8.1 The exponential, parabolic & bi-parabolic profile

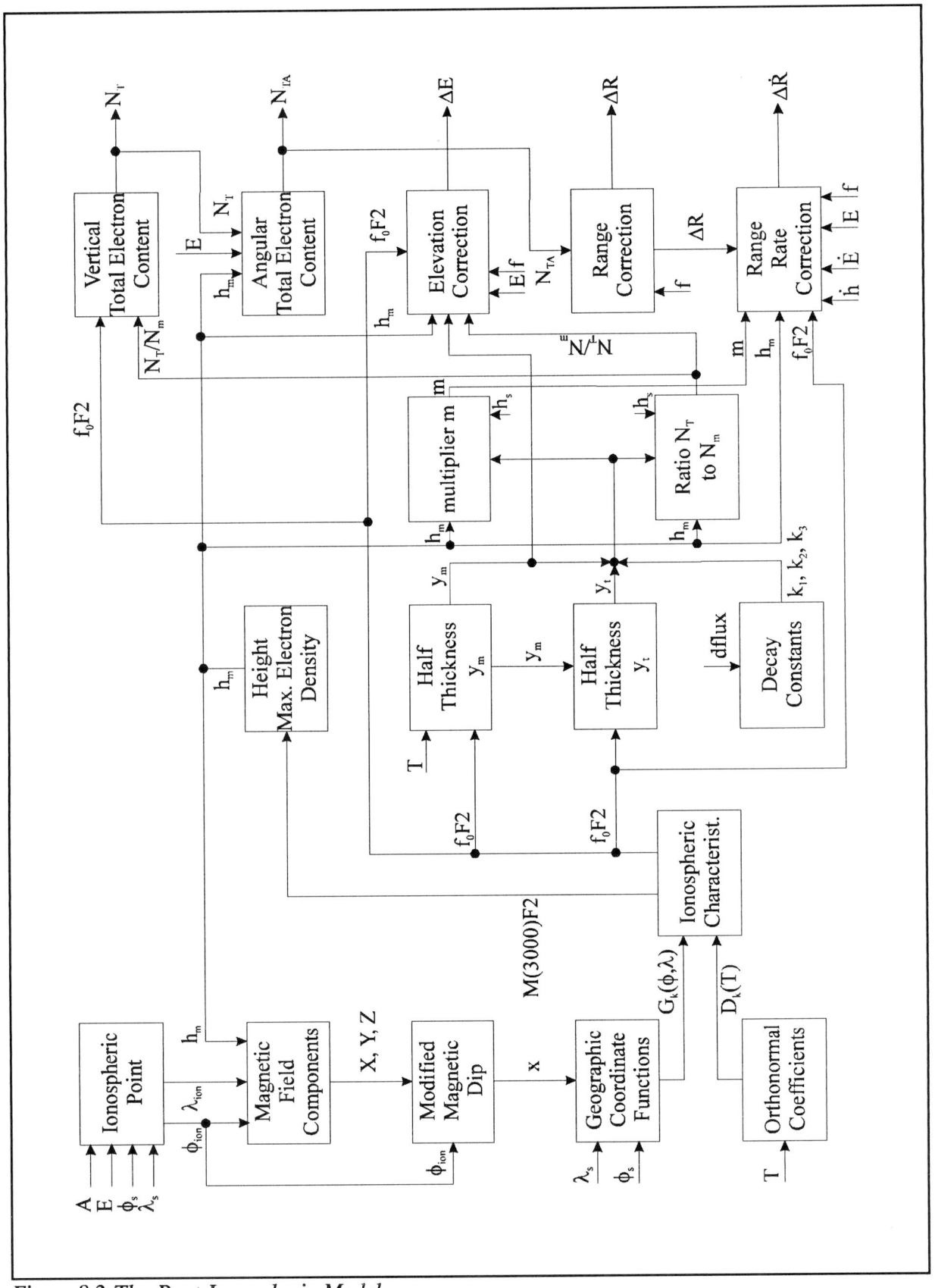

Figure 8.2 The Bent Ionospheric Model

8.2.2 The ionospheric point

The ionospheric point is defined by the latitude ϕ_{ion} and longitude λ_{ion} at which the ray from the station to the satellite passes through the ionosphere. It is calculated from the station latitude ϕ_s, longitude λ_s, the elevation angle E and azimuth A to the satellite. From spherical trigonometry follows (figure 8.3):

$$\begin{aligned} \phi_{ion} &= \arcsin(\sin\phi_s \cos\alpha + \cos\phi_s \sin\alpha \cos A) \\ \lambda_{ion} &= \lambda_s + \arcsin\left(\frac{\sin A \sin\alpha}{\cos\phi_{ion}}\right) \end{aligned} \tag{8.3}$$

where α is the earth central angle between the station and the ionospheric point (figure 8.4):

$$\begin{aligned} \alpha &= \frac{\pi}{2} - E - \beta \\ \beta &= \arcsin\left(\frac{R_e \cos E}{R_e + h_m}\right) \end{aligned} \tag{8.4}$$

β is the zenith angle, R_e is the mean earth radius, and h_m is the height of the ionosphere at the maximum electron density above the surface of the earth.

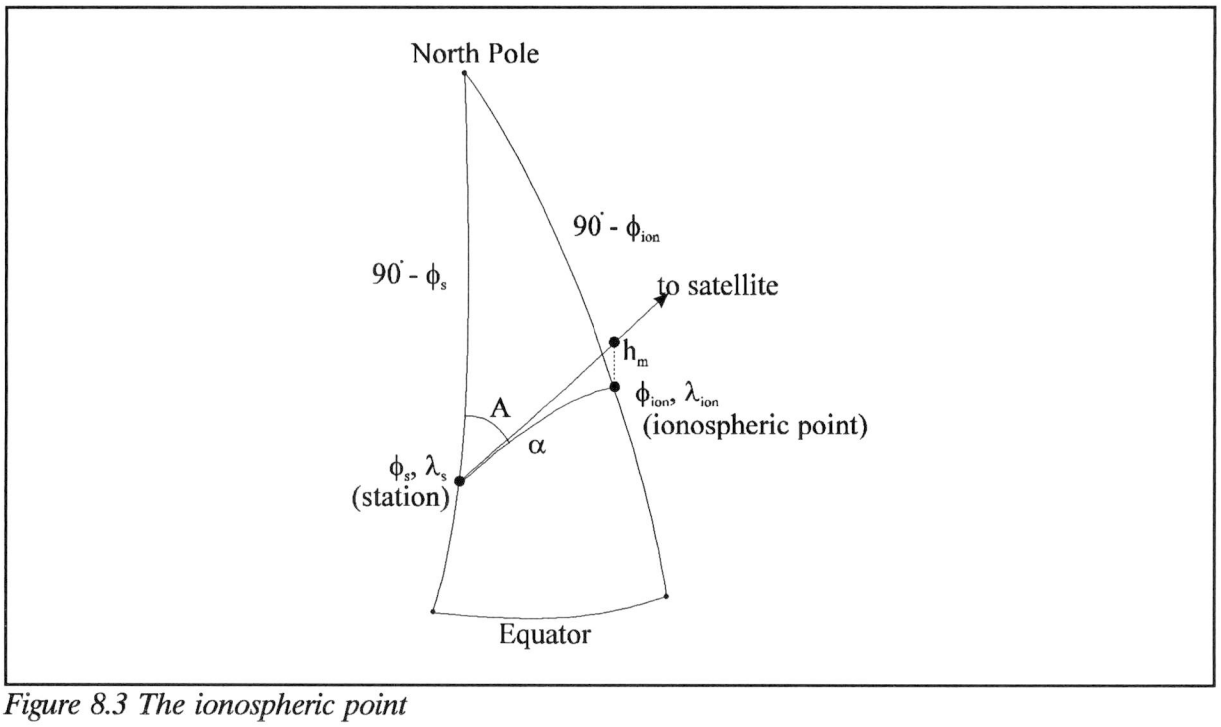

Figure 8.3 The ionospheric point

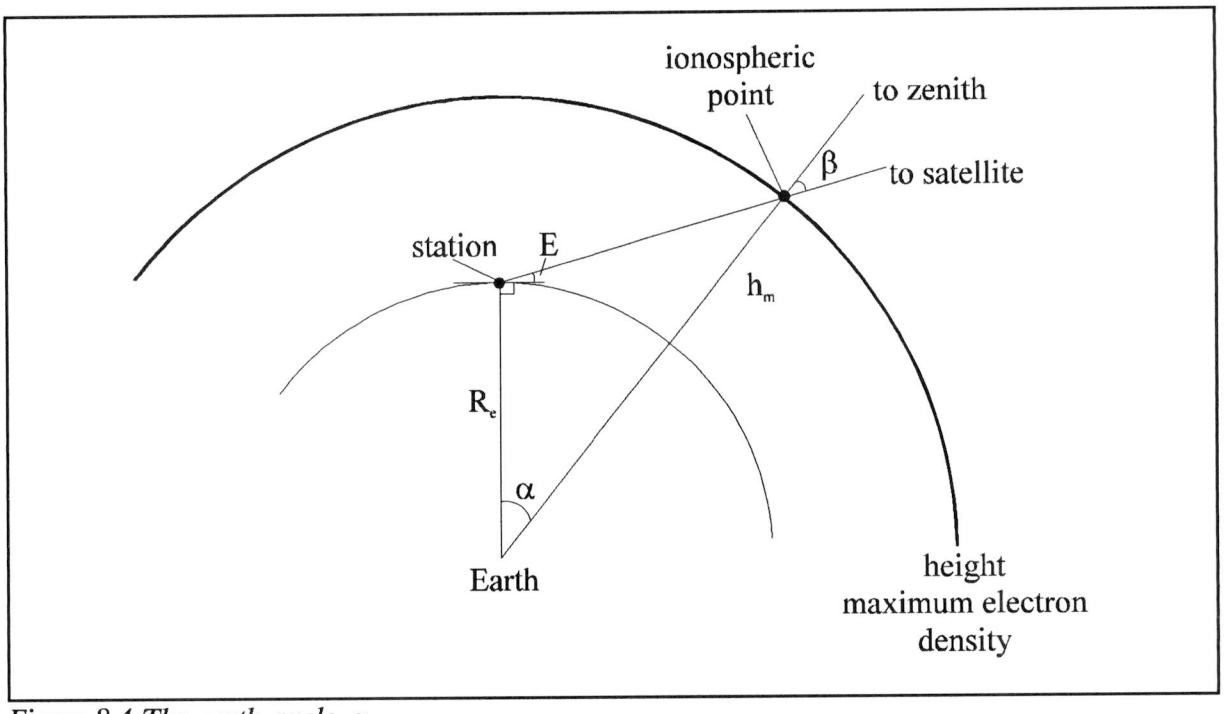

Figure 8.4 The earth angle α

At the ionospheric point the X, Y and Z-components of the earth's magnetic field are determined. These components are required for the calculation of the modified magnetic dip (section 8.2.3).

8.2.3 Modified magnetic dip

The magnetic field has a certain magnitude and direction in each point P of space (figure 8.5). The intensity of the magnetic field at point P is indicated by F and can be specified by its downward vertical component Z and its vector horizontal component H. F can also be specified by H and the angle I by which F dips below the horizontal [23]. This angle I is called the magnetic dip. The direction of H is specified by the angle D between H and the geographic north; D is called the magnetic declination and is reckoned positive if eastward. The northward and eastward components of H are denoted by X, Y, respectively, and

$$\tan D = \frac{X}{Y} \qquad H = \sqrt{X^2 + Y^2}$$
$$X = H\cos D \qquad Y = H\sin D \tag{8.5}$$

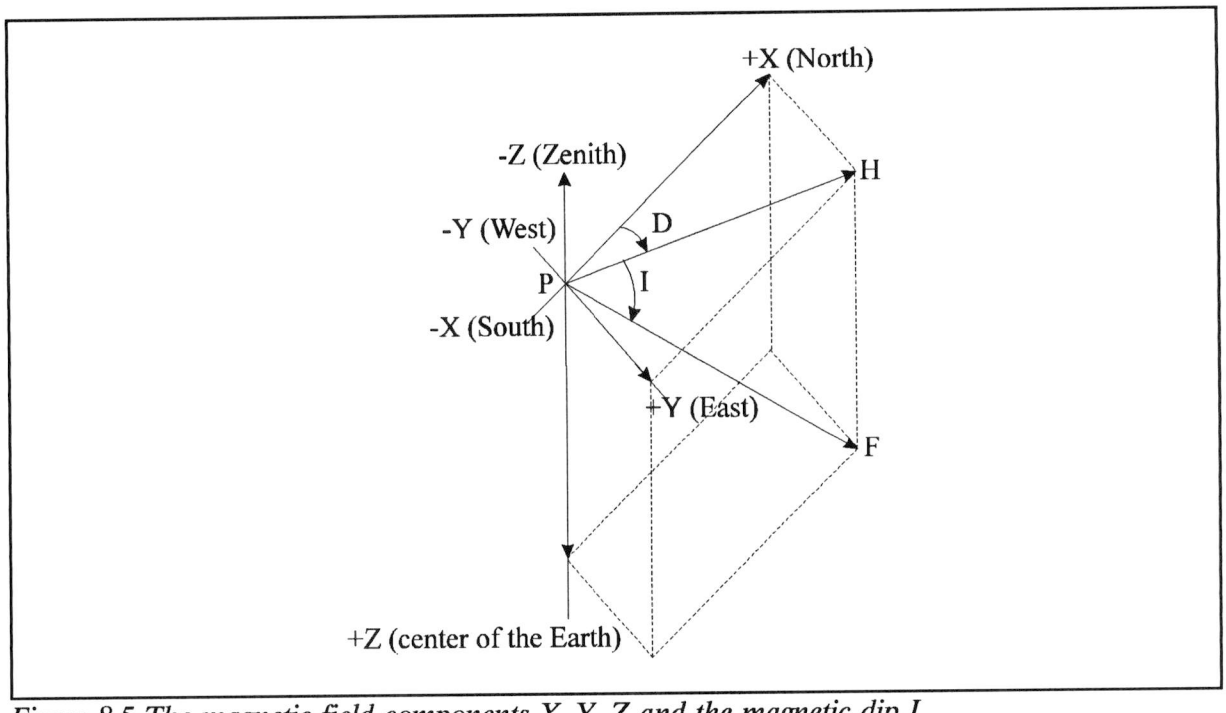

Figure 8.5 The magnetic field components X, Y, Z and the magnetic dip I

From figure 8.5 it can be seen that the magnetic dip I is given by:

$$I = \arctan\left(\frac{Z}{H}\right) = \arctan\left(\frac{Z}{\sqrt{X^2+Y^2}}\right) \tag{8.6}$$

As indicated by formula 8.6, to calculate the magnetic dip the X, Y, Z components of the magnetic field have to be known. These components are derived from the earth's magnetic potential V. As a result of spherical harmonic analysis of the earth's magnetic field, the potential V at a point with latitude ϕ, longitude λ and height h can be expressed as a series of harmonic functions (appendix B and [25]):

$$V = a\sum_{n=0}^{\infty}\sum_{m=0}^{n}\left(\frac{a}{r}\right)^{n+1} P_n^m(\cos\varphi)\left[g_n^m \cos m\lambda + h_n^m \sin m\lambda\right] \tag{8.7}$$

where a is the radius of the earth, $r = a+h$, $\varphi = 90°-\phi$ and

$$P_n^m(\cos\varphi) = \sin^m\varphi\left[\cos^{n-m}\varphi - \frac{(n-m)(n-m-1)}{2(2n-1)}\cos^{n-m-2}\varphi + \frac{(n-m)(n-m-1)(n-m-2)(n-m-3)}{(2)(4)(2n-1)(2n-3)}\cos^{n-m-4}\varphi - ..\right] \tag{8.8}$$

The function $P_n^m(\cos\varphi)$ is a function related to the Legendre function and is called the multiple of the associated Legendre function. The coefficients g_n^m and h_n^m are the Gauss coefficients. These coefficients are determined by measurements of the magnetic field strength, magnetic inclination and declination. In the Bent Ionospheric Model Gauss coefficients determined for the year 1960 are used ($n, m \leq 6$). The coefficients are listed in tables C.1 and C.2 of appendix C.

For the calculation of the magnetic dip I, the magnetic field components have to be determined at the ionospheric point (ϕ_{ion}, λ_{ion}, $\hat{h}_m$[1]). The magnetic field components at the ionospheric point are obtained from the potential V by partial differentiation of formula 8.7:

$$
\begin{aligned}
X &= \sum_{n=1}^{6} \left\{ R^{n+2} \sum_{m=0}^{n} \frac{d}{d\varphi} P_n^m(\cos\varphi) \left[g_n^m \cos(m\lambda) + h_n^m \sin(m\lambda) \right] \right\} \\
Y &= \frac{1}{\sin\varphi} \sum_{n=1}^{6} \left\{ R^{n+2} \sum_{m=0}^{n} m P_n^m(\cos\varphi) \left[g_n^m \sin(m\lambda) - h_n^m \cos(m\lambda) \right] \right\} \\
Z &= -\sum_{n=1}^{6} \left\{ (n+1) R^{n+2} \sum_{m=0}^{n} \frac{d}{d\varphi} P_n^m(\cos\varphi) \left[g_n^m \cos(m\lambda) + h_n^m \sin(m\lambda) \right] \right\}
\end{aligned}
\tag{8.9}
$$

where R is the ratio $R_e/(R_e+\dot{h}_m)$, R_e the mean radius of the earth, $\varphi=90°-\phi_{ion}$ and $\lambda=\lambda_{ion}$.

In the determination of the ionospheric characteristics f_0F2 and M(3000)F2 a function called modified magnetic dip is required. This modified magnetic dip x is a function of the latitude ϕ and longitude λ (at the ionospheric point) and is used as the main latitude coordinate (instead of the geographic latitude ϕ) in the "numerical mapping" technique (section 8.2.4 and appendix B). The modified magnetic dip x is defined as:

$$
x = \arcsin\left(\frac{I}{\sqrt{I^2 + \cos\phi}} \right) \tag{8.10}
$$

---

1 The determination of the height of maximum electron density h_m is an iterative process and is determined from the factor M(3000)F2 as will be shown in section 8.2.4. The modified magnetic dip is required (and thus the magnetic field components X, Y, Z) for the determination of h_m. However the value of h_m is not known when the calculations are performed for the first time and is approximated by 300 km. Based on this value, h_m is determined iteratively (see section 8.2.4).

8.2.4 Determination of the ionospheric profile parameters

To determine the ionospheric profile the following parameters are required (section 8.2.1):

- f_0F2
- M(3000)F2
- h_m
- y_t
- y_m
- d
- k_1, k_2 and k_3

This section starts with the determination of the first two parameters: the critical frequency f_0F2 and the factor M(3000)F2. These ionospheric characteristics are required to calculate the other ionospheric parameters of the list given above.

Both ionospheric characteristics depend on geographic longitude λ, geographic latitude ϕ and time T. To represent the diurnal and geographic variations of f_0F2 and M(3000)F2 the "numerical mapping" technique is used [26, 27, 28]. This technique is described shortly in appendix B. The term "numerical map" is used to denote a function $\Omega(\phi,\lambda,T)$, of three variables (latitude ϕ, longitude λ and time T) which represents the world-wide geographic and diurnal variations of an ionospheric characteristic. Based on analysis of a specific ionospheric characteristic, the diurnal and world-wide geographic variations of this characteristic is represented in the general form of a Fourier time series:

$$\Omega(\phi,\lambda,T) = a_0(\phi,\lambda) + \sum_{j=1}^{H} [a_j(\phi,\lambda)\cos jT + b_j(\phi,\lambda)\sin jT] \qquad (8.11)$$

where:

λ: geographic longitude ($0° \le \lambda \le 360°$)

ϕ: geographic latitude ($-90° \le \phi \le 90°$)

T: universal time (UTC) expressed as an angle ($-180° \le T \le 180°$)

H: the maximum number of harmonics used to represent the diurnal variation

The Fourier coefficients, $a_j(\phi,\lambda)$ and $b_j(\phi,\lambda)$, vary with the geographic coordinates, and are represented by series of the form:

$$a_j(\phi,\lambda) = \sum_{k=0}^{K} U_{2j,k} G_k(\phi,\lambda), \qquad j = 0,1,2,....,H \tag{8.12}$$

$$b_j(\phi,\lambda) = \sum_{k=0}^{K} U_{2j-1,k} G_k(\phi,\lambda), \qquad j = 0,1,2,....,H \tag{8.13}$$

in which $G_k(\phi,\lambda)$ are called the geographic functions representing the geographic variation of the ionospheric characteristic (table B.1, appendix B). $G_k(\phi,\lambda)$ are a function of the latitude ϕ, the longitude λ, and the modified magnetic dip x, which itself is dependent on the geographic position. The numerical map function as described in [27, 28] did not make use of the modified magnetic dip. The change of using the modified magnetic dip as the main latitude coordinate resulted in a better world representation of the ionospheric variations, particularly in equatorial and polar regions [26]. The particular choice of the function $G_k(\phi,\lambda)$ is determined by specifying the integers k (k_0, k_1, k_2, ..., k_i, ..., k_m; k_m = K) where i is the order in longitude. Therefore, a numerical map can be written more explicitly in the form:

$$\begin{aligned} \Omega(\phi,\lambda,T) &= \sum_{k=0}^{K} U_{0,k} G_k(\phi,\lambda) + \\ &+ \sum_{j=1}^{H} \left[\cos jT \sum_{k=0}^{K} U_{2j,k} G_k(\phi,\lambda) + \sin jT \sum_{k=0}^{K} U_{2j-1,k} G_k(\phi,\lambda) \right] \end{aligned} \tag{8.14}$$

In the Bent Ionospheric Model formula 8.14 is written as:

$$\Omega(\phi,\lambda,T) = \sum_{k=0}^{K} D_k(T) G_k(\phi,\lambda) \tag{8.15}$$

The functions $G_k(\phi,\lambda)$ represent the main latitudinal variation and the first order through 8th order longitudinal variation terms. The main latitudinal variation is expressed as:

$$G_k = \sin^k x \qquad , \text{for } k = 0,1,....,11 \tag{8.16}$$

The jth order longitude terms are calculated by:

$$G_k = \begin{cases} (\sin x)^{\frac{(k-m_j)}{2}} \cos^j\phi\cos(j\lambda) & \text{, for k even} \\ (\sin x)^{\frac{(k-m_j-1)}{2}} \cos^j\phi\cos(j\lambda) & \text{, for k odd} \end{cases} \qquad (8.17)$$

where $k = m_j, m_j+1,..., m_{j+1}-1$. The longitude orders are $j = 1, 2,..., 8$ while $k = 12, 13,...., 75$. The indexing is defined by: $m_1 = 12$, $m_2 = 36$, $m_3 = 54$, $m_4 = 64$, $m_5 = 68$, $m_6 = 70$, $m_7 = 72$ and $m_8 = 74$ (see also table B.1, appendix B).

The orthonormal coefficients D_k for a fixed time T are represented by the Fourier series representation:

$$D_k(T) = U_{0,k} + \sum_{j=1}^{H} [U_{2j,k}\cos(jT) + U_{2j-1,k}\sin(jT)] \quad , k = 1,...,K \qquad (8.18)$$

$D_k(T)$ represents the diurnal variation of the ionospheric characteristic. The number of harmonics retained in the series is H. H is the number of harmonics which are produced by real physical variation. Higher harmonics are caused more by noise. For the f_0F2 computation H=6 and for the M(3000)F2 computation H=4 are sufficient.

The coefficients that represent the monthly median values of f_0F2 and M(3000)F2 are the values of $U_{i,k}$ (i is either 2j or 2j-1) that define the function $\Omega(\phi,\lambda,T)$, of the numerical map function of the given characteristic for the indicated month and level of solar activity. The coefficients $U_{i,k}$ are either a monthly predicted coefficient set for M(3000)F2 or a ten day predicted coefficient set for f_0F2, which are both specific subsets derived from the generalized f_0F2 and M(3000)F2 coefficients. The coefficients are computed for each term in a series with a cutoff point K, K=75 for the series expressing f_0F2 and K=48 for the series representing M(3000)F2. The general f_0F2 and M(3000)F2 coefficients are valid for any condition and do not have to be updated or replaced, but can be adjusted for any time in the past or future.

The general f_0F2 coefficients $W_{s,i,k}$ provide annual continuity and are valid for approximate 10 day periods: for the spans from day 1 to 10, day 11 to 20 and day 21 to 30 (or 28, 29, 31) of each month. There are coefficients for 36 periods to cover the whole year. The general f_0F2 coefficients represent the coefficients to a second order polynomial in the 12-month running

average solar flux F_{12} (observed Ottawa 10.7 cm solar flux)[2]. The specific f_0F2 coefficient set $U_{i,k}$ is calculated from the generalized f_0F2 by:

$$U_{i,k} = W_{1,i,k} + W_{2,i,k} \times F_{12} + W_{3,i,k} \times F_{12}^2 \quad , \text{for} \begin{cases} i = 0,1,...,12 \\ k = 0,1,....,75 \end{cases} \tag{8.19}$$

The general M(3000)F2 coefficients are valid for monthly periods. There are coefficients for 12 periods to cover the whole year. For each period there are two sets $V_{i,k}(0)$ and $V_{i,k}(100)$, one for a 12-month running average of sunspot number[3] $S_{12}=0$ and the other for $S_{12}=100$. The coefficients are adjusted by interpolating or extrapolating the two sets to the specific S_{12} of the evaluation date yielding the specific M(3000)F2 coefficients set:

$$U_{i,k} = V_{i,k}(0) + [V_{i,k}(100) - V_{i,k}(0)] \times \frac{S_{12}}{100} \quad , \text{for} \begin{cases} i = 0,1,....,8 \\ k = 0,1,....,48 \end{cases} \tag{8.20}$$

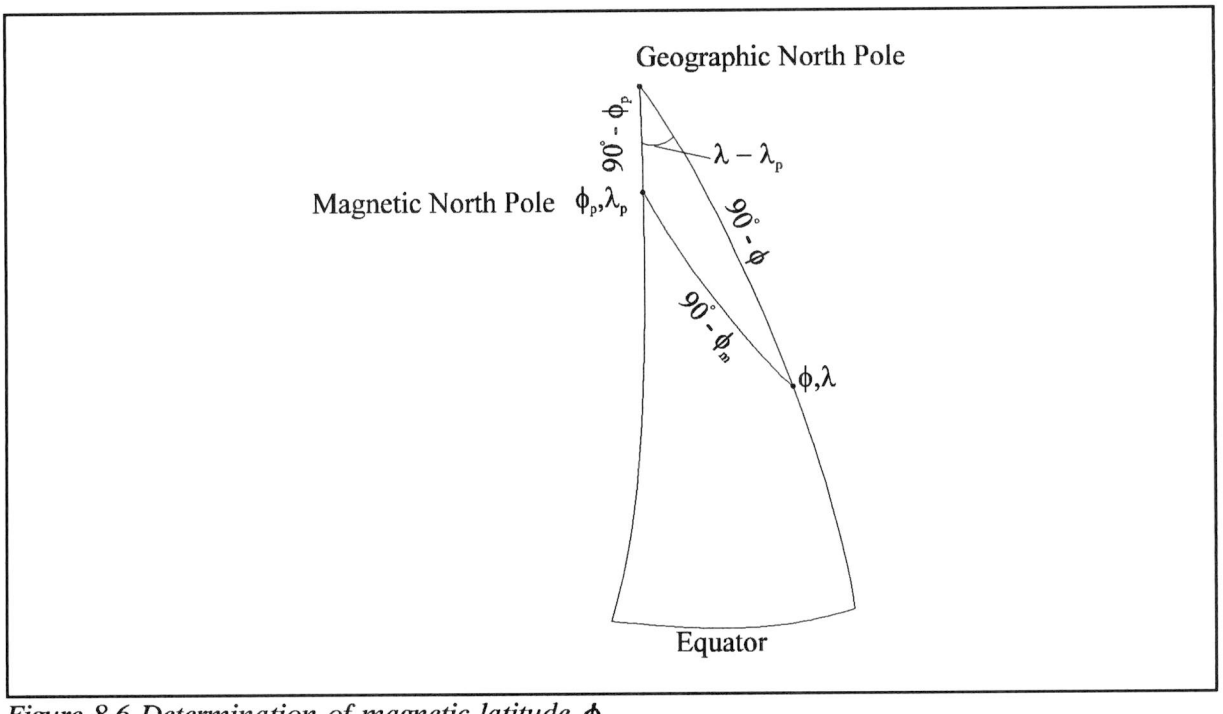

Figure 8.6 Determination of magnetic latitude ϕ_m

2 The sun emits radio energy with a slowly varying intensity. Solar flux density at 2800 MHz (10.7 cm wavelength) has been determined near Ottawa since 1947. Unit: 10^{-22} Wm^{-2} Hz^{-1}.

3 The 12-month running average sunspot number is a measure of the solar activity. Sunspots are dark areas on the surface on the sun. These areas appear dark because of relatively low temperature (3000 °K). Sunspots tend to group together. A group may contain a few isolated spots or dozens of spots.

Using formula 8.15, the 10 day mean of the critical frequency f_0F2 is determined. This f_0F2 is adjusted for day to day changes in the ionosphere and for additional magnetic latitude variations. Using spherical trigonometry, the magnetic latitude ϕ_m of the ionospheric point can be expressed as (figure 8.6):

$$\phi_m = \arcsin[\sin\phi\sin\phi_p + \cos\phi\cos\phi_p\cos(\lambda - \lambda_p)] \tag{8.21}$$

where ϕ_p, λ_p are the latitude and longitude of the magnetic north pole and λ the ionospheric longitude and ϕ the ionospheric latitude. The adjustment factor is given by: $c_1\Delta F+c_2$. ΔF[4] is the difference between the daily value and the 12-month running average of the solar flux, F_{12}. The value of c_2 is obtained by interpolation (depending on the magnetic latitude ϕ_m of the ionospheric point) of three model constants given for three specific magnetic latitudes: ϕ_m=59°, constant is 1.035; ϕ_m=28°, constant is 0.957; ϕ_m=-33°, constant is 0.9. The value of c_1 is 0.00133. The 10 day mean is multiplied by the adjustment factor to yield the final predicted f_0F2.

When the ionospheric characteristics f_0F2 and M(3000)F2 are known, the other parameters of the ionospheric profile can be determined.

First the height of the maximum electron density h_m is determined. This height (in meters) is obtained by a second order polynomial in M(3000)F2:

$$h_m = \left\{1346.92 - 526.40 \times M(3000)F2 + 59.825[M(3000)F2]^2\right\} \times 10^3 \tag{8.22}$$

The determination of h_m is an iterative process. As can be seen from figure 8.1, h_m is required for the calculation of the ionospheric point (section 8.2.1). When the calculations are performed for the first time h_m is not known: a first estimate of h_m is required and is assumed to be h_m=300 km. Based on this assumption, a new value of h_m is predicted. This value is compared with its estimate and if the difference is greater than 1 km, the determination of h_m is performed again (starting with the determination of the ionospheric point, section 8.2.1) using the new value of h_m.

[4] If the daily solar flux F is not available, F_{12} is substituted. If F is greater than 130, 130 is substituted which is a limit imposed by the data base on which development of the model was founded.

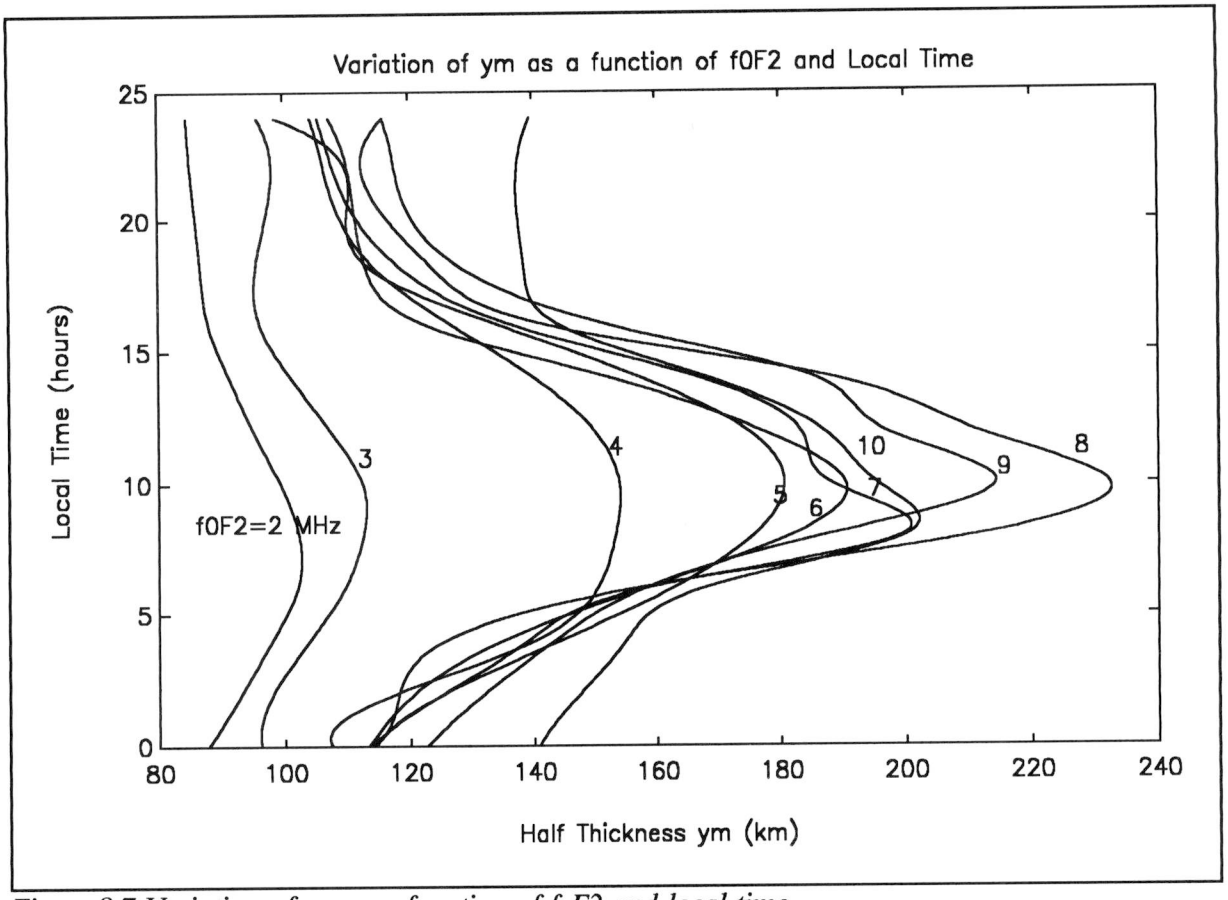

Figure 8.7 Variation of y_m as a function of f_0F2 and local time

Before the half thickness of the topside parabola y_t is calculated, first the half thickness of the bottomside bi-parabola y_m is determined. The half thickness y_m varies with the critical frequency f_0F2 and local time t_{loc}. The local time is calculated from the universal time t (converted to radians or degrees) and the longitude λ_{ion} of the ionospheric point:

$$t_{loc} = t + \lambda_{ion} \tag{8.23}$$

In the Bent Ionospheric Model, the values of y_m are given for values of f_0F2 with increments of 1 MHz (f_0F2 = 2, 3,....10 MHz) and for 2 hour intervals of t_{loc} (t_{loc} = 0, 2,....22 hours) (see table C.3, appendix C, figure 8.7). To obtain y_m for the given conditions (certain f_0F2 and t_{loc}), the fixed values of y_m are interpolated.

In the above description of the determination of y_m, seasonal effects are not taken into account. For seasonal adjustments computation of the parameter $\Delta\chi$ is required. $\Delta\chi$ is the

deviation of the daily value χ from the yearly average $\bar{\chi}$ of the noontime solar zenith angle (figure 8.8). First the solar declination δ is evaluated for the given day:

$$\delta = \delta_{max} \sin\left[\frac{2\pi}{365}(JDAY - 80)\right] \tag{8.24}$$

where δ_{max}=23.4444°. δ_{max} is the maximum solar declination and JDAY is the day of the year. For stations in the northern hemisphere and outside the tropics, with latitudes ≥ 23.4444°, $\Delta\chi=\delta$; for stations in the southern hemisphere and outside the tropics, $\Delta\chi=-\delta$. In the tropics the yearly average of the noontime solar zenith angle is computed as:

$$\bar{\chi} = \frac{2}{\pi}\left(\sqrt{\delta^2_{max} - \phi^2} + \phi \arcsin\frac{\phi}{\delta_{max}}\right) \tag{8.25}$$

where ϕ is the latitude of the ionospheric point. The daily noontime solar zenith angle is $\chi = |\phi - \delta|$, and the difference $\Delta\chi = \bar{\chi} - \chi$.

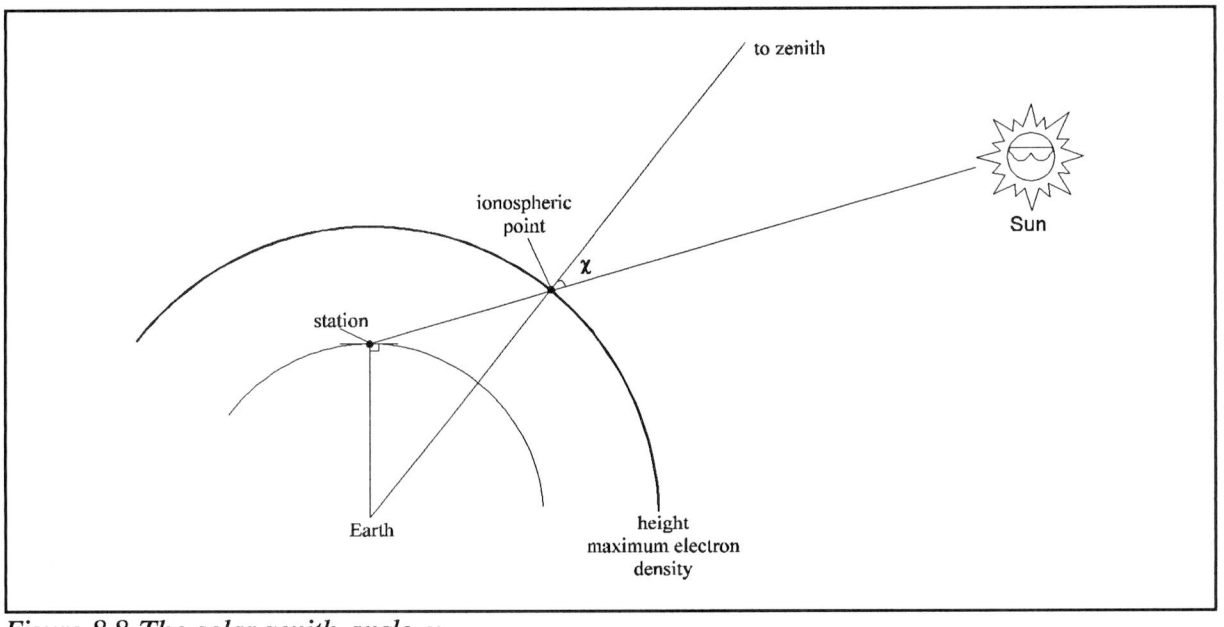

Figure 8.8 The solar zenith angle χ

The half thickness of the bottomside parabola y_m is multiplied by the seasonal adjustment factor that varies with $\Delta\chi$, local time and magnetic latitude ϕ_m.

In the Bent Ionospheric Model, the adjustment factors are given with increments for $\Delta\chi$=24, 16, 8, 0, -8, -16, -24 degrees, at 6 hour intervals for t_{loc}=5.5, 11.5, 17.5, 24.5 hours where the absolute value of the magnetic latitude is greater or equal 15°, and at 12 hour intervals t_{loc}=3, 15 hours where $|\phi_m| \leq 5°$. The seasonal adjustment factor for the given conditions is obtained by interpolation.

From the half thickness of the bottomside bi-parabola y_m and the critical frequency f_0F2 the half thickness of the topside parabola y_t is determined. The half thickness of the topside parabola y_t, extending from the point of maximum electron density to the lower exponential layer, is dependent on y_m and f_0F2 through the relationship:

$$y_t = \begin{cases} y_m & , \text{for } f_0F2 \leq 10.5 \\ y_m[1 + 0.133333(f_0F2 - 10.5)] & , \text{for } f_0F2 > 10.5 \end{cases} \qquad (8.26)$$

There remain four ionospheric profile parameters to be determined: the decay constants k_1, k_2 and k_3, and the distance d above the height at maximum electron density h_m.

The decay constants k_1, k_2 and k_3 for the lower, middle and upper layer of the exponential topside are related to the daily solar flux F through the first order polynomial:

$$k_i = S_i \times F + C_i \qquad , i = 1,2,3 \qquad (8.27)$$

The slopes S_i and the intercepts C_i of this straight line relationship vary with geomagnetic latitude ϕ_m and f_0F2. For each of the three topside layers, S_i (table C.5, appendix C) and C_i (table C.6, appendix C) are given at 30° intervals for $|\phi_m|$=15, 45, 75 degrees, and at 3 MHz increments for f_0F2=2, 5, 8, 11 MHz. To obtain the decay constants for the given conditions, the S_i and C_i values are interpolated. The boundary values are used whenever f_0F2 is outside the limits 2 and 11 Mhz or $|\phi_m|$ is outside 15 and 75 degrees.

Seasonal effects are imposed on the topside by multiplying the decay constants by season adjustment factors that vary with the deviation $\Delta\chi$ in the solar zenith angle and with local time. The adjustment factors are given for each of the three topside layers at 8° increments for $\Delta\chi$=24, 16, 8, 0, -8, -16, -24 degrees, and at 6 hour intervals for t_{loc}=2, 8, 14, 20 hours (table C.6, appendix C). They are interpolated for each k_i to the given conditions.

As the parameters y_t and k_1 are known, the distance d above the height at maximum electron density h_m where the slopes of the parabola and the lower exponential layer are the same can be determined. The distance d is calculated by:

$$d = \frac{1}{k_1}\left(\sqrt{1+k_1^2 y_t^2} - 1\right) \tag{8.28}$$

As the ionospheric profile parameters are determined, the electron density profile is known. When the electron density profile is integrated from zero to the height h_s of the satellite, the vertical and angular total electron content are obtained. This will be described in the next section.

8.2.5 The vertical and angular total electron content

The vertical total electron content N_T and the angular total electron content N_{TA} are obtained by integrating the electron density profile (formulae 8.1 and 8.2) from zero to the height of the satellite h_s. First the ratio of vertical total electron content to the maximum electron density N_T/N_m is determined. The ratio is determined by one of the following six equations, depending on the upper integration limit.

For a satellite below the bi-parabolic layer of the ionosphere:

$$\frac{N_T}{N_m} = 0 \tag{8.29}$$

For a satellite in the bottomside bi-parabolic layer with half thickness y_m formula 8.1a has to be integrated from h_m-h_s to y_m, resulting in:

$$N_T = N_m\left[\frac{8}{15}y_m - (h_m - h_s) + \frac{2}{3}\frac{(h_m - h_s)^3}{y_m^2} - \frac{1}{5}\frac{(h_m - h_s)^5}{y_m^4}\right] \tag{8.30}$$

To obtain the ratio N_T/N_m for a satellite in the topside parabolic layer with half thickness y_t, the electron density profile of the first layer (formula 8.1a) is integrated over the interval 0 to

y_m: this is the total vertical electron content contained in the first layer. To the content of this layer, the content of the parabolic layer to the height of the satellite has to be added (integration of formula 8.1b over the interval 0 to h_s-h_m). For a satellite in the topside parabolic layer with half thickness y_t the ratio N_T/N_m is determined by:

$$N_T = N_m\left[\frac{8}{15}y_m - (h_m - h_s) + \frac{1}{3}\frac{(h_m - h_s)^3}{y_t^2}\right] \tag{8.31}$$

For a satellite in the lower exponential of the topside with decay constant k_1, first the electron density of the bi-parabolic layer (formula 8.1a) and the parabolic layer (formula 8.1b) have to be integrated over respectively 0 to y_m and 0 to h_0-h_m: the total vertical electron content in the first two layers is obtained. To this content, the content extending from the bottom of the lower exponential layer to the satellite has to be determined: integration of formula 8.1c over the interval 0 to h_s-h_0. As a result the ratio N_T/N_m is obtained:

$$N_T = N_m\left(1 - \frac{d^2}{y_t^2}\right)\left[\frac{1}{k_1}\left(1 - e^{-k_1(h_s - h_0)}\right)\right] + N_B \tag{8.32}$$

and the height of the bottom of the lower exponential layer is $h_0 = h_m + d$, and:

$$N_B = N_m\left[\frac{8}{15}y_m - (h_m - h_0) + \frac{1}{3}\frac{(h_m - h_0)^3}{y_t^2}\right] \tag{8.33}$$

For a satellite in the middle exponential layer of the topside with decay constant k_2, first the total vertical electron content of the bi-parabolic layer (integration of formula 8.1a over interval 0 to y_m), the parabolic layer (integration of formula 8.1b over interval 0 to h_0-h_m) and the lower exponential layer (integration of formula 8.1c over interval 0 to h_1-h_0) are determined. Adding the electron content extending from the bottom of the middle exponential layer to the height of the satellite (integration of formula 8.1d over interval 0 to h_s-h_1) gives the ratio N_T/N_m:

$$N_T = N_m\left(1-\frac{d^2}{y_t^2}\right)\left[\frac{1}{k_1}+e^{-k_1(h_1-h_0)}\left[-\frac{1}{k_1}+\frac{1}{k_2}(1-e^{-k_2(h_s-h_1)})\right]\right]+N_B \qquad (8.34)$$

and the height of the bottom of the middle exponential layer is:

$$h_1 = h_0 + \frac{1}{3}(1.012\times10^6-h_0) \qquad (8.35)$$

For a satellite in the upper exponential layer of the topside with decay constant k_3, the total vertical electron content of the bi-parabolic layer (integration of formula 8.1a over interval 0 to y_m), the parabolic layer (integration of formula 8.1b over interval 0 to h_0-h_m), the lower exponential layer (integration of formula 8.1c over interval 0 to h_1-h_0) and the middle exponential layer (integration of formula 8.1d over interval 0 to h_2-h_1) is determined. Adding the electron content extending from the bottom of the higher exponential layer to the height of the satellite (integration of formula 8.1e over interval 0 to h_s-h_2) gives the ratio N_T/N_m:

$$N_T = N_m\left(1-\frac{d^2}{y_t^2}\right)\times \\ \times\left[\frac{1}{k_1}+e^{-k_1(h_1-h_0)}\left[-\frac{1}{k_1}+\frac{1}{k_2}+e^{-k_2(h_2-h_1)}\left(-\frac{1}{k_2}+\frac{1}{k_3}-\frac{1}{k_3}e^{-k_3(h_s-h_2)}\right)\right]\right]+N_B \qquad (8.36)$$

and the height of the bottom of the upper exponential layer is:

$$h_2 = h_0 + \frac{2}{3}(1.012\times10^6-h_0) \qquad (8.37)$$

When the ratio N_T/N_m is known, the total integrated electron content N_T along a vertical path through the ionosphere is obtained by multiplying this ratio by N_m(= $1.24\times10^{10}f_0F2^2$, formula 8.2). This results in:

$$N_T = 1.24\times10^{10}\ f_oF2^2\left(\frac{N_T}{N_M}\right) \qquad (8.38)$$

As discussed in section 7.3, the vertical total electron content has to be multiplied by a

correction factor if the angular total electron content N_{TA} along the line of sight is required. So, N_{TA} is calculated from N_T by:

$$N_{TA} = \frac{N_T}{\sqrt{1-\left(\frac{R_e \cos E}{R_e + h_m}\right)^2}} \tag{8.39}$$

From N_{TA} the ionospheric refraction range correction can be determined. This correction as well as the range rate and elevation corrections will be discussed in the next section of this report.

8.2.6 Ionospheric corrections

From the Bent Ionospheric Model three ionospheric corrections can be obtained: range correction, range rate correction and elevation correction. Range and range rate errors are of more importance in GNSS accuracy than elevation errors caused by the ionosphere. Therefore these errors will be discussed more extensively.

The first ionospheric correction output by the model is the range correction. In chapter 7, the dependence of the range correction on the angular total electron content has been discussed (formulae 7.7, 7.8 and 7.9). Replacing TEC of formula 7.7 by N_{TA} gives the ionospheric range correction as used in the Bent Ionospheric Model. The one-way ionospheric range correction ΔR is given by:

$$\Delta R = \frac{40.3 \times 10^{-12}\, N_T}{f^2 \sqrt{1-\left(\frac{R_e \cos E}{R_e + h_m}\right)^2}} = \frac{40.3 \times 1.24 \times 10^{-2} \left(\frac{f_o F2}{f}\right)^2 \frac{N_T}{N_m}}{\sqrt{1-\left(\frac{R_e \cos E}{R_e + h_m}\right)^2}} \tag{8.40}$$

where f is the transmission frequency.

The second ionospheric correction which can be obtained from the Bent Ionospheric Model is the ionospheric range rate correction. The range rate $\Delta \dot{R}$ consists of two terms, one

multiplied by the altitude rate $\dot{h}$, the other by the elevation rate $\dot{E}$. If it is assumed that the only variation in the total electron content over the time of the observation is due to the positional change of the satellite and the ionosphere between station and satellite remains constant for the duration of the measurement, the one-way ionospheric range rate correction range rate $\Delta\dot{R}$ is given by:

$$\Delta\dot{R} = -\frac{40.3\times1.24\times10^{-2}\left(\frac{f_oF2}{f}\right)^2 m\dot{h} + \frac{\Delta R\left(\frac{R_e}{R_e+h_m}\right)^2 \sin E\cos E}{1-\left(\frac{R_e\cos E}{R_e+h_m}\right)^2}\dot{E}}{\sqrt{1-\left(\frac{R_e\cos E}{R_e+h_m}\right)^2}} \tag{8.41}$$

In formula (8.41) the multiplier m depends on the height of the satellite. For a satellite below the bi-parabolic layer of the ionosphere:

$$m = 0 \tag{8.42}$$

For a satellite in the bottomside bi-parabolic layer with half thickness y_m:

$$m = \left[1-\left(\frac{h_m-h_s}{y_m}\right)^2\right]^2 \tag{8.43}$$

For a satellite in the topside parabolic layer with half thickness y_t:

$$m = 1-\left(\frac{h_m-h_s}{y_t}\right)^2 \tag{8.44}$$

For a satellite in the lower exponential layer of the topside:

$$m = \left(1-\frac{d^2}{y_t^2}\right)e^{-k_1(h_s-h_0)} \tag{8.45}$$

For a satellite in the middle exponential layer of the topside:

$$m = \left(1-\frac{d^2}{y_t^2}\right)e^{-k_1(h_1-h_0)}e^{-k_2(h_s-h_1)} \tag{8.46}$$

For a satellite in the upper exponential layer of the topside:

$$m = \left(1 - \frac{d^2}{y_t^2}\right) e^{-k_1(h_1 - h_0)} e^{-k_2(h_2 - h_1)} e^{-k_3(h_s - h_2)} \tag{8.47}$$

The final ionospheric correction which can be determined with the Bent Ionospheric Model is the ionospheric elevation correction. For more information on this correction is referred to the documentation on the Bent Ionospheric Model [24].

8.3 Improvement of the accuracy of the model

The model as described in the previous section has an prediction accuracy which accounts for approximately 75 to 80 percent of the ionosphere. This accuracy can be improved to 90 percent by an updating technique. This technique will be discussed briefly. For more information is referred to [24].

The predicted f_0F2 can be updated with observations of f_0F2 or with vertical or angular electron content measurements from other stations. Up to eight update observations of either type separated by different amounts in time and space from the evaluation time and station can be accepted. To obtain the best possible update, the observation times and stations should be the closest to the evaluation condition available, in any case, the update station should be within 2000 km of the evaluation site.

9. GLONASS ionospheric influence simulation model

9.1 Introduction

The influence of the ionosphere on the propagation of GLONASS signals is determined by applying the Bent Ionospheric Model. The possible updating technique [24] is not implemented. From this simulation model the range error on GLONASS signals due to the ionosphere is determined.

The Bent Ionospheric Model requires both satellite and station position information (elevation, azimuth and height of the satellite) and time and solar data. The satellite position is calculated from GLONASS almanac data (section 9.2). In section 9.3 the conversion from geodetic station coordinates (latitude, longitude and height) to ECEF coordinates is described. This section is followed by a section on the determination of the elevation and azimuth to the satellite (section 9.4). This chapter is concluded with a section on the complete simulation model.

9.2 GLONASS position algorithm

The positions of the satellites at a certain moment in time are calculated using GLONASS almanac data[1]. The almanac parameters are:

- Satellite ID (consisting of satellite and slot number)
- Health
- Eccentricity: ϵ

[1] The GLONASS almanac data was obtained from the MIT Lincoln Laboratory. The format of this almanac is similar to that of GPS, and differs from the format of the almanac transmitted by the GLONASS satellites. At the MIT the received GLONASS almanac data has been converted to the described format. Although GLONASS satellites do not transmit clock correction terms Af0 and Af1, these terms have been added for completeness (and will always be zero).

- Time of Applicability: $T_{Applicability}$ (s)
- Orbital Inclination: i (rad)
- Rate of Right Ascension: $\dot{\Omega}$ (rad/s)
- Square Root of the Semi Major Axis: $\sqrt{A}$ ($m^{1/2}$)
- Right Ascension at Time of Applicability: Ω (rad)
- Argument of Perigee: ω (rad)
- Mean Anomaly: M_0 (rad)
- Clock correction terms: Af0 (s) and Af1 (s/s)

The GLONASS satellite position is determined by applying the following calculations.

First the semi-major axis A is given by:

$$A = \left(\sqrt{A}^{-}\right)^2 \tag{9.1}$$

The satellite mean motion n is defined as:

$$n = \sqrt{\frac{\mu}{A^3}} \tag{9.2}$$

where μ is the gravitational constant.

The mean anomaly M is given by:

$$M = M_0 + n \times t_k \tag{9.3}$$

where the time of calculation t_k is defined by:

$$t_k = T_{Position} - T_{Applicability} \tag{9.4}$$

and M_0 is the mean anomaly at $T_{Applicability}$.

The eccentric anomaly E_k of the satellite orbit is determined by iteratively solving the Kepler equation:

$$E_k = M_k + \epsilon \sin E_k \tag{9.5}$$

where ϵ is the eccentricity of the satellite orbit.

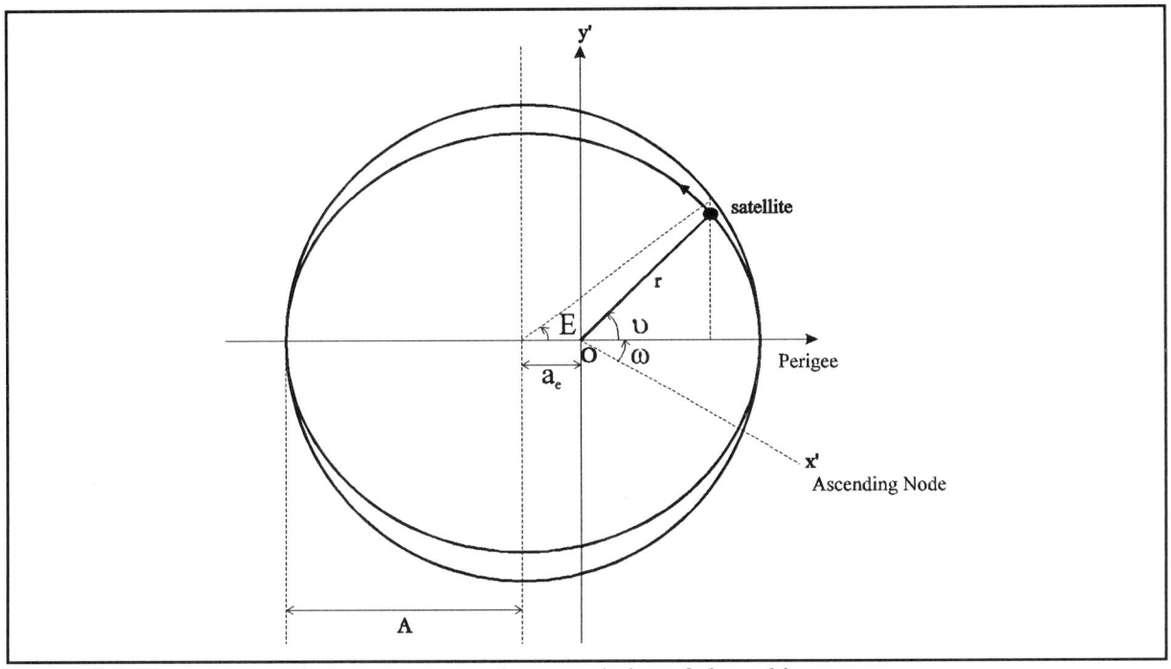

Figure 9.1 Keplerian orbital parameters: shape and size of the orbit

The relation between the true anomaly υ_k and eccentric anomaly E_k is (figure 9.1):

$$\tan\left(\frac{E_k}{2}\right) = \left(\frac{1-\epsilon}{1+\epsilon}\right)^{\frac{1}{2}} \tan\left(\frac{\upsilon_k}{2}\right) \tag{9.6}$$

The corrected radius r_k is given by:

$$r_k = A(1-\epsilon\cos E_k) \tag{9.7}$$

The position in the orbital plane (x_k', y_k') is calculated from r_k, υ_k and ω by (figure 9.2):

$$\begin{aligned} x_k' &= r_k\cos(\upsilon_k+\omega) \\ y_k' &= r_k\sin(\upsilon_k+\omega) \end{aligned} \tag{9.8}$$

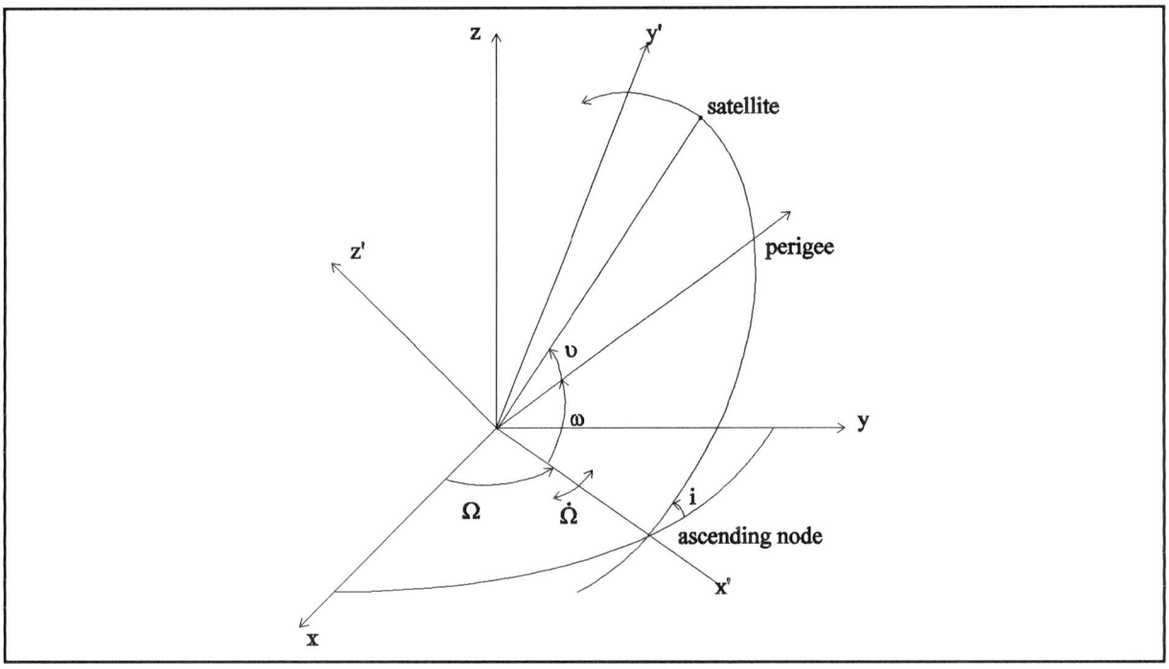

Figure 9.2 Keplerian orbital parameters: position and orientation of the orbit

The position in SGS-85/PZ-90[2] ECEF coordinates follows from:

$$\begin{aligned} x_k &= x_k' \cos\Omega_k - y_k' \sin\Omega_k \cos i \\ y_k &= x_k' \cos\Omega_k + y_k' \sin\Omega_k \cos i \\ z_k &= y_k' \sin i \end{aligned} \tag{9.9}$$

where Ω_k is the corrected right ascension (with ω_{earth} the angular rotation velocity of the earth) given by:

$$\Omega_k = \Omega_0 + (\dot{\Omega}_k - \omega_{earth}) t_k - \omega_{earth} T_{Applicability} \tag{9.10}$$

The SGS-85/PZ-90 coordinate reference system is defined by the following parameters:

---

2 The GLONASS coordinate reference system has been changed from SGS-85 to PZ-90. At the time of writing this report (March 1995), the third edition of the GLONASS Interface Control Document is being prepared in which the transition from SGS-85 to PZ-90 will be described. Before its approval and publication the Coordinational Scientific Information Center (CSIC) of the Russian Space Forces could only give the following information concerning the parameters of the PZ-90 ellipsoid: equatorial radius: a_e = 6378136 m and the flattening of the earth: f = 1/298.25783903. Some necessary parameters defining the coordinate reference system PZ-90 are therefore not exactly known. In this case, the values of the SGS-85 reference system are taken from [4]. The errors introduced can be neglected

- angular velocity of the earth ω_{earth} : 0.7292115×10^{-4} rad/s;
- flattening of the earth f : 1/298.257839303;
- equatorial radius of the earth a_e : 6378.136 km;
- gravitational constant μ : 398600.44 km^3/s^2;
- value of pi : 3.145926536;

9.3 Conversion of station geodetic coordinates to ECEF coordinates

The ECEF coordinates $x_{station}$, $y_{station}$ and $z_{station}$ of the station position are calculated from the geodetic station coordinates: latitude ϕ, longitude λ and height h above the SGS-85/PZ-90 ellipsoid by (figure 9.3):

$$\begin{aligned} x_{station} &= [N+h]\cos\phi\cos\lambda \\ y_{station} &= [N+h]\cos\phi\sin\lambda \\ z_{station} &= [N(1-e^2)+h]\sin\phi \end{aligned} \qquad (9.11)$$

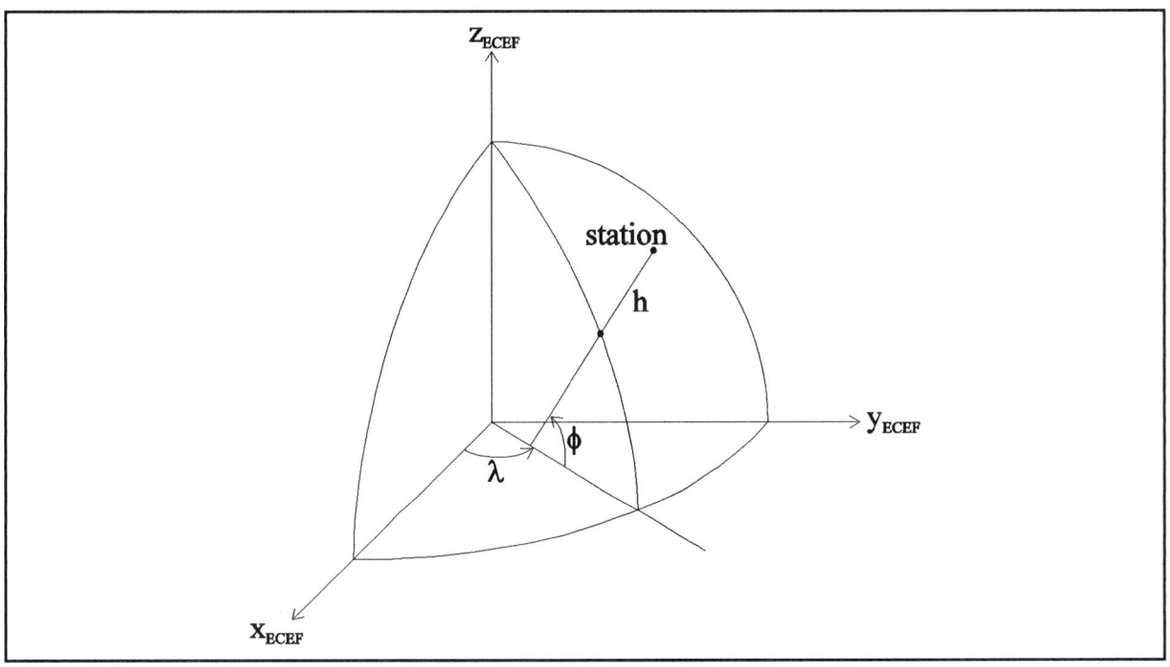

Figure 9.3 Conversion of latitude, longitude and height to ECEF coordinates

In formula 9.11:

$$N = \frac{a_e}{(1 - e^2 \sin^2 \phi)^{\frac{1}{2}}} \tag{9.12}$$

and

$$e^2 = \frac{a_e^2 - b_e^2}{a_e^2} \tag{9.13}$$

The value of the polar axis b_e follows from:

$$b_e = a_e(1 - f) \tag{9.14}$$

From formulae 9.13 and 9.14 the value of e^2 follows: $e^2 = 6.694366 \times 10^{-3}$.

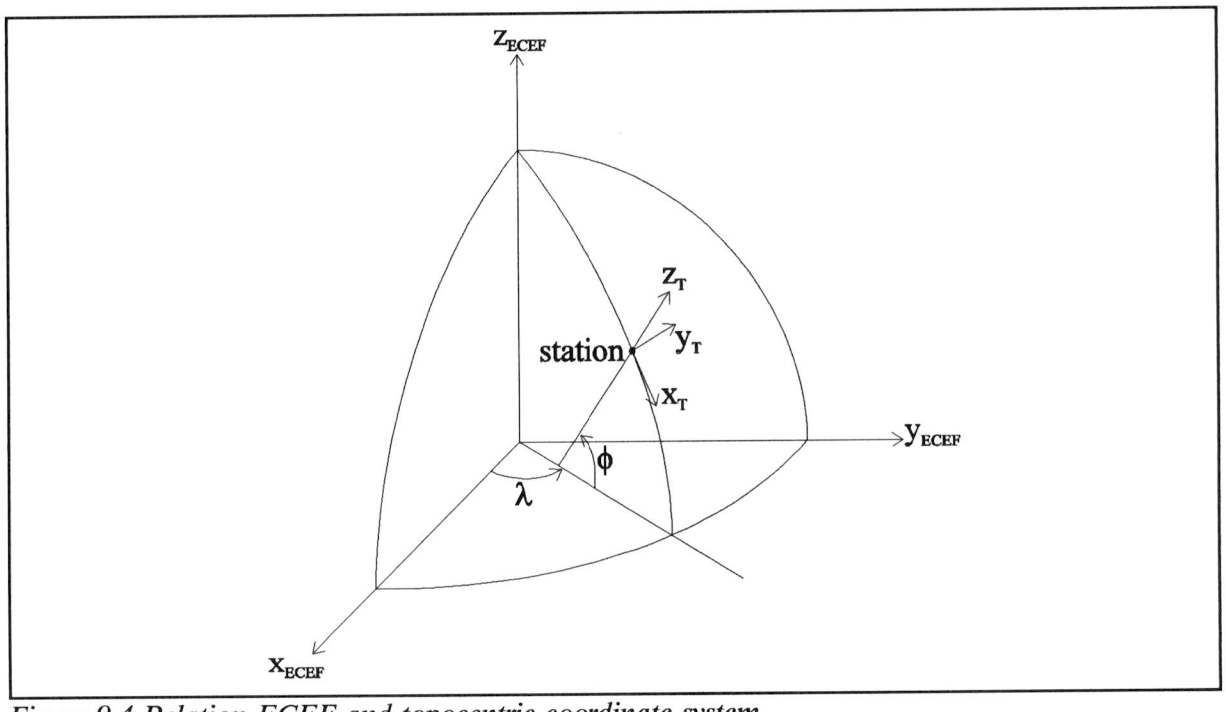

Figure 9.4 Relation ECEF and topocentric coordinate system

9.4 Elevation and azimuth determination

The elevation and azimuth are calculated in a topocentric coordinate system. Topocentric coordinates have their origin on the surface of the earth (figure 9.4). The reference plane is

the local horizon, which is taken as perpendicular to the line defining the geodetic latitude. The X-axis lies in the horizon plane and points towards the south. The Y-axis lies in this plane and points eastwardly. The Z-axis coincides with the zenith.

The ECEF coordinates x_{ECEF}, y_{ECEF}, z_{ECEF} are transformed to topocentric coordinates x_T, y_T, z_T by:

$$\begin{pmatrix} x_T \\ y_T \\ z_T \end{pmatrix} = \begin{pmatrix} \sin\phi\cos\lambda & \sin\phi\sin\lambda & -\cos\phi \\ -\sin\lambda & \cos\lambda & 0 \\ \cos\lambda\cos\phi & \sin\lambda\cos\phi & \sin\phi \end{pmatrix} \begin{pmatrix} x_{ECEF} \\ y_{ECEF} \\ z_{ECEF} \end{pmatrix} \tag{9.15}$$

where λ the longitude and ϕ the latitude of the station are.

The position of a satellite in the topocentric coordinate system is defined by the magnitude of the range R to the satellite, the elevation el (angle between range vector R and the horizon plane) and the azimuth az (angle between north direction and the projection of vector R onto the horizon plane) (figure 9.5).

The distance R is calculated from the station and satellite ECEF-coordinates:

$$R = \sqrt{(x_{satellite} - x_{station})^2 + (y_{satellite} - y_{station})^2 + (z_{satellite} - z_{station})^2} \tag{9.16}$$

The elevation el is determined by:

$$\sin el = \frac{z'_T}{R} \tag{9.17}$$

Using formula 9.15, el is given by:

$$el = \arcsin\left(\frac{x'\cos\phi\cos\lambda + y'\cos\phi\sin\lambda + z'\sin\phi}{\sqrt{x'^2 + y'^2 + z'^2}}\right) \tag{9.18}$$

where

$$\begin{aligned} x' &= x_{satellite} - x_{station} \\ y' &= y_{satellite} - y_{station} \\ z' &= z_{satellite} - z_{station} \end{aligned} \tag{9.19}$$

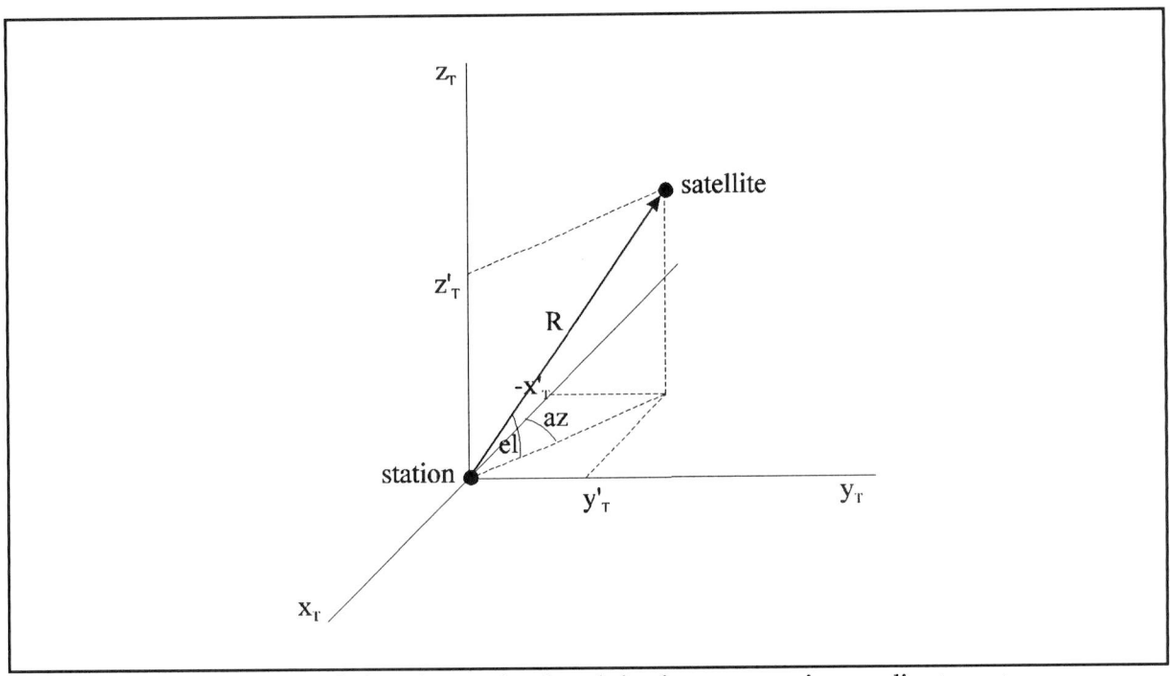

Figure 9.5 Determination of elevation and azimuth in the topocentric coordinate system

The azimuth az is determined by:

$$\cos az = \frac{-x'_T}{R \cos el} \tag{9.20}$$

Using formula 9.15, az is determined by:

$$\cos az = \frac{z' \cos\phi - x' \sin\phi \cos\lambda - y' \sin\phi \sin\lambda}{R \cos el} \tag{9.21}$$

Multiplying nominator and denominator by $\cos\phi$ results in:

$$\cos az = \frac{z' \cos^2\phi - \sin\phi (x' \cos\phi \cos\lambda + y' \cos\phi \sin\lambda)}{R \cos el \cos\phi} \tag{9.22}$$

Formula 9.22 can be written as:

$$\cos az = \frac{z'\cos^2\phi - \sin\phi(x'\cos\phi\cos\lambda + y'\cos\phi\sin\lambda + z'\sin\phi) + z'\sin^2\phi}{R\cos el\cos\phi} \quad (9.23)$$

Finally, the azimuth az is given by:

$$az = \arccos\left(\frac{\frac{z'}{\sqrt{x'^2+y'^2+z'^2}} - \sin(el)\sin\phi}{\cos(el)\cos\phi}\right) \quad (9.24)$$

and x′, y′, z′ as in formula 9.19.

9.5 The simulation model

The GLONASS ionospheric influence simulation model is given in figure 9.6. The model consists of the follwing parts:

- satellite position calculation (ECEF coordinates) (section 9.2)
- conversion of the station geodetic coordinates to ECEF coordinates (section 9.3)
- azimuth and elevation determination (section 9.4)
- the Bent Ionospheric Model (chapter 8, section 8.2); the updating technique [24] is not implemented.

The input data, which will be described in chapter 10, to this model are:

- GLONASS almanac data
- geodetic coordinates of the ground station
- time/date information
- solar input data
- transmission frequency of the satellite

The output data of this model are:

- Total Vertical Electron Content
- Total Angular Electron Content
- Range Error

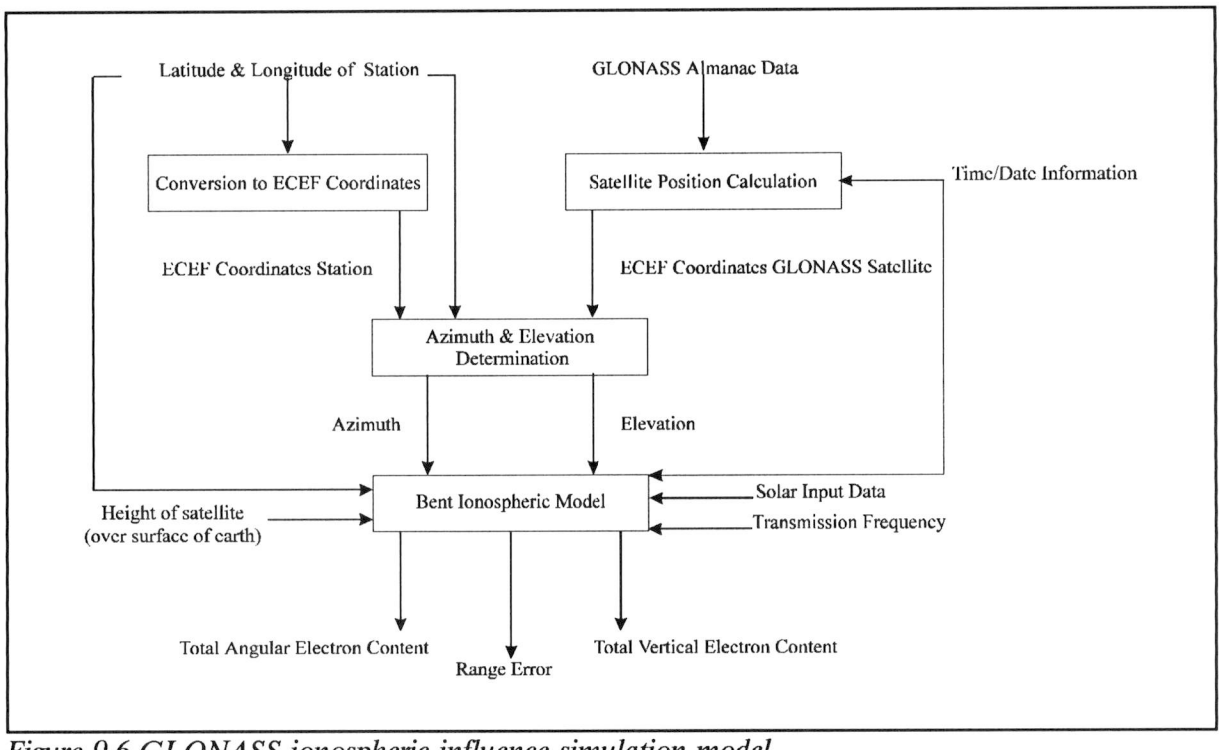

Figure 9.6 GLONASS ionospheric influence simulation model

The model is implemented in Matlab (appendix D). In chapter 10 of this report the results of the simulations will be discussed.

10. Description and evaluation of the simulations

10.1 Introduction

This chapter discusses the simulations performed for March 23rd 1995, assuming high solar activity. For comparison some plots representing low solar activity are given. Section 10.2 describes the input data to the model, followed by a section (section 10.3) discussing the output of the simulations. In section 10.4 the temporal decorrelation of the range error due to the ionosphere is discussed. Section 10.5 discusses the differential error growth of GLONASS as given by the RIRT [29]. From the temporal decorrelation of the range error due to the ionosphere (section 10.4) and the differential error growth of GLONASS as given by the RIRT [26] (section 10.5) the differential GLONASS message update rate will be determined (section 10.6). This chapter will be concluded with a section on sudden changes of the ionosphere. The message update rate determined in this chapter, is based on a more or less standard ionosphere. Sudden changes in the ionosphere may introduce large errors.

10.2 Input to the Bent Ionospheric Model

10.2.1 Position and time information

Simulations were performed for March 23rd 1995. For different locations on earth ranging in latitude from -60 to 60 degrees (in steps of 20 degrees, leaving out the equatorial region) and in longitude from 0 to 180 degrees (latitude 52 degrees, longitude 4 degrees is also included) range errors were determined for a period of 24 hours, with intervals of 6 minutes. Furthermore, the Angular Total Electron Content ($=N_{TA}$ from chapter 8) and Vertical Total Electron Content ($=N_T$ from chapter 8) as well as the elevation to the satellites were determined.

On March 23rd, 16 GLONASS satellites were operational. For the determination of the GLONASS satellite positions (and elevation and azimuth to these satellites) GLONASS

almanac data (appendix E), with week number 793, obtained from the MIT Lincoln Laboratory have been used.

10.2.2 Solar data

The Bent Ionospheric Model requires solar data. This data consist of:

- the 12-month running average (= smoothed) of the sunspot number S_{12} (or SSN)
- the 12-month running average of the solar flux F_{12}

The 12-month running average of the sunspot number represents the activity of the sun: a large S_{12} means high solar activity, a small S_{12} low solar activity. In table 10.1 the values of S_{12} are listed for the period January 1976 to July 1995. This period almost equals two (approximately) 11-year cycles of solar activity (see also figure 10.1). The values of the months April, May, June and July of 1994 are provisional; for the period August 1994 - July 1995 predicted values are given. From table 10.1 and figure 10.1 it can be seen that the sun had a maximum activity during the years 1979 and 1989. In the years 1976 and 1986 a minimum of solar activity was encountered.

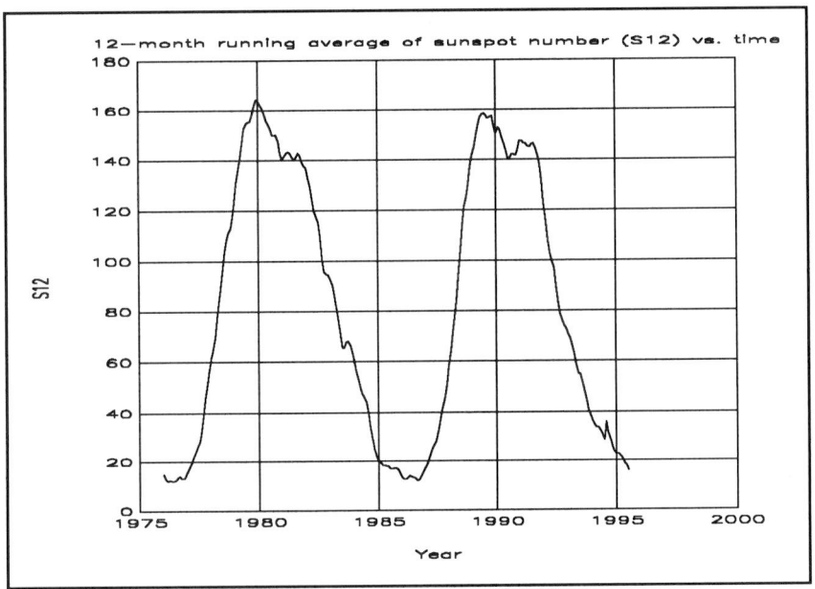

Figure 10.1 The 12-month running average of sunspot number (S_{12}) versus time

To investigate the effect of high solar activity a value of S_{12} had to be assumed: the GLONASS almanac data was valid for week number 793 which is in the period of low solar activity.

Table 10.1 12-month running average of sunspot number (S_{12}) (January 1976 - July 1995)[1]

Year	Month											
	Jan	**Feb**	**Mar**	**Apr**	**May**	**Jun**	**Jul**	**Aug**	**Sep**	**Oct**	**Nov**	**Dec**
1976	15.2	13.2	12.2	12.6	12.5	12.2	12.9	14.0	14.3	13.4	13.5	14.8
1977	16.7	18.1	20.0	22.2	24.2	26.3	29.0	33.4	39.1	45.6	51.9	56.9
1978	61.3	64.5	69.6	76.9	83.2	89.3	97.4	104.0	108.4	111.1	113.3	117.7
1979	123.7	130.9	136.5	141.1	147.2	153.0	155.0	155.4	155.7	157.8	162.3	164.5
1980	163.9	162.6	160.9	158.7	156.3	154.7	152.8	150.3	150.1	150.2	147.7	142.7
1981	140.3	141.5	143.0	143.4	142.9	141.5	140.3	141.1	142.8	142.2	138.9	137.8
1982	137.0	133.3	129.2	124.3	119.9	117.3	115.2	109.4	101.0	95.7	94.7	94.6
1983	92.8	90.3	85.9	81.5	77.1	70.5	65.5	65.8	67.9	68.2	66.8	64.0
1984	60.2	56.4	53.0	49.8	47.5	46.5	44.2	39.6	33.9	28.9	24.7	21.7
1985	20.5	19.6	18.6	18.3	18.3	18.0	17.4	17.1	17.3	17.3	16.8	15.3
1986	13.8	13.1	13.0	13.7	14.3	13.8	13.7	13.2	12.3	13.2	14.9	16.3
1987	17.6	19.6	22.1	24.4	26.5	28.4	31.2	34.8	39.0	43.6	46.7	51.3
1988	58.2	64.6	71.3	77.5	83.8	93.7	104.3	113.7	121.2	125.3	130.4	137.6
1989	142.0	145.0	149.7	153.5	156.9	158.4	158.5	157.7	156.6	157.4	157.5	153.5
1990	150.6	152.9	152.0	149.3	147.0	143.8	140.6	140.5	142.1	142.1	141.7	143.9
1991	147.6	147.6	146.6	146.5	145.5	145.2	146.3	146.6	144.9	141.7	138.1	131.7
1992	123	115	108	103	100	97	90	84	79	76	74	73
1993	71	69	66	63	59	55	55	52	49	45	41	39
1994	37	35	34	34*	33*	31*	29*	36**	32**	29**	26**	24**
1995	23**	23**	22**	21**	19**	18**	16**					

*: Provisional values
**: Predicted values

1 Data obtained from the National Geophysical Data Center (NGDC) of the National Oceanic & Atmospheric Administration (NOAA) in Boulder, Colorado, USA. This data was updated on 1/2/1995.

For the simulations a S_{12}-value of 150 was taken. As an assumed S_{12}-value was used in the simulations, the value of F_{12} had to be approximated from S_{12}. This was done by applying formula [24]:

$$F_{12}^{approximate} = 63.75 + 0.728 \times S_{12} + 0.00089 \times S_{12}^2 \qquad (10.1)$$

giving a F_{12}-value of approximately 193 (10^{-22} Wm^{-2} Hz^{-1}).

10.3 Output of the Bent Ionospheric Model

The Bent Ionospheric Model outputs the Vertical Total Electron Content (VTEC), the Angular Total Electron Content (ATEC) and the Range Error. In this section representative plots are given for VTEC, ATEC and range error for space vehicles (SV) 205 and 2401 and latitude 52° and longitude 4°.

10.3.1 The Vertical Total Electron Content

In figures 10.2 and 10.3 the Vertical Total Electron Content is plotted versus the time of day. These figures show the variability of the VTEC during satellite passages of SV 205 and SV 2401. The VTEC is smaller at night-time than at day-time: night-time values are in the range of about 3×10^{17} to 5×10^{17} el/m^2; day-time values range from about 5×10^{17} to 9×10^{17} el/m^2 (SSN = 150). Furthermore, differences between figures 10.2 and 10.3 can be seen. These differences are caused by the fact that signals, originating from different satellites, will pass through different parts of the ionosphere. This means different ionospheric points, different local geomagnetic conditions and different solar influence. As a result the VTEC values will be different.

10.3.2 The Angular Total Electron Content

The ionospheric propagation delay depends on the elevation angle at which the signals from the satellites are received: at lower elevation angles the total number of free electrons encountered on the propagation path is larger than at higher elevations. In figures 10.4 and

10.5 the elevation angle (≥ 5 degrees) during the satellite passages is plotted versus the time of day (SV's 205 and 2401).

The Vertical Total Electron Content has to be corrected for this changing elevation angle: this results in the Angular Total Electron Content. In figures 10.6 and 10.7 the ATEC is plotted versus the time of day.

Correcting the VTEC for changing elevation angles, increases the actual total electron content encountered on the transmission path by a factor of about 1 at high elevation angles (nearly 90 degrees) to 3 at low elevation angles (about 5 degrees). Furthermore, the figures show an increasing ATEC when the elevation angle decreases. At a maximum elevation angle the ATEC has a minimum value.

10.3.3 The range error

The ATEC causes a propagation delay of the signals transmitted by the satellites, resulting in a range error. In figures 10.8 and 10.9 the range error (SV's 205 and 2401) is plotted versus the time of day. Range errors from about 10 to 40 m can be observed during a satellite passage.

Figures 10.8 and 10.9 have the similar shape as figures 10.6 and 10.7 indicating the strong ATEC-dependency (and implicitly elevation-dependency) of the ionospheric range error.

10.3.4 Solar activity

One of the factors influencing the range error is the solar activity. During high solar activity the VTEC (and ATEC) values are larger. To illustrate the effect of solar activity plots of VTEC, ATEC and range error are given for SV 2401 and SSN = 20 (representing a solar minimum). From these figures (10.10 to 10.12) the lower VTEC, ATEC and range error values due to lower solar activity can be seen.

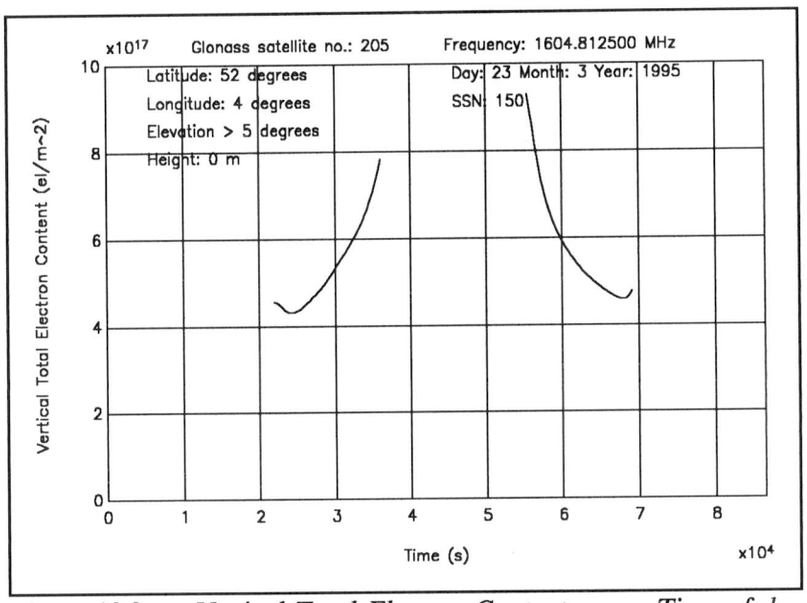

Figure 10.2 Vertical Total Electron Content versus Time of day (SV = 205)

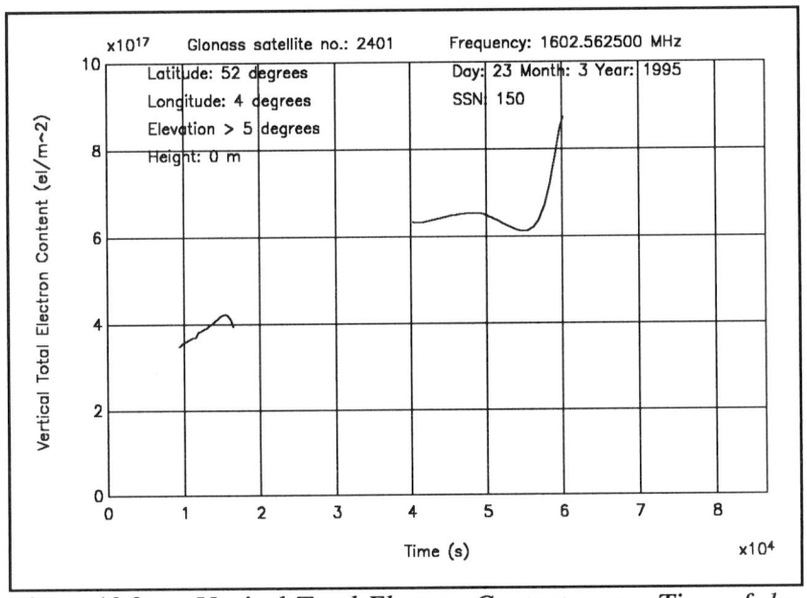

Figure 10.3 Vertical Total Electron Content versus Time of day (SV = 2401)

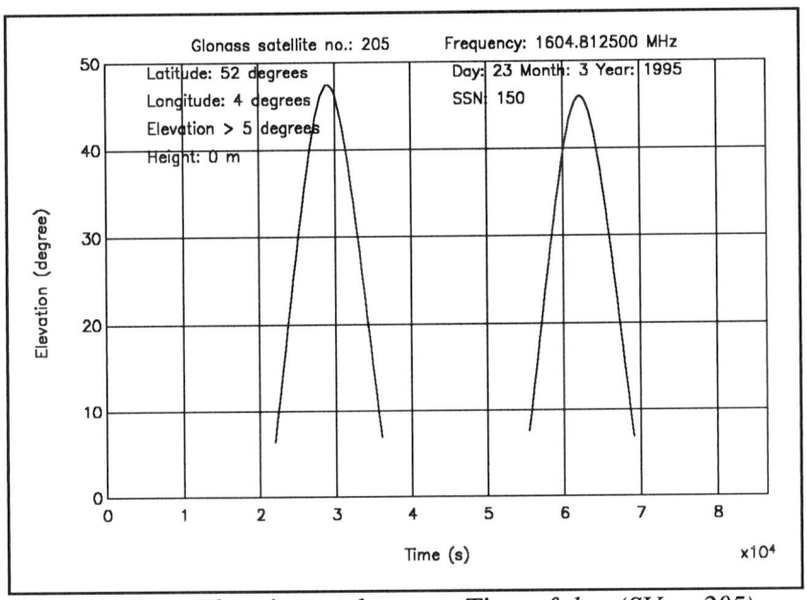

Figure 10.4 Elevation angle versus Time of day (SV = 205)

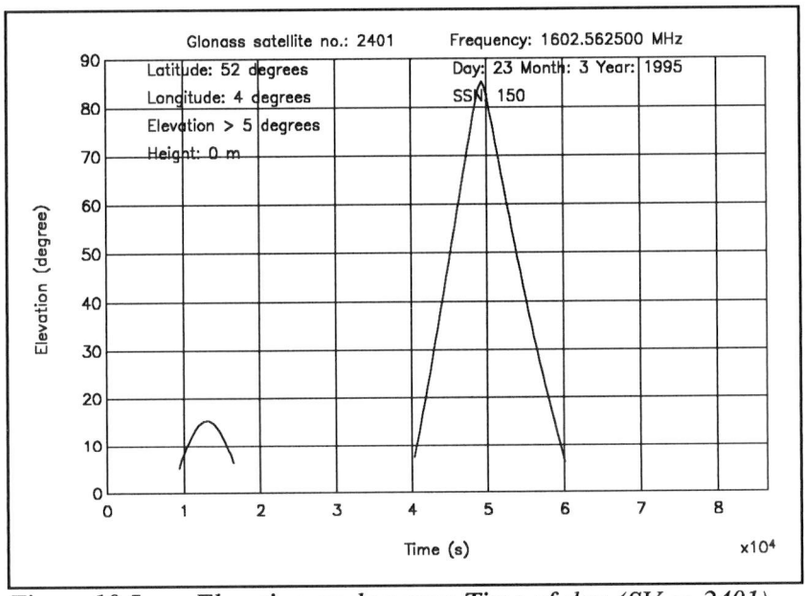

Figure 10.5 Elevation angle versus Time of day (SV = 2401)

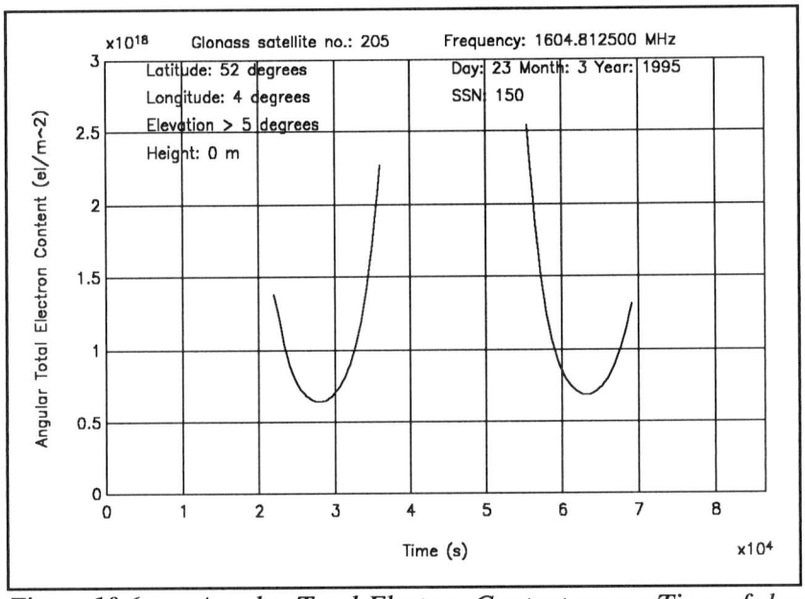

Figure 10.6 Angular Total Electron Content versus Time of day (SV = 205)

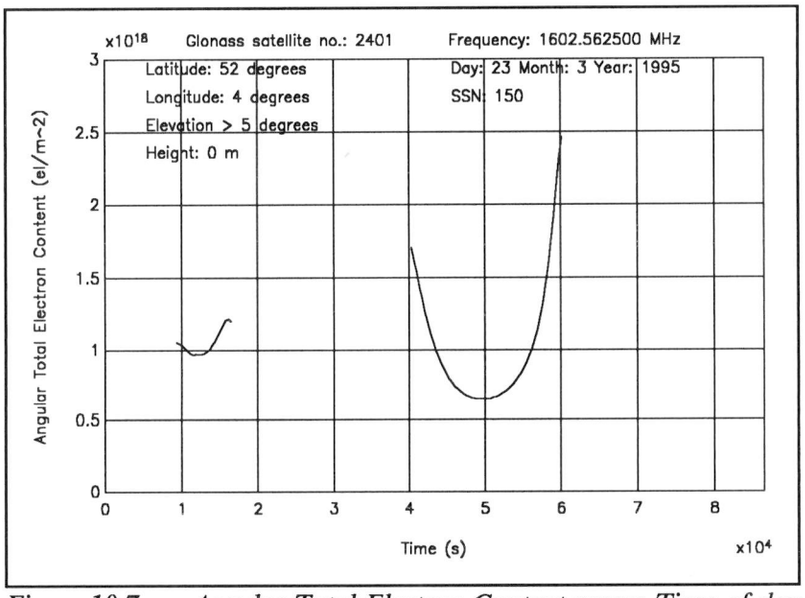

Figure 10.7 Angular Total Electron Content versus Time of day (SV = 2401)

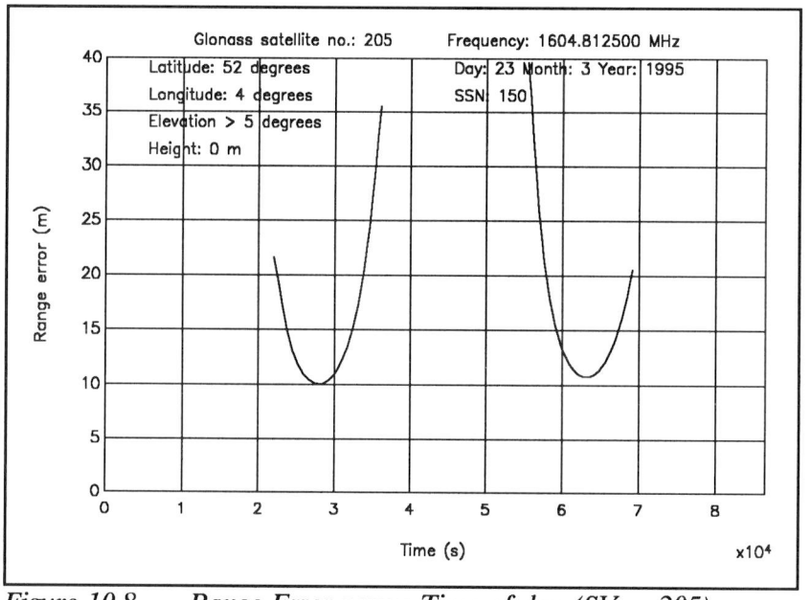

Figure 10.8 Range Error versus Time of day (SV = 205)

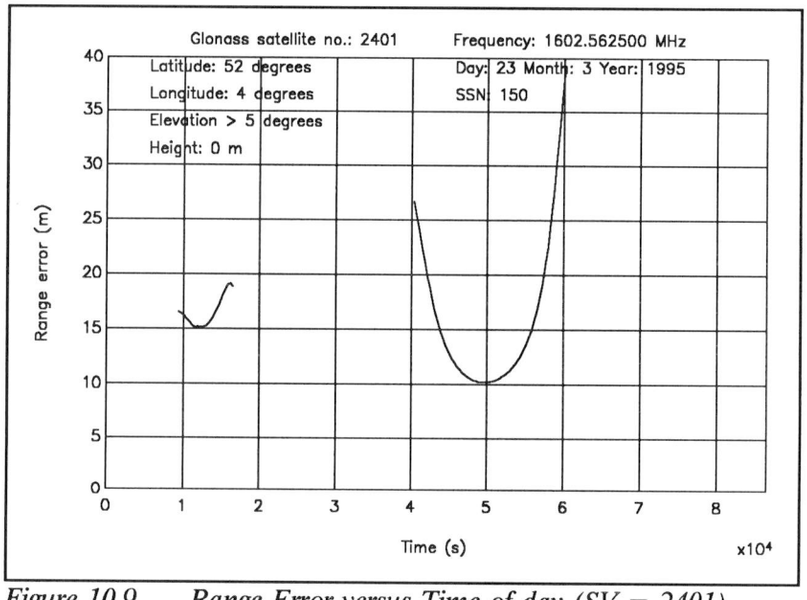

Figure 10.9 Range Error versus Time of day (SV = 2401)

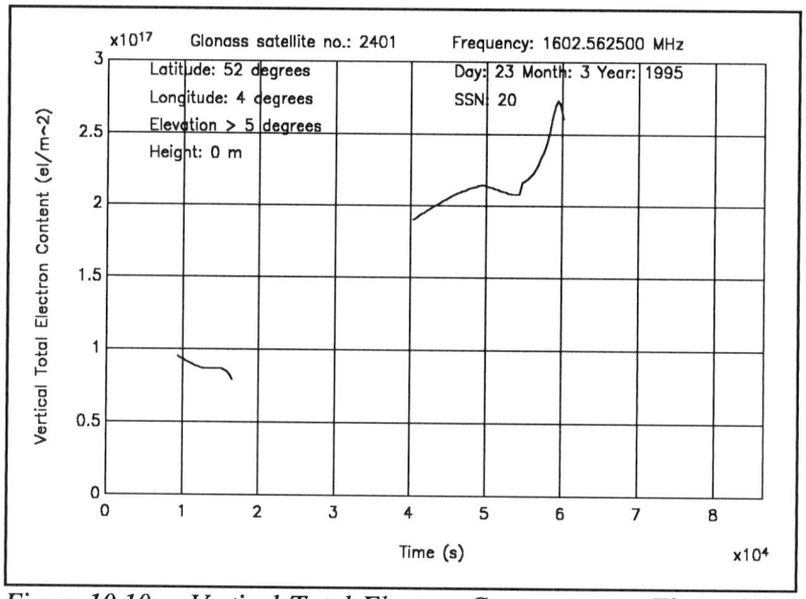

Figure 10.10 Vertical Total Electron Content versus Time of day (SV = 2401, SSN = 20)

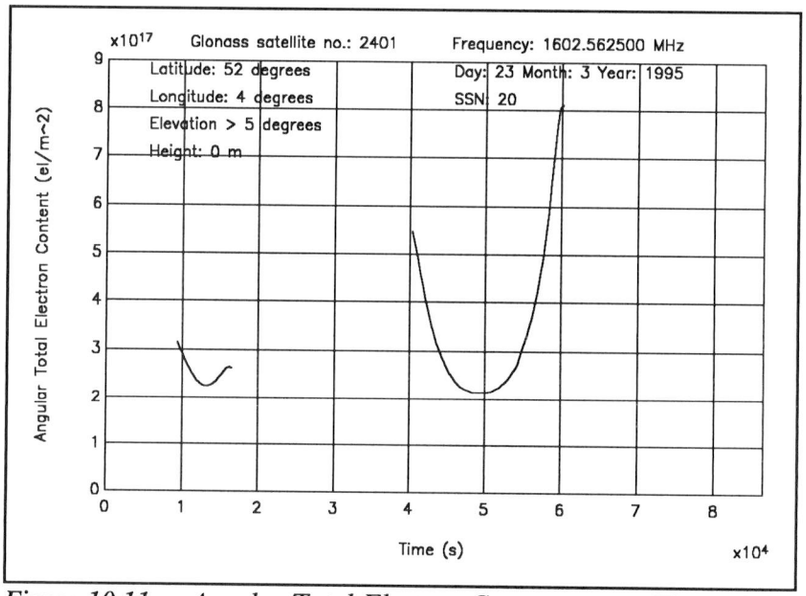

Figure 10.11 Angular Total Electron Content versus Time of day (SV = 2401, SSN = 20)

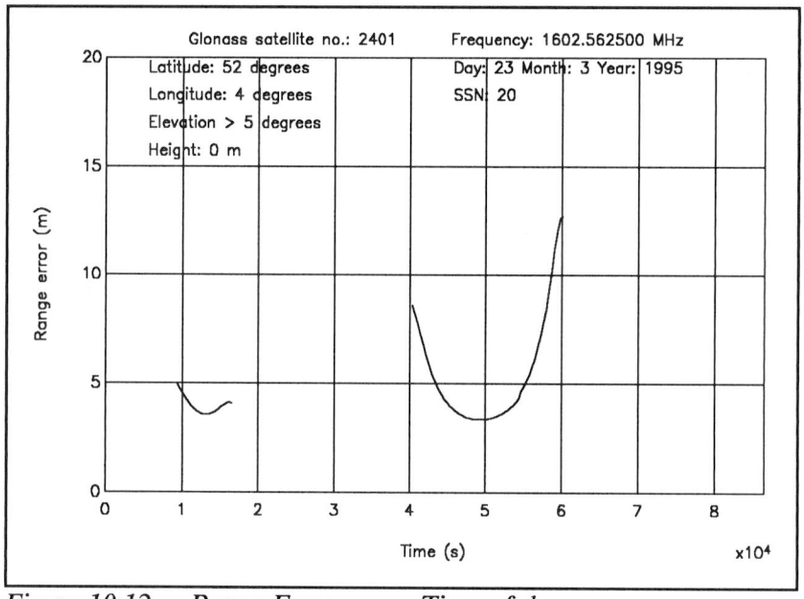

Figure 10.12 Range Error versus Time of day (SV = 2401, SSN = 20)

10.4 Temporal decorrelation

10.4.1 RMS Range Error Difference plots

The Bent Ionospheric Model outputs range errors for every 360s interval. Within these intervals, the course of the range errors is not expected to differ much from the smooth curves presented in section 10.3 (the ionosphere is not expected to change dramatically in short periods). Therefore, values of the range errors at intervals of 10 seconds are obtained by cubic spline data interpolation[2]. These range errors x(t) are put into vector **x(t)**:

$$\mathbf{x(t)} = \begin{bmatrix} x(t_1) \\ x(t_2) \\ . \\ . \\ x(T) \end{bmatrix} \qquad t_1 = 10s,\ t_2 = 20s, \ldots,\ T = n_1 \times 10s \qquad (10.2)$$

where n_1 is the number of intervals of 10 seconds in the period of a satellite passage.

2 Determination of the range errors for 16 satellites during a period of 24 hours requires a lot of processing time. Using intervals of 360 seconds required approximately 1.5 hours on a 486DX2-66 MHz personal computer. Therefore the range errors on the 10 second intervals are determined by interpolation.

To investigate the ionospheric error contribution to the pseudorange error the RMS Range Error Difference Function $Y(\tau)$ is used[3]. This function is given by:

$$Y(\tau) = \left(E\left\{ \left[x(t+\tau) - x(t) \right]^2 \right\} \right)^{\frac{1}{2}} \tag{10.3}$$

$Y(\tau)$ is a measure of the decorrelation of the function x(t) (in this case, x(t) is the pseudorange error as a function of time) over an interval τ. The temporal decorrelation of the range error strongly depends on the moment of update. Therefore formula 10.3 is applied to different subsets of vector **x(t)**, vector **x(t')**:

$$\mathbf{x(t')} = \begin{bmatrix} x(t_1') \\ x(t_2') \\ . \\ . \\ x(T) \end{bmatrix} \qquad t_1' = t_1 + n_2 \times 10s,\ t_2' = t_2 + n_2 \times 10s, \ldots, T = n_1 \times 10s \tag{10.4}$$

where n_2 is the number of intervals of 10 seconds since the satellite came into view.

First time SV in view

Figures 10.13 and 10.14 show the plots of the RMS Range Error Difference of the range errors of SV's 205 and 2401 (in meters) versus the time τ (in seconds) since the SV's where for the first time in view during a passage (= moment of update). In table 10.2 the 1-σ values and the corresponding horizontal position errors are listed for τ = 60, 120, 180, 240, 300 and 360 seconds.

After 60 seconds the 1-σ differential range error is in the range of 0.1 to 0.2 meters. If a HDOP of 1.5[4] is assumed, the corresponding position error (95%) ranges form 0.3 to 0.6

---

3 This method is applied earlier in investigations of the effect of Selective Availability on differential GPS corrections [30].

4 Determination of the 95% horizontal position accuracy given by 2×HDOP×σ is a conservative approach: it assumes equal σ's for all visible satellites. These σ's are elevation dependent. Usually, low-elevation angle satellites (largest ionospheric errors) will be left out of the position solution and the real σ-values will be smaller.

meters. After 360 seconds the 1-σ differential range error has the range of 0.3 to 1.4 meters. Again assuming a HDOP of 1.5 gives a 95%-position error ranging from 0.9 to 4.2 meters.

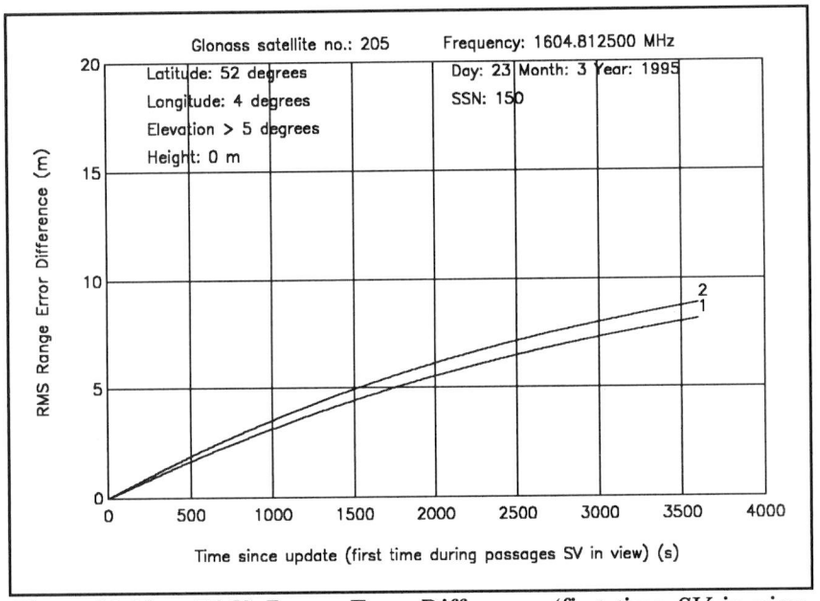

Figure 10.13 RMS Range Error Difference (first time SV in view, 2 passages of SV 205)

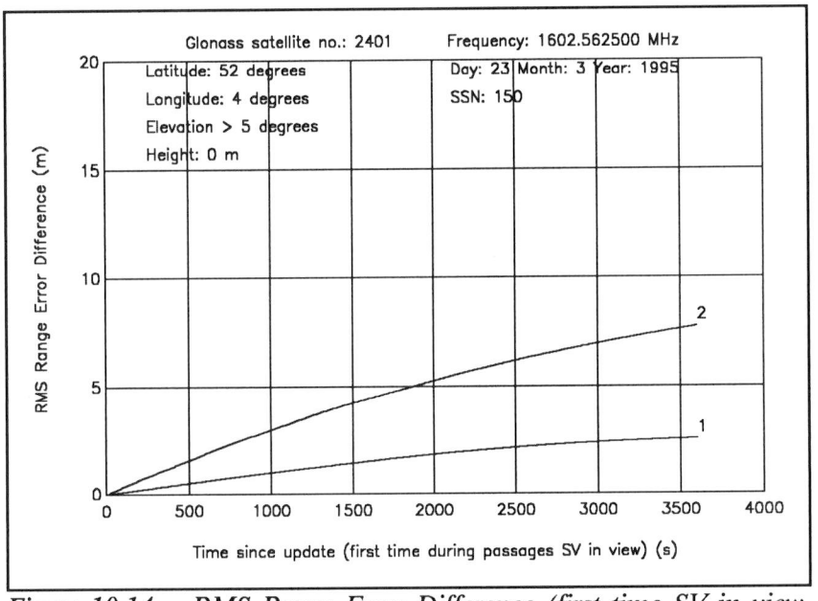

Figure 10.14 RMS Range Error Difference (first time SV in view, 2 passages of SV 2401)

Table 10.2 *1-σ values and position errors (τ = 60, 120, 180, 240, 300 and 360 s, HDOP = 1.5, first time SV in view, RMS Range Error Difference)*

	SV = 205				SV = 2401			
	1-σ (m)		position error (m) (95%, HDOP=1.5)		1-σ (m)		position error (m) (95%, HDOP=1.5)	
	1st	2nd	1st	2nd	1st	2nd	1st	2nd
τ=60 s	0.2	0.2	0.6	0.6	0.1	0.2	0.3	0.6
τ=120 s	0.4	0.5	1.2	1.5	0.1	0.4	0.3	1.2
τ=180 s	0.6	0.7	1.8	2.1	0.2	0.6	0.6	1.8
τ=240 s	0.8	0.9	2.4	2.7	0.2	0.8	0.6	2.4
τ=300 s	1.0	1.2	3.0	3.6	0.3	0.9	0.9	2.7
τ=360 s	1.2	1.4	3.6	4.2	0.3	1.1	0.9	3.3

Minimum range error

Figures 10.15 and 10.16 show the plots of the RMS Range Error Difference of the range errors of SV's 205 and 2401 (in meters) versus the time τ (in seconds) since the moment of maximum elevation angle (= minimum range error) to the SV's (= moment of update). In table 10.3 the 1-σ values and the corresponding horizontal position errors are listed for τ = 60, 120, 180, 240, 300 and 360 seconds. The 1-σ values and 95%-position errors are in the same order of magnitude as the values of table 10.2.

After 60 seconds the 1-σ differential range error is in the range of 0.1 to 0.2 meters. If a HDOP of 1.5 is assumed, the corresponding position error (95%) ranges from 0.3 to 0.6 meters. After 360 seconds the 1-σ differential range error has the range of 0.4 to 1.4 meters. Again assuming a HDOP of 1.5 gives a 95%-position error ranging from 1.2 to 4.2 meters.

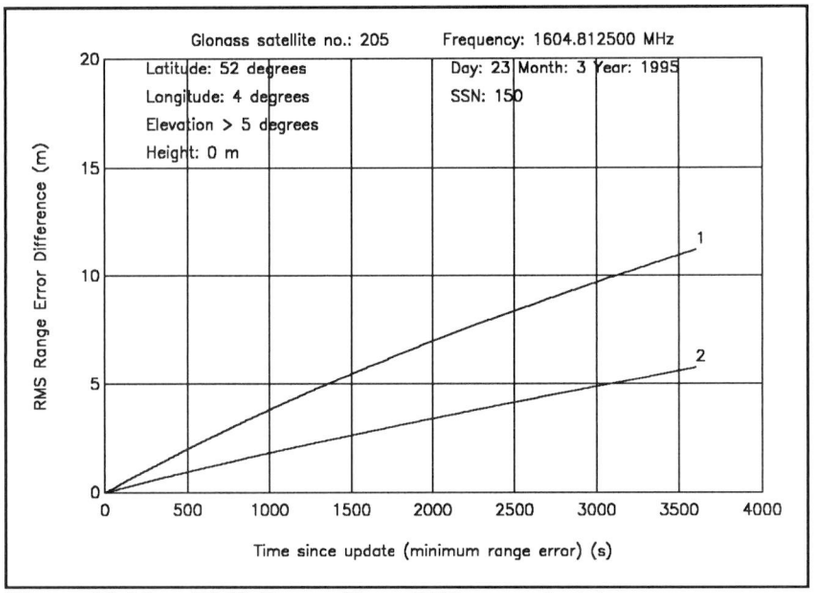

Figure 10.15 RMS Range Error Difference (minimum range error, 2 passages of SV 205)

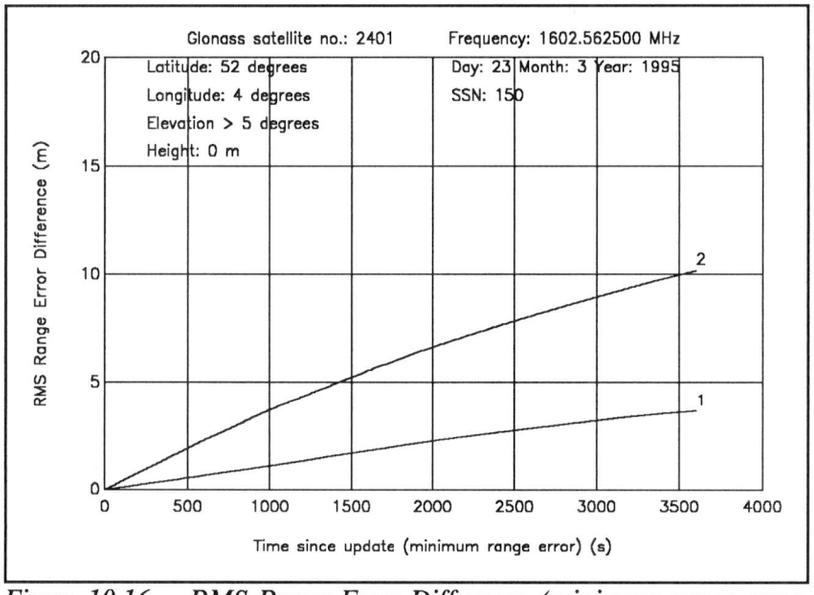

Figure 10.16 RMS Range Error Difference (minimum range error, 2 passages of SV 2401)

Table 10.3 1-σ values and position errors (τ = 60, 120, 180, 240, 300 and 360 s, HDOP = 1.5, minimum range error, RMS Range Error Difference)

	SV = 205				SV = 2401			
	1-σ (m)		position error (m) (95%, HDOP=1.5)		1-σ (m)		position error (m) (95%, HDOP=1.5)	
	1st	2nd	1st	2nd	1st	2nd	1st	2nd
τ=60 s	0.2	0.1	0.6	0.3	0.1	0.2	0.3	0.6
τ=120 s	0.5	0.2	1.5	0.6	0.1	0.5	0.3	1.5
τ=180 s	0.7	0.4	2.1	1.2	0.2	0.7	0.6	2.1
τ=240 s	1.0	0.5	3.0	1.5	0.3	0.9	0.9	2.7
τ=300 s	1.2	0.6	3.6	1.8	0.3	1.2	0.9	3.6
τ=360 s	1.4	0.7	4.2	2.1	0.4	1.4	1.2	4.2

10.4.2 RMS Extrapolated Range Error Difference plots

The proposed RTCM SC-104 Message Type 31: differential GLONASS corrections include range rate corrections. These range rate corrections compensate for the predicted rate of change of the pseudorange correction. Including range rate corrections in the differential GLONASS messages should reduce the error growth. The RMS Extrapolated Range Error Difference Function estimates the effect of including range rate corrections. If formula 10.3 is modified, the RMS Extrapolated Range Error Difference Function can be obtained[5]:

$$Y(\tau) = \left(E\left\{ \left[x(t+\tau) - (x(t) + \tau \dot{x}(t)) \right]^2 \right\} \right)^{\frac{1}{2}} \qquad (10.5)$$

In formula 10.5 $\dot{x}(t)$ is the range error rate as a function of time. The range error rate as a function of time is determined from the range errors by derivation.

5 This method is applied earlier in investigations of the effect of Selective Availability on differential GPS corrections [30].

First time SV in view

Figures 10.17 and 10.18 show the plots of the RMS Extrapolated Range Error Difference of the range errors of SV's 205 and 2401 (in meters) versus the time τ (in seconds) since the SV's where for the first time in view during a passage (= moment of update). In table 10.4 the 1-σ values and the corresponding horizontal position errors are listed for τ = 60, 120, 180, 240, 300 and 360 seconds.

After 60 seconds the 1-σ differential range error is in the range of 0.1 to 0.2 meters. If a HDOP of 1.5 is assumed, the corresponding position error (95%) ranges form 0.3 to 0.6 meters. After 360 seconds the 1-σ differential range error has the range of 0.3 to 1.3 meters. Again assuming a HDOP of 1.5 gives a 95%-position error ranging from 0.9 to 3.9 meters.

Table 10.4 *1-σ values and position error (τ = 60, 120, 180, 240, 300 and 360 s, HDOP = 1.5, first time SV in view, RMS Extrapolated Range Error Difference)*

	SV = 205				**SV = 2401**			
	1-σ (m)		**position error (m) (95%, HDOP=1.5)**		**1-σ (m)**		**position error (m) (95%, HDOP=1.5)**	
	1st	**2nd**	**1st**	**2nd**	**1st**	**2nd**	**1st**	**2nd**
τ=60 s	0.2	0.2	0.6	0.6	0.1	0.2	0.3	0.6
τ=120 s	0.4	0.4	1.2	1.2	0.1	0.4	0.3	1.2
τ=180 s	0.6	0.7	1.8	2.1	0.2	0.5	0.6	1.5
τ=240 s	0.8	0.9	2.4	2.7	0.2	0.7	0.6	2.1
τ=300 s	0.9	1.1	2.7	3.3	0.3	0.9	0.9	2.7
τ=360 s	1.1	1.3	3.3	3.9	0.3	1.0	0.9	3.0

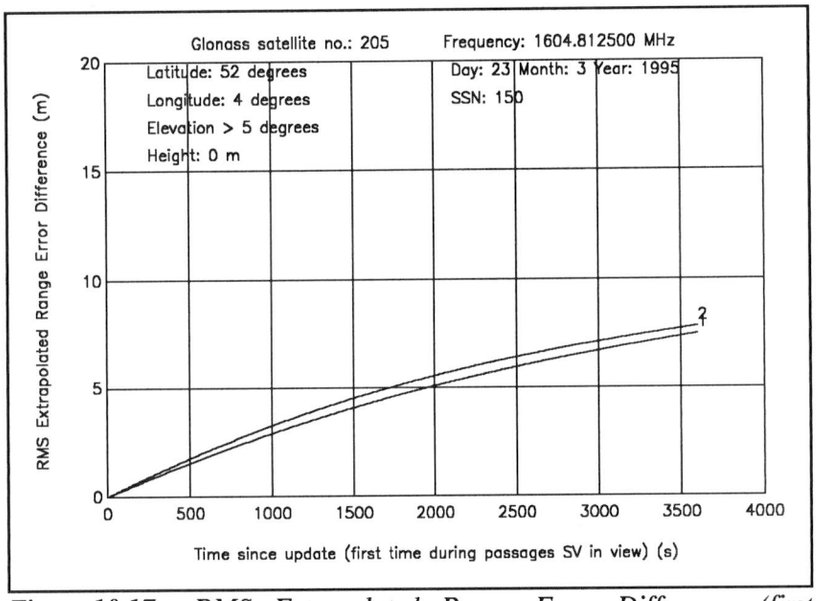

Figure 10.17 RMS Extrapolated Range Error Difference (first time SV in view, 2 passages of SV 205)

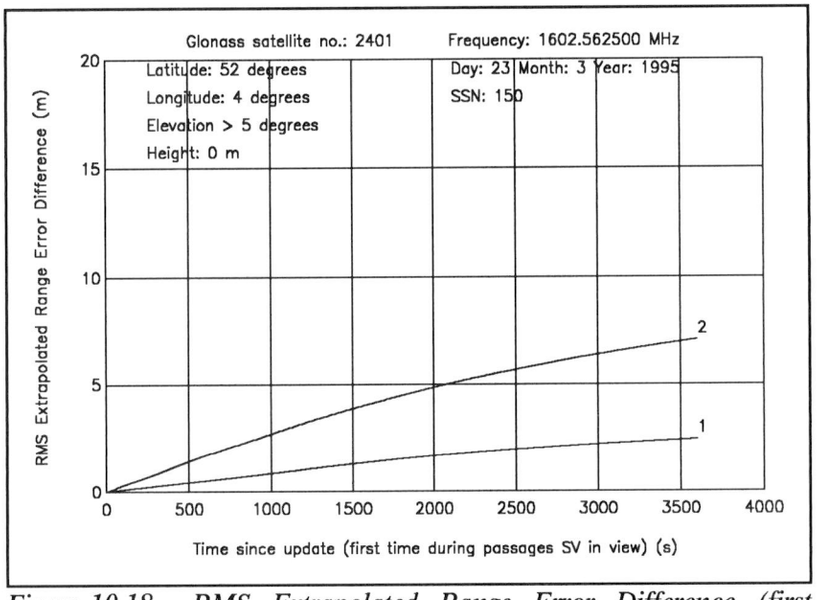

Figure 10.18 RMS Extrapolated Range Error Difference (first time SV in view, 2 passages of SV 2401)

Minimum range error

Figures 10.19 and 10.20 show the plots of the RMS Extrapolated Range Error Difference of the range errors of SV's 205 and 2401 (in meters) versus the time τ (in seconds) since the moment of maximum elevation angle (= minimum range error) to the SV's (= moment of update). In table 10.5 the 1-σ values and the corresponding horizontal position errors are listed for τ = 60, 120, 180, 240, 300 and 360 seconds. The 1-σ values and 95%-position errors are in the same order of magnitude as the values of table 10.4.

After 60 seconds the 1-σ differential range error is in the range of 0.1 to 0.2 meters. If a HDOP of 1.5 is assumed, the corresponding position error (95%) ranges form 0.3 to 0.6 meters. After 360 seconds the 1-σ differential range error has the range of 0.4 to 1.3 meters. Again assuming a HDOP of 1.5 gives a 95%-position error ranging from 1.2 to 3.9 meters.

Table 10.5 *1-σ values and position error (τ = 60, 120, 180, 240, 300 and 360 s, HDOP = 1.5, minimum range error, RMS Extrapolated Range Error Difference)*

	SV = 205				**SV = 2401**			
	1-σ (m)		**position error (m) (95%, HDOP=1.5)**		**1-σ (m)**		**position error (m) (95%, HDOP=1.5)**	
	1st	**2nd**	**1st**	**2nd**	**1st**	**2nd**	**1st**	**2nd**
τ=60 s	0.2	0.1	0.6	0.3	0.1	0.2	0.3	0.6
τ=120 s	0.5	0.2	1.5	0.6	0.1	0.4	0.3	1.2
τ=180 s	0.7	0.3	2.1	0.9	0.2	0.7	0.6	2.1
τ=240 s	0.9	0.4	2.7	1.2	0.2	0.9	0.6	2.7
τ=300 s	1.1	0.5	3.3	1.5	0.3	1.1	0.9	3.3
τ=360 s	1.3	0.6	3.9	1.8	0.4	1.3	1.2	3.9

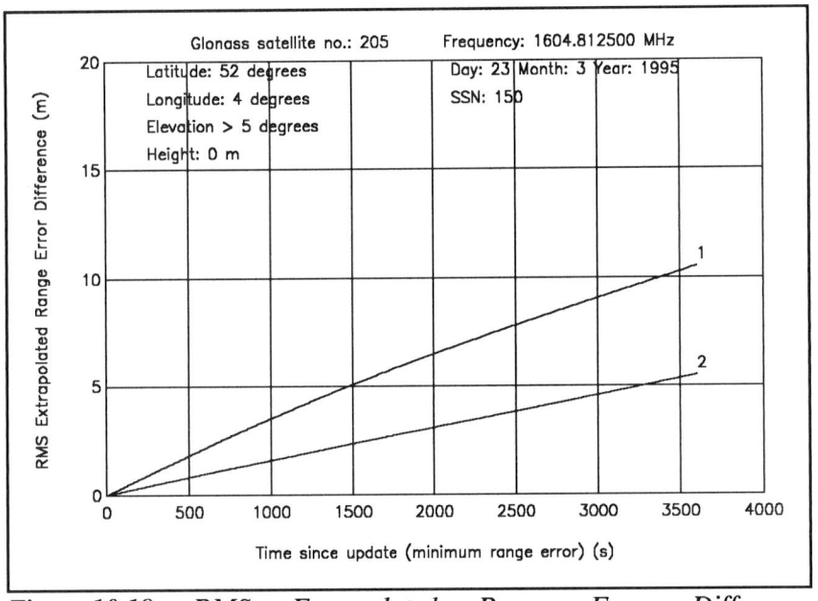

Figure 10.19 RMS Extrapolated Range Error Difference (minimum range error, 2 passages of SV 205)

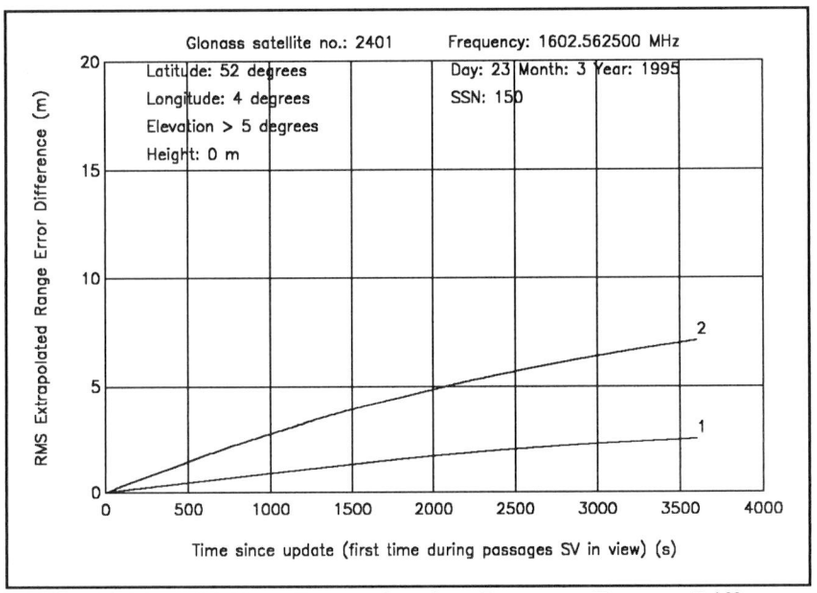

Figure 10.20 RMS Extrapolated Range Error Difference (minimum range error, 2 passages of SV 2401)

10.5 Differential error growth

Temporal decorrelation results in a position error. Assuming an average HDOP of 1.5, the DGLONASS position error (95%) can be approximated conservatively by [29]:

$$S(t) = \sqrt{S_0^2 + \left(\frac{1}{2}S_\Sigma t^2\right)^2} \tag{10.6}$$

where S_0 = 0.4 m and S_Σ = 0.00014 m/s^2. This function is plotted in figure 10.21. In this figure, the differential error growth for DGPS is also given. The positioning error growth for DGPS is mainly determined by SA, having a nominal SA pseudorange acceleration of 0.0037 m/s^2 [12]. Assuming a HDOP of 1.5 the DGPS position error can be approximated (also conservatively) by [29]:

$$S(t) = \sqrt{S_0^2 + \left(\frac{1}{2}S_\Sigma t^2\right)^2 + \left(\frac{1}{2}at^2\right)^2} \tag{10.7}$$

with S_0 = 0.4 m, S_Σ = 0.00014 m/s^2 and a = 0.011 m/s^2.

From figure 10.21 it can be seen that the position accuracy of DGLONASS is still within 5 m (95%) after 4 minutes. For DGPS a position error of 5 m has already been reached after 30 seconds.

Using formula 10.6 (and 10.7) the DGLONASS and DGPS position errors (when transmitting DGLONASS corrections together with DGPS corrections) can be investigated (see chapter 11). But is formula 10.6 in agreement with the results of the simulations presented in this chapter? Therefore, the position error growth for the first passage of SV 205 is also displayed in figure 10.21 (assuming an HDOP of 1.5, see figure 10.13). It can be seen that for short periods after moment of update (up to 200 seconds), the differential error growth as given by [29] approximates the results of the simulations. Due to the quadratic factor in formula 10.6, the error growth as given by [29], will diverge from the error growth determined in the simulations after long periods (> 200 seconds). The cause of this quadratic factor is not known at this moment. Future research will have to clarify this fact. Therefore, for relatively short periods it is suited to use formula 10.6 (together with formula 10.7) to determine

DGLONASS/DGPS position errors when transmitting DGLONASS corrections together with DGPS corrections through the same datalink (see chapter 11).

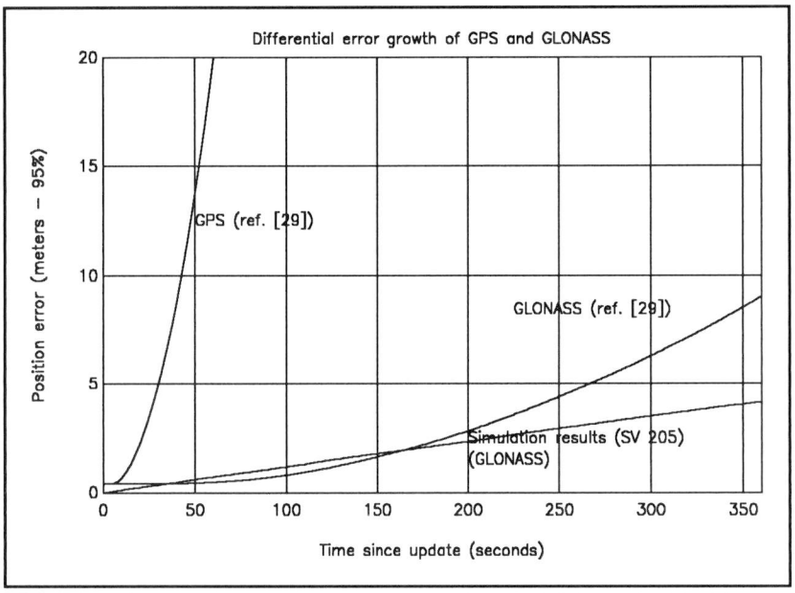

Figure 10.21 Differential error growth of GPS and GLONASS according to [29] and simulation results

10.6 The DGLONASS message update rate

The DGLONASS message update rate mainly depends on the accuracy and the time to alarm (integrity). In Eurofix, the integrity will be serviced by transmission of integrity messages (chapter 11). So, the accuracy is really the factor determining the update rate.

The FRP requires a horizontal position accuracy (95%) of 8-20 meters for harbour approaches [9]. From the simulations and the differential error growth displayed in figure 10.21, it can be seen that the 95%-accuracy is still within 5 meters after approximately 4 minutes. So, a DGLONASS correction message can have a latency of approximately 4 minutes. Depending on the time elapsed between the generation of the correction and the moment the correction is available to the user, the update rate can be determined. For example: assuming it will take 2 minutes before a generated correction (for one satellite) is available to the user, the correction will have to be used for another 2 minutes. In this case the minium update rate is one message (for one satellite) per 2 minutes.

10.7 Sudden ionospheric changes

In the ionosphere sudden changes may occur in the TEC. As the Bent Ionospheric Model represents (more or less) a standard ionosphere, these changes were not taken into account when determining the GLONASS differential correction message update rate. The major source of variation in the TEC from monthly mean conditions is due to geomagnetic activity. The Bent Ionospheric Model is not capable of sufficiently predicting the behaviour of the TEC during magnetic storms, caused by solar activity.

Sudden ionospheric changes may lead to unusable range measurements which have to be discarded. This results in an integrity problem. This problem is beyond the scope of this report and should be investigated in the future.

11. Integration of GLONASS into Eurofix

11.1 Introduction

Integration of GLONASS into Eurofix will have its consequences. First of all the Eurofix message format has to be enlarged with a differential GLONASS correction message (section 11.2). As differential GLONASS and GPS corrections are to be transmitted through the same datalink, the effective DGPS update rate will reduce and thus the GPS position accuracy will degrade. In section 11.3 this problem is discussed and illustrated with examples.

As discussed in chapter 2, GLONASS and GPS show some differences. The consequences of these differences on Eurofix supporting DGLONASS and DGPS will be discussed in section 11.4.

11.2 A proposed DGNSS-Eurofix message format

In chapter 6 of this report differential GLONASS messages as proposed by the RIRT and the RTCM SC-104 have been discussed. As the currently proposed RTCM SC-104 differential GPS messages (Version 2.1) are widely accepted, it is to be expected that this will be the case for the proposed RTCM DGLONASS messages as well. The RTCM proposed to enlarge the DGPS standards with *new* messages supporting the differential use of GLONASS. These messages have the same format (as far as this is possible) in which the differential GPS messages are transmitted.

Due to the low bitrate of the Eurofix datalink it is not possible to transmit the DGNSS messages in the RTCM format. Therefore an asynchronous Eurofix data format has been proposed which is convertible to the RTCM format (see chapter 4 and [7]). To service the differential use of GLONASS as well, the Eurofix data format has to be enlarged. It is proposed to add one new message type: *Asynchronous GLONASS pseudorange correction*. For reasons of commonality this new message type is transmitted in the same format as the

Asynchronous GPS pseudorange correction is. The Eurofix data format may consist of 4 message types:

type 1: Asynchronous GPS pseudorange correction
type 2: Delta Asynchronous pseudorange correction (like RTCM SC-104 message type 2: old navigation data)
type 3: Asynchronous GLONASS pseudorange correction
type 4: Integrity message

The message types 1 and 3 are almost similar (table 11.1). There is one difference. GPS transmits the Issue of Data (IOD). In GLONASS an IOD is not transmitted. Instead of the IOD the T_b (chapter 2, appendix A), transmitted by GLONASS, can be used. T_b has a length of 7 bits. The IOD is 8 bits long. So, there is 1 spare bit in the type 3 message.

Table 11.1 The asynchronous GPS/GLONASS pseudorange correction

Function	**Number of bits**	**Range**	**Resolution**
Message No.	2	4 messages	
Satellite ID	5	32 satellites	
Issue of Data (IOD)/T_b *)	8		
Time Reference	10	1 hour	3.6 seconds
Range	12	-655.32...+655.32 m	0.32 m
Range Rate	7	-2.048...+2.048 m/s	0.032 m/s
UDRE	1	2 states	
Total Number of bits	45		

*) Depending on the message type IOD (type 1) or T_b (type 3) is transmitted.

11.3 Transmission of GPS and GLONASS pseudorange corrections

Eurofix had been proposed to provide GPS users with differential corrections. If Eurofix is also to be used to provide GPS/GLONASS users (and GLONASS-only users) with differential GLONASS corrections, transmission of GLONASS pseudorange corrections certainly will affect the GPS performance. This will be explained by some examples. In these examples the horizontal position errors in meters (95%, HDOP 1.5) of GPS and GLONASS are given by [12, 29]:

$$S_{GPS}(t) = \sqrt{(0.4)^2 + \left(\frac{1}{2}0.00014t^2\right)^2 + \left(\frac{1}{2}0.011t^2\right)^2}$$
$$S_{GLONASS}(t) = \sqrt{(0.4)^2 + \left(\frac{1}{2}0.00014t^2\right)^2} \qquad (11.1)$$

The average position error (in meters) is calculated by:

$$\bar{S} = \sqrt{\frac{1}{t_2 - t_1}\int_{t_1}^{t_2} S^2(t)dt} \qquad (11.2)$$

where S(t) is $S_{GLONASS}(t)$ or $S_{GPS}(t)$.

In examples 1 and 2, 9 GPS corrections and 9 GLONASS corrections are transmitted. In example 1 this is done with a data rate of 15 bps. In example 2 a data rate of 30 bps is assumed. The sequence of transmission is as follows: 9 GPS correction messages followed by 3 GLONASS corrections. After these corrections 9 new GPS corrections and the next 3 GLONASS corrections are transmitted. The sequence is concluded with 9 new GPS corrections and the last 3 (of the 9) GLONASS corrections.

Example 1

The following is assumed:

Data rate:	15 bps
Message length:	45 bits (≙ 3 seconds)
Number of GPS satellites:	9

Number of GLONASS satellites: 9

With a transmission time of 3 seconds per message the interval of use of a GPS pseudorange correction is 3 to 39 (13 message lengths) seconds; for GLONASS the interval is 3 to 111 (37 message lengths) seconds. The resulting position error ranges for GPS from 0.4 to 8.4 meters (95%), with an average of 3.9 meters; for GLONASS this is 0.4 to 1.0 meters (95%), with an average of 0.6 meters.

Example 2

The following is assumed:

Data rate:	30 bps
Message length:	45 bits (≙ 1.5 seconds)
Number of GPS satellites:	9
Number of GLONASS satellites:	9

Assuming the same transmission sequence as in example 1 this results in an interval of use for GPS ranging from 1.5 to 19.5 (13 message lengths) seconds and for GLONASS 1.5 to 55.5 (37 message lengths) seconds. This results in a GPS position error from 0.4 to 2.1 meters (95%), with an average of 1.1 meters and a GLONASS position error ranging from 0.4 to 0.5 meters (95%), with an average of approximately 0.4 meters.

In examples 1 and 2 it is assumed that each GLONASS and GPS correction message is transmitted and received correctly. What will happen if 1 GLONASS or 1 GPS message is received incorrectly or even missed? This will be illustrated by examples 3 and 4: in example 3 one GLONASS message is missed, in example 4 one GPS message is not received.

Example 3

The following is assumed:

Data rate:	15 bps
Message length:	45 bits (≙ 3 seconds)
Number of GPS satellites:	9
Number of GLONASS satellites:	9
One missed GLONASS correction	

A transmission sequence as in examples 1 and 2 is assumed. If one GLONASS message is missed, the interval of use changes from 3 to 111 seconds to an interval of 3 to 219 seconds (73 message lenghts). This results in a GLONASS position error ranging from 0.4 to 3.4 meters (95%), with an average of 1.6 meters.

If the datarate is increased to 30 bps, the GLONASS position error decreases to 0.4 to 0.9 meters (95%), with an average of 0.6 meters (interval of use: 1.5 to 109.5 seconds).

The position errors for GPS are not changed (see examples 1 and 2).

Example 4

The following is assumed:

Data rate:	15 bps
Message length:	45 bits (≙ 3 seconds)
Number of GPS satellites:	9
Number of GLONASS satellites:	9
One missed GPS correction	

A transmission sequence as in examples 1 and 2 is assumed. If one GPS message is missed, the interval of use changes from 3 to 39 seconds to an interval of 3 to 75 seconds (25 message lenghts). This results in a GPS position error ranging from 0.4 to 30.9 meters (95%), with an average of 14.1 meters.

If the datarate is increased to 30 bps, the GPS position error decreases to 0.4 to 7.7 meters (95%), with an average of 3.6 meters (interval of use: 1.5 to 37.5 seconds).

The position errors for GLONASS are not changed (see examples 1 and 2).

In the above examples a sequence of 9 GPS followed by 3 GLONASS corrections, repeated after every 9 GLONASS corrections, was assumed. What will happen if the sequence is changed to 9 GPS and 2 corrections (repeated after every 8 GLONASS corrections). This is shown in the next two examples: example 5 with a data rate of 15 bps and example 6 with a data rate of 30 bps.

Example 5

The following is assumed:

Data rate:	15 bps
Message length:	45 bits (≙ 3 seconds)
Number of GPS satellites:	9
Number of GLONASS satellites:	8

A transmission sequence of 9 GPS corrections followed by 2 GLONASS corrections is assumed. If one GLONASS correction message is missed, the interval of use changes (compared to example 3) from 3 to 75 seconds to an interval of 3 to 267 seconds (89 message lenghts). This results in a GLONASS position error ranging from 0.4 to 5 meters (95%), with an average of 2.3 meters.

If one GPS correction message is missed, the interval of use will be 3 to 69 seconds, resulting in a position error ranging from 0.4 to 26.2 meters (95%), with an average of 12 meters.

The position error for GPS (all messages received correctly) ranges from 0.4 to 7.1 meters (95%), with an average of 3.4 meters (interval of use: 3 to 36 seconds). For GLONASS this is 0.4 to 1.3 meters (95%), with an average of 0.7 meters (interval of use: 3 to 135 seconds).

Example 6

Only the data rate is changed: from 15 bps to 30 bps. Further assumptions are the same as in example 5. This will give the following position errors:

1 missed GLONASS message:

The interval of use is 1.5 to 133.5 seconds, resulting in a GLONASS position error ranging from 0.4 to 1.3 meters (95%, average 0.7 meters).

1 missed GPS message:

The interval of use is 1.5 to 34.5 seconds, resulting in a GPS position error ranging from 0.4 to 6.6 meters (95%, average 3.0 meters).

All GLONASS messages received correctly:

The interval of use is 1.5 to 67.5 seconds, resulting in a GLONASS position error ranging from 0.4 to 0.5 meters (95%, average approximately 0.4 meters).

All GPS messages received correctly:
The interval of use is 1.5 to 18 seconds, resulting in a GPS position error ranging from 0.4 to 1.8 meters (95%, average 0.9 meters).

Finally, two examples are given in which the transmission sequence is changed to 9 GPS corrections followed by 1 GLONASS correction. The next 9 (new) GLONASS corrections are transmitted after 81 GPS corrections have been transmitted.

Example 7

The following is assumed:

Data rate:	15 bps
Message length:	45 bits (≙ 3 seconds)
Number of GPS satellites:	9
Number of GLONASS satellites:	9

A transmission sequence of 9 GPS corrections followed by 1 GLONASS correction is assumed. If one GLONASS correction message is missed, the interval of use changes (compared to example 3) from 3 to 75 seconds to an interval of 3 to 543 seconds (181 message lenghts). This results in a GLONASS position error ranging from 0.4 to 20.6 meters (95%), with an average of 9.3 meters.

If one GPS correction message is missed, the interval of use will be 3 to 63 seconds, resulting in a position error ranging from 0.4 to 21.8 meters (95%), with an average of 10.0 meters.

The position error for GPS (all messages received correctly) ranges from 0.4 to 6.0 meters (95%), with an average of 2.8 meters (interval of use: 3 to 33 seconds. For GLONASS this is 0.4 to 5.2 meters (95%), with an average of 2.4 meters (interval of use: 3 to 273 seconds).

Example 8

Only the data rate is changed: from 15 bps to 30 bps. Further assumptions are the same as in example 7. This will give the following position errors:

1 missed GLONASS message:
The interval of use is 1.5 to 271.5 seconds, resulting in a GLONASS position error ranging from 0.4 to 5.2 meters (95%, average 2.3 meters).

1 missed GPS message:
The interval of use is 1.5 to 31.5 seconds, resulting in a GPS position error ranging from 0.4 to 5.5 meters (95%, average 2.5 meters).

All GLONASS message received correctly:
The interval of use is 1.5 to 136.5 seconds, resulting in a GLONASS position error ranging from 0.4 to 1.4 meters (95%, average 0.7 meters).

All GPS message received correctly:
The interval of use is 1.5 to 16.5 seconds, resulting in a GPS position error ranging from 0.4 to 1.6 meters (95%, average 0.8 meters).

In table 11.2 a summary is given.

If no GLONASS corrections are transmitted, the GPS horizontal position accuracy ranges from 0.4 to 5.0 meters (95%, assuming transmission of GPS 9 corrections with a data rate of 15 bps, HDOP of 1.5) with an average of 2.4 meters. When a data rate of 30 bps is assumed, the GPS position error ranges from 0.4 to 1.3 meters (95%), with an average of 0.7 meters.

The (average) position accuracy of DGPS positioning degrades when transmitting DGLONASS corrections from 2.8 (15 bps, 9 GPS corrections followed by 1 GLONASS correction) to 3.9 meters (15 bps, 9 GPS corrections followed by 3 GLONASS corrections). When the data rate is changed to 30 bps, the accuracy will be better: 0.8 meters (1 GLONASS correction per 9 GPS corrections) to 1.1 meters (3 GLONASS corrections per 9 GPS corrections).

Table 11.2 Position errors (95%) when transmitting GLONASS and GPS corrections (HDOP=1.5, no spatial decorrelation assumed)

	sequence	data rate (bps)	interval of use (s)	95% position error (m)	average (m)
GLONASS (no missed GLONASS corrections)	9 GPS 3×3 GLONASS	15	3-111	0.4-1.0	0.6
		30	1.5-55.5	0.4-0.5	0.4
	9 GPS 4×2 GLONASS	15	3-135	0.4-1.3	0.7
		30	1.5-67.5	0.4-0.5	±0.4
	9 GPS 9×1 GLONASS	15	3-273	0.4-5.2	2.4
		30	1.5-136.5	0.4-1.4	0.7
GPS (no missed GPS corrections)	9 GPS 3×3 GLONASS	15	3-39	0.4-8.4	3.9
		30	1.5-19.5	0.4-2.1	1.1
	9 GPS 4×2 GLONASS	15	3-36	0.4-7.1	3.4
		30	1.5-18	0.4-1.8	0.9
	9 GPS 9×1 GLONASS	15	3-33	0.4-6.0	2.8
		30	1.5-16.5	0.4-1.6	0.8
GLONASS (one missed GLONASS correction)	9 GPS 3×3 GLONASS	15	3-219	0.4-3.4	1.6
		30	1.5-109.5	0.4-0.9	0.6
	9 GPS 4×2 GLONASS	15	3-267	0.4-5.0	2.3
		30	1.5-133.5	0.4-1.3	0.7
	9 GPS 9×1 GLONASS	15	3-543	0.4-20.6	9.3
		30	1.5-271.5	0.4-5.2	2.3
GPS (one missed GPS correction)	9 GPS 3×3 GLONASS	15	3-75	0.4-30.9	14.1
		30	1.5-37.5	0.4-7.7	3.6
	9 GPS 4×2 GLONASS	15	3-69	0.4-26.2	12.0
		30	1.5-34.5	0.4-6.6	3.0
	9 GPS 9×1 GLONASS	15	3-63	0.4-21.8	10.0
		30	1.5-31.5	0.4-5.5	2.5

At a data rate of 15 bps the (average) position accuracy of DGLONASS positioning ranges from 0.6 (3 GLONASS corrections per 9 GPS corrections) to 2.4 meters (1 GLONASS correction per 9 GPS corrections). At a data rate of 30 bps, the DGLONASS position

accuracy ranges from 0.4 (3 GLONASS corrections per 9 GPS corrections) to 0.7 meters (1 GLONASS correction per 9 GPS corrections).

In the examples also the effect of a missed GPS or GLONASS correction is shown. If one GPS correction is missed the average position accuracy of DGPS ranges from 10.0 (1 GLONASS correction per 9 GPS corrections) to 14.1 meters (3 GLONASS corrections per 9 GPS corrections) at a data rate of 15 bps. When the data rate is increased to 30 bps, the accuracy ranges from 2.3 to 3.6 meters. If one GLONASS correction is missed the average position accuracy of DGLONASS ranges from 0.6 (3 GLONASS correction per 9 GPS corrections) to 9.3 meters (3 GLONASS corrections per 9 GPS corrections) at a data rate of 15 bps. When the data rate is increased to 30 bps, the accuracy ranges from 0.6 to 2.3 meters.

The support of integrated differential use of GLONASS and GPS implies a contradiction: increasing the GLONASS position accuracy (increasing DGLONASS update rate) results in decreasing the GPS position accuracy (decreasing DGPS update rate). Integrated differential GNSS is to support three types of users:

1. GPS-only users
2. GLONASS-only users
3. Integrated GPS-GLONASS users

These three different user groups have their own requirements and demands. A GPS-only user would like to have the best GPS position accuracy: a high update rate of differential GPS corrections is required. A high update rate of DGPS corrections is only possible if the DGLONASS update rate is relatively low resulting in a less accurate GLONASS positioning than if the DGLONASS update rate was set at a higher level. The best GLONASS position accuracy is required by GLONASS-only users: to get a better DGLONASS accuracy differential GLONASS corrections are to be transmitted with a higher update rate than the GPS-only users would like these to be transmitted. A higher DGLONASS update rate would lead to a better GLONASS position accuracy and a worse GPS position accuracy.

If Eurofix is to support GPS and GLONASS as well, a compromise has to be made which satisfies both the independent use of GPS and GLONASS and the integrated use of both

systems. Probably the best and most satisfying position accuracy can be reached when 9 GPS differential corrections are transmitted followed by the first two GLONASS differential corrections. These 11 corrections are followed by 9 new GPS corrections and the next two GLONASS corrections. After 4 sets of 9 different GPS corrections and 1 set of 8 different GLONASS corrections, the next 4 sets of GPS corrections and the next set GLONASS corrections are transmitted. When these corrections are transmitted with a data rate of 15 bps, the (average) 95%-position accuracy should be within 4 meters for GPS and 1 meter for GLONASS. When the data rate is increased to 30 bps, the accuracies are even better: a 95%-position error (average) of about 0.5 meter for GLONASS and 1 meter for GPS. These accuracies are valid for a HDOP of 1.5.

11.4 The consequence of GNSS differences

11.4.1 Two different coordinate reference systems

The coordinates of a position in one Cartesian coordinate frame may be related to those in another via a similarity transformation of the three axes, and a scale factor. Specifically, a Cartesian coordinate system WGS-84: (X,Y,Z) is related to the coordinate system SGS-85/SGS-90: (U,V,W), nearly aligned to it, by (figure 11.1):

$$\begin{bmatrix} X \\ Y \\ Z \end{bmatrix}_{WGS-84} = \begin{bmatrix} \Delta X \\ \Delta Y \\ \Delta Z \end{bmatrix} + (1+\delta s) \begin{bmatrix} 1 & \omega & -\phi \\ -\omega & 1 & \epsilon \\ \phi & -\epsilon & 1 \end{bmatrix} \begin{bmatrix} U \\ V \\ W \end{bmatrix}_{SGS-85/SGS-90} \tag{11.3}$$

where $(\Delta X, \Delta Y, \Delta Z)$: coordinates of the origin of frame (U,V,W) in frame (X,Y,Z)

ϵ, ϕ, ω: differential rotations (in radians) around the axes (U,V,W), respectively, to establish parallelism with the (X,Y,Z) frame

δs: differential scale change

Many attempts have been made to determine an accurate transformation between SGS-85 and WGS-84. Probably the best estimation of the coordinate reference transformation has been determined at the Lincoln Laboratory of the Massachusetts Institute of Technology [31]. The determination was based on tracking the GLONASS satellites by radar and comparing the

position of the satellites (expressed in SGS-85 coordinates) with their position in WGS-84. The estimated transformation parameters are given by:

$\Delta X = 0$, $\Delta Y = 0$, $\Delta Z = 4$ m, $\delta = 0$, $\epsilon = 0$, $\phi = 0$ and $\omega = -3\times10^{-6}$ rad (0.6")

The rms difference between the coordinates of positions on earth in WGS-84 and SGS-85 has been estimated to be less than 20 m.

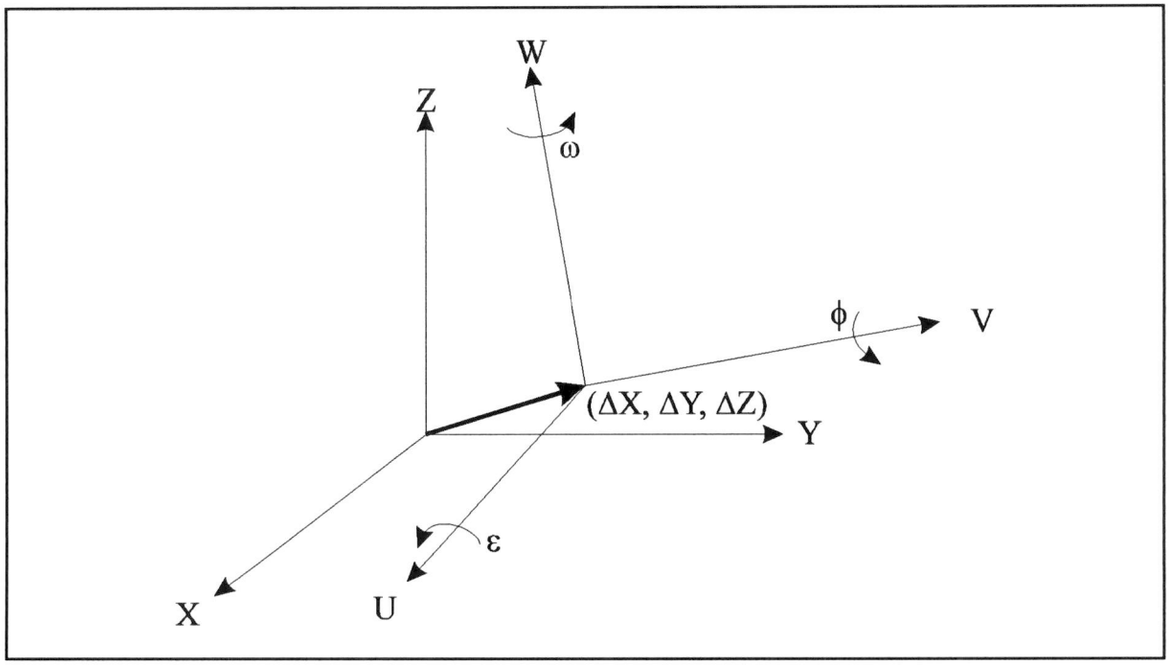

Figure 11.1 Transformation between SGS-85/90 and WGS-84

As SGS-85 has been changed to SGS-90 (PZ-90) the transformation between both coordinate systems has to be reviewed. While the MIT intends to investigate the transformation between SGS-90 and WGS-84, the Russian CSIC has provided the following transformation parameters:

$\Delta X = 0$, $\Delta Y = 0$, $\Delta Z = 1.5$ m, $\delta = 0$, $\epsilon = 0$, $\phi = 0$ and $\omega = -3.7\times10^{-7}$ rad (0.076")

The difference between the two coordinate reference systems certainly will have its consequences on the development of a system supporting the differential use of both GLONASS and GPS. The consequences imposed by the differences between SGS-90 and

WGS-84 depend on the way GPS and GLONASS are being used: *(1)* Independent use of GPS and GLONASS or *(2)* Integrated use of GPS and GLONASS.

(1) Independent use of GLONASS and GPS

As the positions determined with GLONASS and GPS are referenced to different coordinate systems, it is recommended to determine the differential corrections in both coordinate systems, (i.e. SGS-90 and WGS-84) and transmitted to independent GLONASS and GPS users. This can be done in two ways:

a. Differential corrections are determined by a reference station of which the position is known in both coordinate systems
b. Differential corrections referenced to one coordinate system are determined. Corrections for users of the other system is determined by means of a coordinate transformation

(2) Integrated use of GLONASS and GPS

Integrated use of GLONASS and GPS requires positions referenced to one coordinate system. Therefore, integration of GLONASS and GPS always requires a coordinate transformation between SGS-90 and WGS-84.

From the above it can be concluded that providing DGNSS corrections referenced to both coordinate systems, is preferred. This makes it possible that the differential GLONASS and GPS corrections can be used by both types of users. The integrated user itself has to transform the differentially corrected positions to one of the coordinate reference systems, for example: a GPS user making use of GLONASS pseudoranges has to transform the corrected SGS-90 positions to WGS-84. It is therefore recommended that Eurofix (when supporting GPS and GLONASS) will determine differential corrections referenced to SGS-90 and WGS-84.

11.4.2 Two different system times

The system times of GLONASS and GPS are different. Consequently, the clock offsets measured to GPS and GLONASS are different. If GLONASS and GPS are used integrated,

the difference between the system times has to be known. To determine this difference two approaches are possible:

- an external measure of the system time difference and solve for a single clock offset
- determination of the clock offset as part of the navigation solution.

The first approach could be performed at the Eurofix reference station. At the reference station the system time difference is determined and transmitted to the integrated users. This means an adaption of the DGNSS-Eurofix message format proposed in section 11.2. If the number of bits is maintained at 45, addition of the system time difference means reducing the bits available (and thus the range or resolution of the range, range rate correction and the time reference) for the GLONASS corrections. If the number of bits is increased to transmit the system time difference, GPS and GLONASS correction messages will have unequal lengths, influencing the final DGPS (and DGLONASS) accuracy.

In the second approach the determination of the time difference is left to the GPS/GLONASS user. It is possible to calculate the difference between the system times by using five (instead of four) range measurement as there are five unknowns to be determined.

12. Conclusions and recommendations

Conclusions

The provision of differential GLONASS corrections through the Eurofix datalink is opportune. The development of GLONASS is still in progress: at the end of 1995 the full constellation will be reached.

Based on DGLONASS correction messages proposed by the RTCM, a Eurofix message format has been proposed supporting both DGPS and DGLONASS. To support DGLONASS, the Eurofix message format has to be enlarged with one new message type: the asynchronous GLONASS pseudorange correction. This message type is very similar to the asynchronous GPS pseudorange correction. The determined DGLONASS corrections should be referenced to PZ-90, the coordinate reference system applied by GLONASS. This makes application of DGLONASS corrections by GLONASS-only or GPS-GLONASS users possible. The latter will have to transform the positions to one coordinate reference system.

The largest and most varying range errors in GLONASS are caused by the ionosphere. Using the Bent Ionospheric Model, range errors and their temporal decorrelation have been investigated. Based on simulations the DGLONASS correction message update rate has been determined. The GLONASS 95% horizontal position accuracy should be within 5 meters when asynchronous DGLONASS corrections are transmitted with an update rate of 1 message per 1 to 2 minutes.

Transmission of DGLONASS corrections together with DGPS corrections should be possible without severe degradation of DGPS position accuracy. Different sequences of GLONASS and GPS corrections have been evaluated at different data rates. The number of DGLONASS messages per DGPS messages determines the final DGPS and DGLONASS 95% horizontal position accuracy. Increasing the number of GLONASS corrections reduces the DGPS accuracy. If a sequence of 9 GPS corrections followed by 2 GLONASS corrections (repeated

after four 9-GPS/2-GLONASS corrections) are transmitted the requirement of a 95% horizontal position accuracy of 8-20m should be met. The DGPS/DGLONASS accuracy is higher when the data rate is higher.

Recommendations

In the ionosphere sudden changes may occur which are not represented by the Bent Ionospheric Model. These sudden changes may have a large impact on the integrity of the GNSS-Eurofix system. It should be possible to monitor the ionosphere, for example by a dual-frequency receiver, and send warning messages to the users of Eurofix by means of an integrity message. It is recommended to perform research concerning this issue of integrity.

In this report, the spatial decorrelation of the ionospheric errors has not been investigated. This spatial decorrelation determines the distance over which the DGLONASS corrections are valid. Therefore, research concerning this spatial decorrelation has to be carried out.

The differential position errors are estimated conservatively. The real errors are probably smaller than presented in this report. It is recommended to perform tests to verify the results presented in this report. First, tests should be performed by transmission of (real) DGPS corrections together with (simulated) GLONASS corrections. Different sequences of GLONASS/GPS messages should be tested at different data rates. These tests should be followed by experiments in which real DGLONASS and DGPS corrections are transmitted. This could be done by using two receivers: a GLONASS and a GPS receiver or by one dual system receiver.

Furthermore, in the literature the differential error growth is determined as having a quadratic course (also conservative). The simulation results, however, show a more linear course of the error growth. This difference should be investigated.

Differential GLONASS and GPS corrections transmitted through the Eurofix datalink could be used to improve GLONASS accuracy (DGLONASS corrections only) or to improve GPS accuracy (DGPS corrections only). Both corrections could by used to improve GNSS, an integrated use of GLONASS and GPS, accuracy. Integrated use of GLONASS and GPS will

have its advantages concerning integrity, availability and reliability. It is therefore recommended to investigate the possibility of application of DGLONASS/DGPS corrections transmitted in Eurofix by integrated use of GLONASS and GPS.

In Russia a system similar to Loran-C is operational: Chayka. In the Bering Sea, a chain consisting of Loran-C and Chayka transmitters is operational. It is suggested to investigate the possible integration of GPS, GLONASS, Loran-C and Chayka. This could lead to a system which will provide differential GLONASS and GPS corrections to GLONASS and GPS users over the entire northern hemisphere.

References

[1] *Interface Control Document GPS-200*, Arinc Research Corporation, Fountain Valley, CA, 3 July 1991

[2] Johnson, N.L., *GLONASS Spacecraft*, GPS World, November 1994

[3] Feairheller, S., *The Russian GLONASS System: A US Air Force/Russian Study*, Proceedings of ION GPS-94, The Institute of Navigation, Albuquerque, New Mexico, September, 1994, pp. 293-304

[4] *GLONASS Interface Control Document (second wording)*, RTCA Paper No. 518-91/SC159-317, 1991

[5] Dale, S.A., Daly, P., Kitching, I.D., *Understanding signals from GLONASS navigation satellites*, International Journal of Satellite Communications, vol.7, 11-12, 1989

[6] Reshetnev, M., Kozlov, A., Cheremisin, V., Kazantsev, V. and Gorev, V., *The results of operation of the "GLONASS" system and the plan for its development*, International Symposium on Precision Approach and Automatic Landing 1995, The German Institute of Navigation, Düsseldorf, Germany, February, 1995, pp. 393-399

[7] Beekhuis, L.J., *The asynchronous correction concept for high precision DGPS in Eurofix*, Thesis Report, Delft University of Technology, The Netherlands, June, 1993

[8] *Intergovernmental Radionavigation Programme of the member states of the Commonwealth of Independent States (Radionavigation Plan)*, Radionavigation Intergovernmental Advisory Council, 1994

[9] *1992 Federal Radionavigation Plan*, Department of Transportation/Department of Defense, DOT-VNTSC-RSPA-92-2/DOD-4650.5, Washington, D.C., USA, January, 1993

[10] Willigen, D. van, *Eurofix*, The Journal of Navigation, Vol. 42, No.3, September, 1989

[11] *Loran-C User Handbook*, U.S. Department of Transportation/United States Coast Guard, COMDTPUB P16562.6, Washington, D.C., USA, 1992

[12] *RTCM Recommended Standards For Differential Navstar GPS Service*, Version 2.1, RTCM Special Committee No. 104, Radio Technical Commission for Maritime ServicesWashington, D.C., USA, January, 1994

[13] Offermans, G.W.A., *Modulation Schemes for the Eurofix Datalink*, Thesis Report, Delft University of Technology, The Netherlands, September, 1994

[14] Offermans, G.W.A., Willigen, D. van, Breeuwer, E.J., *Eurofix: Have we reached the limit?*, Proceedings of the 23rd Annual Technical Symposium of the Wild Goose Association, Newport, RI, October 31-November 4, 1994

[15] Willigen, D. van, Offermans, G.W.A., Breeuwer, E.J., Weber, J.H., Andersen, J.H., *Eurofix: GNSS Augmented Loran-C & Loran-C Augmented GNSS*, Proceedings of the 1995 National Technical Meeting of the Institute of Navigation, Anaheim, CA, January 18-20, 1995

[16] Zwart, J. de, *Testing and Optimizing the Eurofix Datalink*, Thesis Report, Delft University of Technology, The Netherlands, July, 1994

[17] Willemsen, D., *Modelling of the Eurofix Data-Link*, Thesis Report, Delft University of Technology, The Netherlands, August, 1994

[18] Gouzhva, Y.G., e.a., *Development of a combined set of standard messages with respect to the differential mode of navigation determinations for the joint use of GLONASS/NAVSTAR satellite radionavigation systems, Russian Institute of Radionavigation and Time (RIRT)*, Proceedings of DSNS 93, March, 1993

[19] *Proposals on expanding the RTCM recommended standard for differential mode of the NAVSTAR satellite RNS (DPGS), for joint use of NAVSTAR and GLONASS satellite radionavigation systems in the differential mode with due regard for the correction data standard frames recommended for GLONASS* (In Russian), St. Petersburg, CIS, 1992

[20] *Minutes of the Meeting RTCM SC-104, Differential Navstar/GPS Service 19-20 September 1994*

[21] CCIR Report 725-2, *Ionospheric Properties*, Recommendations and Reports of the CCIR, vol. VI, 'Propagation in ionized media', 1986

[22] CCIR Report 263-6, *Ionospheric effects upon earth-space propagation*, Recommendations and Reports of the CCIR, vol. VI, 'Propagation in Ionized Media', 1986

[23] Davies, K., *Ionospheric Radio Propagation*, Dover Publications, Inc., New York, 1966

[24] Llewellyn, S.K., Bent, R.B., *Documentation and Description of the Bent Ionospheric Model*, AFCRL-TR-73-0657 and AD 772733, Atlantic Science Corporation, Florida, 1973

[25] Chapman, S., Bartels, J., *Geomagnetism*, vol. II, Oxford University Press, 1962

[26] CCIR Report 340, *CCIR Atlas of Ionospheric Characteristics*, 1983

[27] Jones, W.B, Gallet, R.M., *The Representation of Diurnal and Geographic Variations of Ionospheric Data by Numerical Methods*, Telecommunication Journal, vol. 29, 5, 129-147, May 1962

[28] Jones, W.B, Gallet, R.M., *Representation of Diurnal and Geographic Variations of Ionospheric Data by Numerical Methods*, Telecommunication Journal, vol. 32, 1, 18-28, January 1965

[29] Chistyakov, V., Filatchenkov, S., Khimulin, V., *Parameters of Differential GLONASS/GPS Service on the Base of Russian Marine Radiobeacons*, Proceedings of DSNS 95, April, 1995

[30] Kremer, G.T., Kalafus, R.M., Loomis, P.V.W., Reynolds, J.C., *The Effect of Selective Availability on Differential GPS Corrections*, Navigation, Journal of the Institute of Navigation, Vol.37, no. 1, Spring, 1990, 39-52

[31] Misra, P.N., Abbot, R.I., Bayliss, E.T., *SGS85-WGS84 Transformation: Interim Results*, Project Report ARC-204, Lincoln Laboratory Massachusetts Institute of Technology, Lexington, Massachusetts, August 1993

Appendix A: GNSS navigational data

The GLONASS message structure is discussed in the GLONASS-ICD [4]. Information on the GPS message structure can be found in the GPS-ICD [1]. This appendix discusses both messages in short and gives an overview of their contents.

A.1 GLONASS navigational data

The basic message format consists of a 1500 bit frame. Each frame consists of 15 subframes with a length of 100 bits (see Figure A.1). The data rate is 50 bits/s, resulting in a duration of a subframe of 2 seconds. A total frame has the length of 30 seconds. The complete navigation message, the superframe, contains 5 frames, making the length of a complete navigation message 2.5 minutes.

As mentioned already, each frame consists of 15 subframes:

subframe 1-4:	ephemeris and clock correction parameters (Table A.1)
subframe 5:	information concerning the validity of the almanac data (Table A.1)
subframe 6-15:	almanac data (Table A.2)

Each subframe is preceded by a 15-bit Time Mark (TM) and an 8-bit Hamming Code (Hc). The last 5 bits in each subframe are formed by a 4-bit line number (m) and a 1 bit which is blank.

For further information on the GLONASS navigation message the reader is referred to [4].

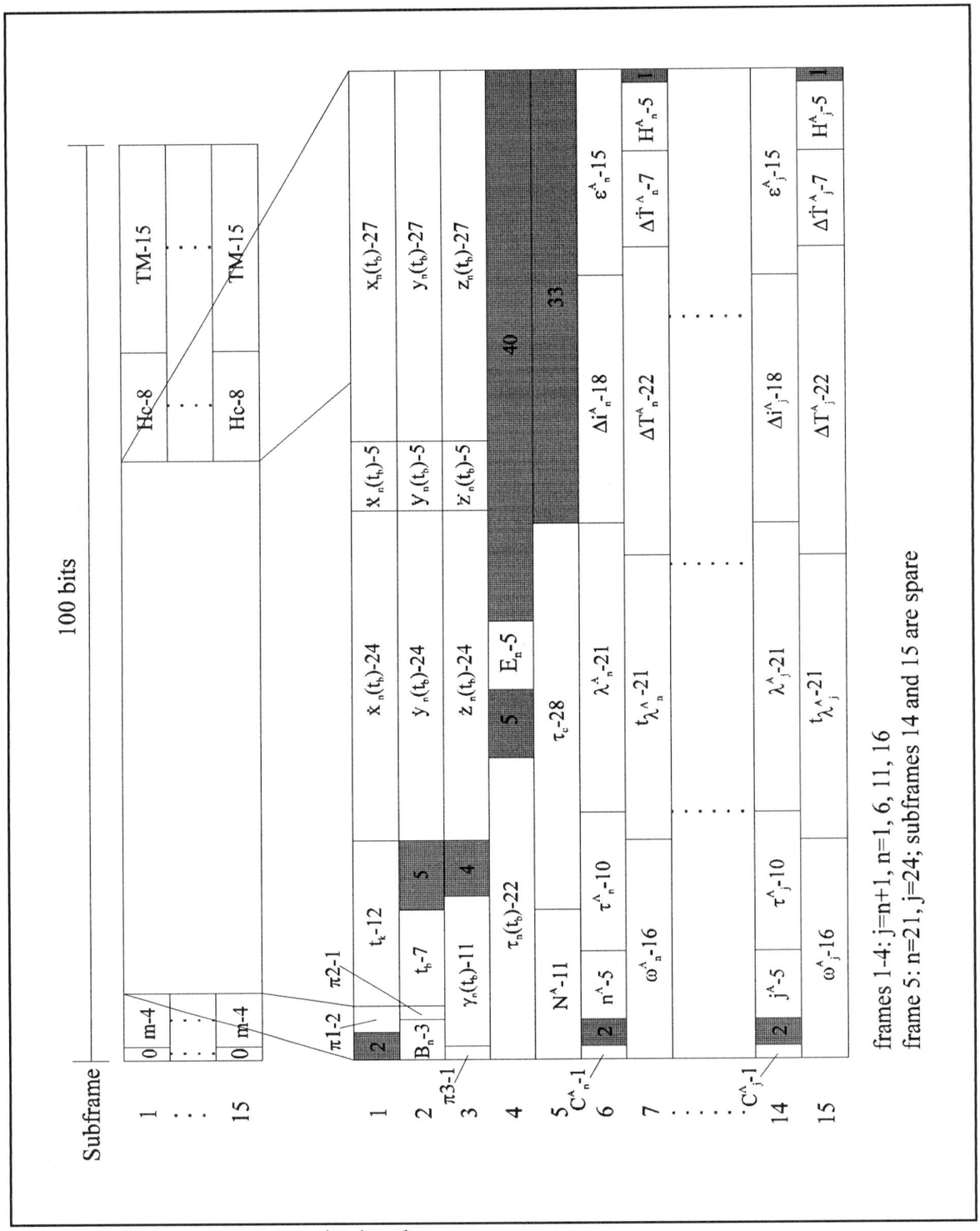

Figure A.1 The GLONASS navigational message

Table A.1 The GLONASS satellite ephemeris parameters: subframes 1 to 5

parameter[1]	contents	bits[2)]	scale factor (LSB)	range	unit
subframe 1					
$\pi 1$[4)]	indicates time period between the t_b in current and previous frames	2			min
t_k	time referenced to the beginning of the frame within the current day (satellite time scale)	5 (MSB) 6 1 (LSB)	1 1 30	0...23 0...59 0;30	h min s
$\dot{x}_n(t_b)$	x-coordinate velocity	24	2^{-20}	±4.3	km/s
$\ddot{x}_n(t_b)$	x-coordinate acceleration (lunar/solar induced)	5	2^{-30}	$\pm 6.2 \cdot 10^{-9}$	km/s^2
$x_n(t_b)$	x-coordinate position	27	2^{-11}	$\pm 2.7 \cdot 10^{4}$	km
subframe 2					
B_n	satellite health; only MSB, 2nd and 3rd bits not used; "1" = unhealthy, "0" healthy	3			
$\pi 2$	indicates the first "1" or second half "0" of an hour	1			
t_b	time reference of the ephemeris (scale UTC(SU)	7	15	15;...;1425	min
$\dot{y}_n(t_b)$	y-coordinate velocity	24	2^{-20}		km/s
$\ddot{y}_n(t_b)$	y-coordinate acceleration (lunar/solar induced)	5	2^{-30}	$\pm 6.2 \cdot 10^{-9}$	km/s^2
$y_n(t_b)$	y-coordinate position	27	2^{-11}	$\pm 2.7 \cdot 10^{4}$	km
subframe 3					
$\pi 3$	number of transmitted almanacs: "1" = 5, "0" = 4	1		0;1	
$\gamma_n(t_b)$	relative frequency offset	11	2^{-40}	$\pm 2^{-30}$	
$\dot{z}_n(t_b)$	z-coordinate velocity	24	2^{-20}	±4.3	km/s
$\ddot{z}_n(t_b)$	z-coordinate acceleration (lunar/solar induced)	5	2^{-30}	$\pm 6.2 \cdot 10^{-9}$	km/s^2
$z_n(t_b)$	z-coordinate position	27	2^{-11}	$\pm 2.7 \cdot 10^{4}$	km
subframe 4					
$\tau_n(t_b)$	offset of satellite time to the system time	22	2^{-30}	$\pm 2^{-9}$	s
E_n	age of day of the ephemeris	5[3)]	1	0...31	day
subframe 5					
N^A	current day within the 4-year period	11	1	1...1461	day
τ_c	system time offset (to UTC-SU)	28[3)]	2^{-27}	±1	s

1) Numerical values of the parameters are presented as the number sign and its module; sign bit MSB
2) See Figure A.1 for bit allocation in subframe
3) Parameters have the range attainable with the maximum range and indicated LSB scale factor
4) See for further information [4]

Table A.2 The contents of the GLONASS subframes 6-15

subframes 6, 8, 10, 12 and 14					
paramter[1)]	**contents**	**bits[2)]**	**scale factor (LSB)**	**range**	**unit**
C^A_n	satellite state; "0" = satellite unfitness for navigation, "1" = unfitness satellite	1	1	0;1	
n^A	satellite number	5	1	1...24	
τ^A_n	satellite time offset (to system time)	10[3)]	2^{-18}	$\pm 1.9 \cdot 10^{-3}$	s
λ^A_n	longitude of the ascending node of the orbit	21[3)]	2^{-20}	±1	semi cycle
Δi^A_n	orbit inclination offset (to mean value 0.35 ≙ 63°)	18[3)]	2^{-20}	±0.067	semi cycle
ϵ^A_n	eccentricity of the orbit of the satellite	15	2^{-20}	0...0.03	
subframes 7, 9, 11, 13 and 15					
ω^A_n	perigee argument	16[3)]	2^{-15}	±1	semi cycle
$t_{\lambda^A_n}$	ascending node passing time	21	2^{-5}	0...44100	s
ΔT^A_n	correction to the mean value (43200 s) of the draconitic period	22	2^{-9}	$\pm 3.6 \cdot 10^3$	s
$\Delta \dot{T}^A_n$	change velocity of the draconitic period of the revolution of the satellite	7	2^{-14}	$\pm 2^{-8}$	s/orbit
H^A_n	frequency number	5	1	1...24	

1) Numerical values of the parameters are presented as the number sign and its module; sign bit MSB
2) See Figure A.1 for bit allocation in subframe
3) Parameters have the range attainable with the maximum range and indicated LSB scale factor

A.2 GPS navigational data

The basic message format consists of a 1500 bit frame. Each frame consists of 5 subframes with a length of 300 bits (see Figure A.2). The data rate is 50 bits/s, resulting in a duration of a subframe of 6 seconds. A subframe consists of 10 words, 30 bits long each. A total frame has the length of 30 seconds. The complete navigation message, the superframe, contains 25 frames, making the length of a complete navigation message 12.5 minutes.

As mentioned already, each frame consists of 5 subframes:

subframe 1: satellite clock parameters (Table A.3)

subframe 2: ephemeris (Table A.4)

subframe 3: ephemeris (Table A.4)

subframe 4: The data in subframe 4 is divided over 25 pages. In the following, a brief summary of the data contained in each page is given.

- ☐ pages 1, 6, 11, 16 and 21: reserved;
- ☐ pages 2, 3, 4, 5, 7, 8, 9 and 10 almanac data for SV 25-32, the format equals the format of pages 1-24 of subframe 5;
- ☐ pages 12, 19, 20, 22, 23 and 24: reserved;
- ☐ pages 13, 14 and 15: spares;
- ☐ page 17: special messages;
- ☐ page 18: ionospheric and UTC data (Table A.5)
- ☐ page 25: A-S flags/SV configurations for 32 SVs, plus SV health for 25-32

subframe 5: Almanac data (Table A.6)

Each subframe is preceded by a Telemetry Word (TLM) and a Handover Word (HOW).

For further information on the GPS navigation message the reader is referred to [1].

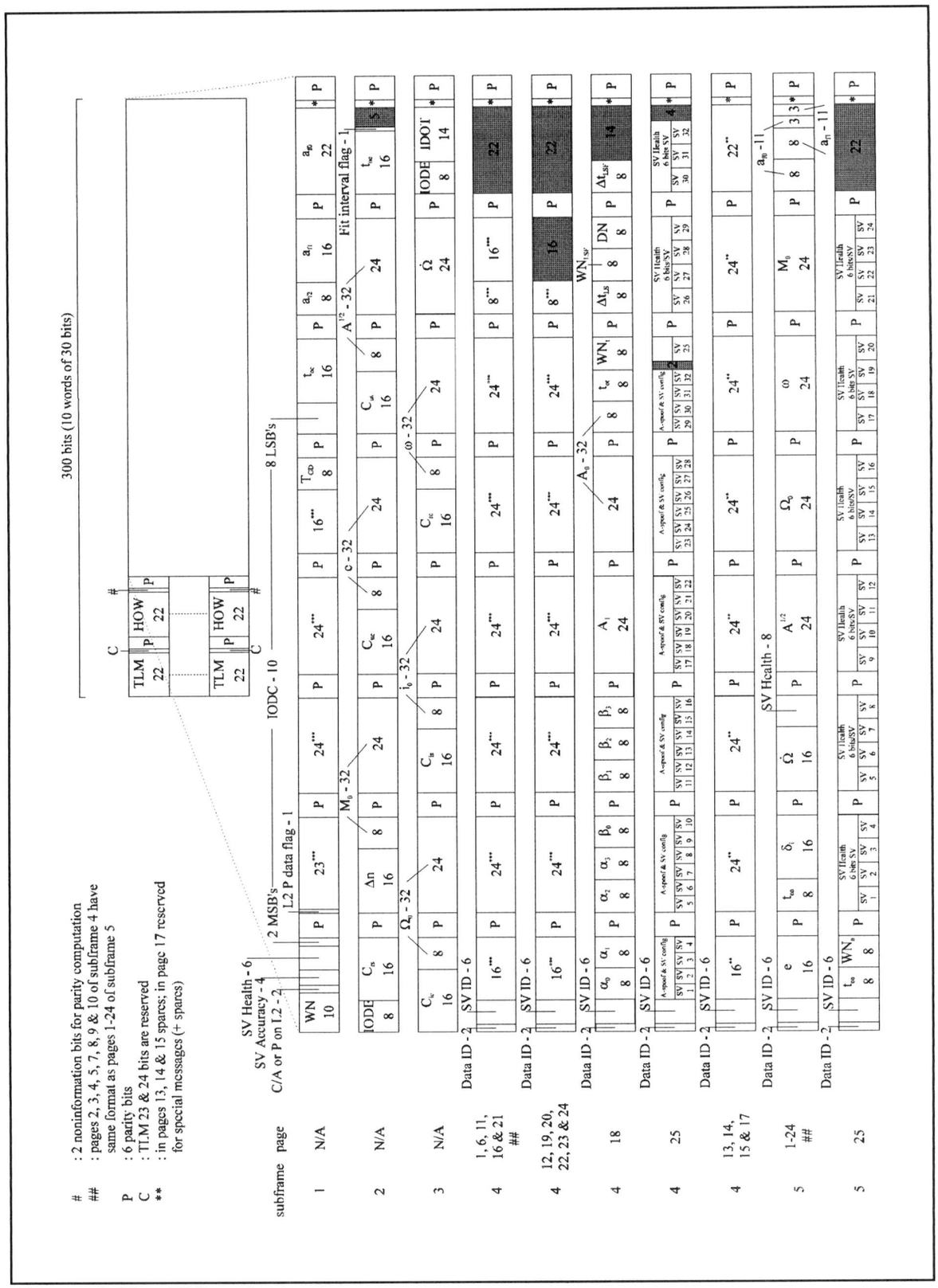

Figure A.2 The GPS navigational message

Table A.3 The contents of GPS subframe 1

subframe 1					
parameter	**contents**	**bits[2)]**	**scale factor (LSB)**	**range[3)]**	**unit**
WN	Week number	10	1		discretes
Code on L2.		2	1		week
SV accuracy		4	-		see [1]
SV health		6	1		discretes
L2 P data flag		1	1		discretes
T_{GD}	L1/L2 Correction Term	8[1)]	2^{-31}		s
IODC	Issue of Data (Clock)	10			see [1]
t_{oc}	Clock Correction Term	16	2^{4}	607,784	s
a_{f2}	idem	8[1)]	2^{-55}		s/s^2
a_{f1}	idem	16[1)]	2^{-43}		s/s
a_{f0}	idem	22[1)]	2^{-31}		s

1) Two's complement, sign bit MSB
2) See Figure A.2 for bit allocation in subframe
3) Unless otherwise indicated in this column, effective range is the maximum range attainable with indicated bit allocation and scale factor

Table A.4 The contents of GPS subframes 2 and 3

subframe 2					
parameter	**contents**	**bit[2)]**	**scale factor (LSB)**	**range[3)]**	**unit**
IODE	Issue of Data (Ephemeris)	8			see [1]
C_{rs}	Amplitude of the Sine Harmonic Correction Term to the Orbit Radius	16[1)]	2^{-5}		m
Δn	Mean Motion Difference from Computed Value	16[1)]	2^{-43}		semi-circles/s
M_0	Mean Anomaly at Reference Time	32[1)]	2^{-31}		semi-circles
C_{uc}	Amplitude of the Cosine Harmonic Correction Term to the Argument of Latitude	16[1)]	2^{-29}		radians
e	Eccentricity	32	2^{-33}	0.03	
C_{us}	Amplitude of the Sine Harmonic Correction Term to the Argument of Latitude	16[1)]	2^{-29}		radians
$(A)^{½}$	Square Root of the Semi-Major Axis	32	2^{-19}		$m^{½}$
t_{oe}	Reference Time Ephemeris	16	2^{4}	607,784	s
subframe 3					
C_{ic}	Amplitude of the Cosine Harmonic Correction Term to the Angle of Inclination	16[1)]	2^{-29}		radians
Ω_0	Longitude of Ascending Node of Orbit Plane at Weekly Epoch	32[1)]	2^{-31}		semi-circles
C_{is}	Amplitude of the Sine Harmonic Correction Term to the Angle of Inclination	16[1)]	2^{-29}		radians
i_0	Inclination Angle at Reference Time	32[1)]	2^{-31}		semi-circles
C_{rc}	Amplitude of the Cosine Harmonic Correction Term to the Orbit Radius	16[1)]	2^{-5}		m
ω	Argument of Perigee	32[1)]	2^{-31}		semi-circles
$\dot{\Omega}$	Rate of Right Ascension	24[1)]	2^{-43}		semi-circles/s
IODE	Issue of Data (Ephemeris)	8			see [1]
IDOT	Rate of Inclination Angle	14[1)]	2^{-43}		semi-circles/s

1) Two's complement, sign bit MSB
2) See Figure A.2 for bit allocation in subframe
3) Unless otherwise indicated in this column, effective range is the maximum range attainable with indicated bit allocation and scale factor

Table A.5 The contents of page 18 in GPS subframe 4

subframe 4, page 18					
parameter	**contents**	**bits[2)]**	**scale factor (LSB)**	**range[3)]**	**unit**
data id[5)]		2			
sv id[5)]		6			
α_0	Ionospheric parameter	8[1)]	2^{-30}		s
α_1	idem	8[1)]	2^{-27}		s/semi-circle
α_2	idem	8[1)]	2^{-24}		s/semi-circle^2
α_3	idem	8[1)]	2^{-24}		s/semi-circle^3
β_0	idem	8[1)]	2^{11}		s
β_1	idem	8[1)]	2^{14}		s/semi-circle
β_2	idem	8[1)]	2^{16}		s/semi-circle^2
β_3	idem	8[1)]	2^{16}		s/semi-circle^3
A_1		24[1)]	2^{-50}		s/s
A_0		32[1)]	2^{-30}		s
t_{ot}	Reference Time for UTC data	8	2^{12}	602,112	s
WN_t	UTC Reference Week No.	8	1		weeks
Δt_{LS}	Delta Time due to leap seconds	8[1)]	1		s
WN_{LSF}	Week Number	8	1		weeks
DN	Day Number	8[4)]	1	7	days
Δt_{LSF}	Delta Time due to leap seconds	8[1)]	1		s

1) Two's complement, sign bit MSB
2) See Figure A.2 for bit allocation in subframe
3) Unless otherwise indicated in this column, effective range is the maximum range attainable with indicated bit allocation and scale factor
4) Right justified
5) See [1] for further information

Table A.6 The contents of pages 1-25 in GPS subframe 5

subframe 5					
pages 1 - 24					
parameter	**contents**	**bits[2)]**	**scale factor (LSB)**	**range[3)]**	**unit**
data id[5)]					
SV id[5)]					
e	eccentricity	16	2^{-21}		
t_{oa}	almanac reference time	8	2^{12}	602,112	s
δ_i	Correction to Inclination[4)]	16[1)]	2^{-19}		semi circles
$\dot{\Omega}$	Rate of Right Ascension	16[1)]	2^{-38}		semi cicles/s
SV health[5)]		8			
$(A)^{1/2}$	Square Root of the Semi-Major Axis	24	2^{-11}		$m^{1/2}$
Ω_0	Longitude of Ascending Node of Orbit Plane at Weekly Epoch	24[1)]	2^{-23}		semi circles
ω	Argument of Perigee	24[1)]	2^{-23}		semi circles
M_0	Mean Anomaly at Reference Time	24[1)]	2^{-23}		semi circles
a_{f0}	Clock Correction Term	11[1)]	2^{-20}		s
a_{f1}	idem	11[1)]	2^{-38}		s/s
page 25					
data id[5)]					
SV id[5)]					
t_{oa}	Almanac Reference Time	8	2^{12}	602,112	s
WN_a	Number of the Week	8			

1) Two's complement, MSB sign bit
2) See Figure A.2 for bit allocation in subframe
3) Unless otherwise indicated in this column, effective range is the maximum range attainable with indicated bit allocation and scale factor
4) relative to i_0=0.30 semi-circles
5) See [1] for further information

Appendix B: Introduction to spherical harmonic analysis and numerical mapping

B.1 Introduction to spherical harmonic analysis

Spherical harmonic functions afford an analytical representation of an arbitrary function of position on a sphere, in a form which facilitates many types of physical investigation. In [25] the subject of spherical harmonic analysis is extensively discussed. This appendix gives a short introduction.

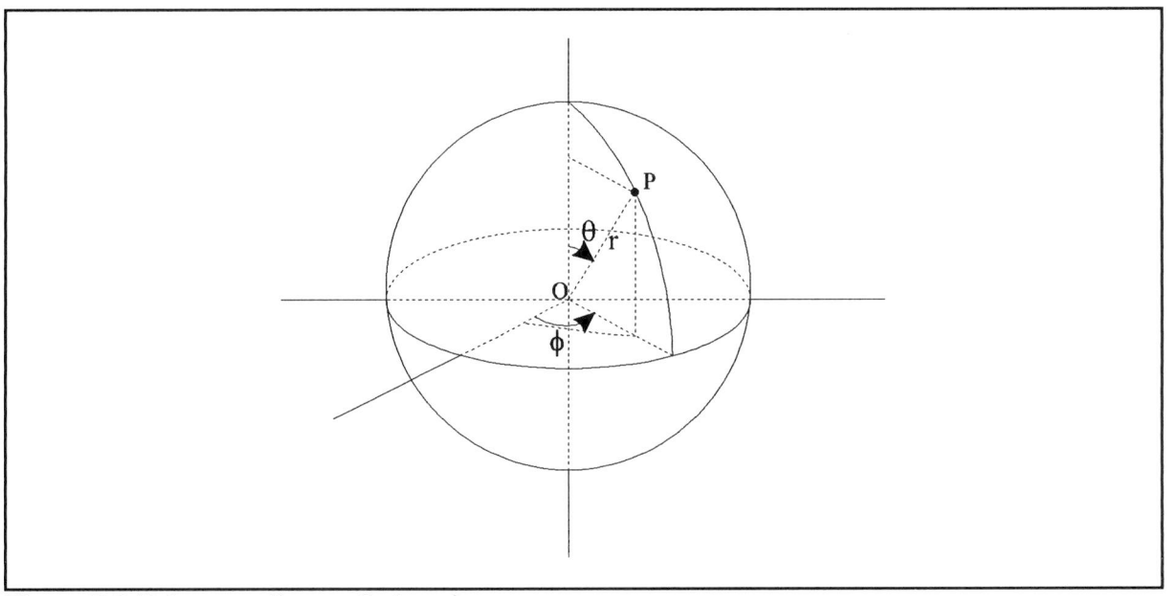

Figure B.1 Polar coordinates θ, ϕ and r

Any function $f(\theta,\phi)$ may be regarded as a function of position P (indicated by the polar coordinates θ, ϕ and r, figure B.1) on a sphere centred at O. Its distribution along any circle of latitude, defined by the polar distance φ is represented by the function $f(\varphi,\phi)$, which can be expressed, by ordinary harmonic analysis, as a trigonometrical series of terms $a_m\cos(m\phi)$ and $b_m\sin(m\phi)$; the coefficients a_m and b_m will be functions of φ:

$$f(\varphi,\phi) = \sum_{m=0}^{\infty} \left\{ a_m(\varphi)\cos(m\phi) + b_m(\varphi)\sin(m\phi) \right\} \tag{B.1}$$

The coefficients $a_m(\varphi)$ and $b_m(\varphi)$ can be expressed in terms of orthogonal functions. A set of real functions $\phi_0(t)$, $\phi_1(t)$, $\phi_2(t)$, ..., which are defined in a finite or infinite interval $t_1<t<t_2$, and which, as also their squares and products, are integrable in this interval, form an orthogonal system, if

$$\int_{t_1}^{t_2} \phi_n(t)\phi_m(t)dt = 0 \qquad \text{for } n \neq m \tag{B.2}$$

The functions $a_m(\varphi)$ and $b_m(\varphi)$, the coefficients of $\cos(m\phi)$ and $\sin(m\phi)$ in formula B.1, will be expressed in terms of Legendre related functions, called multiple of associated Legendre functions, denoted by $P_n^m(\cos\varphi)$ (n is the degree, m the order of P_n^m). Both Legendre and associated Legendre functions are orthogonal functions.

Legendre functions, orthogonal in the interval $-1<x<1$, are formed by the polynomials of the form:

$$\begin{aligned} P_0(x) &= 1 & P_1(x) &= x \\ P_2(x) &= \frac{1}{2}(3x^2-1) & P_3(x) &= \frac{1}{2}(5x^3-3x) \\ P_4(x) &= \frac{1}{8}(35x^4-30x^2+3) & P_5(x) &= \frac{1}{8}(63x^5-70\,x^3+15x) \\ P_6(x) &= \ldots\ldots\ldots \end{aligned} \tag{B.3}$$

The general formula for Legendre functions is given by:

$$P_n(x) = \frac{(2n)!}{2^n(n!)^2}\left\{x^n - \frac{n(n-1)}{2(2n-1)}x^{n-2} + \frac{n(n-1)(n-2)(n-3)}{2.4(2n-1)(2n-3)}x^{n-4} - \ldots\ldots\right\} \tag{B.4}$$

With $x=\cos\varphi$ a set of orthogonal functions at the interval $0<\varphi<\pi$ is obtained:

$$P_n(\cos\varphi) = \frac{(2n)!}{2^n(n!)^2}\left\{\cos^n\varphi - \frac{n(n-1)}{2(2n-1)}\cos^{n-2}\varphi + \frac{n(n-1)(n-2)(n-3)}{2.4(2n-1)(2n-3)}\cos^{n-4}\varphi - \ldots\ldots\right\} \tag{B.5}$$

The associated Legendre functions $P_{n,m}(\cos\varphi)$ are related to the Legendre functions $P_n(\cos\varphi)$ by:

$$P_{n,m}(\cos\varphi) = \sin^m\varphi \frac{d^m P_n(\cos\varphi)}{d(\cos\varphi)^m} \tag{B.6}$$

or:

$$P_{n,m}(\cos\varphi) = \frac{(2n)!}{2^n.n!(n-m)!}\sin^m\varphi\left\{\cos^{n-m}\varphi - \frac{(n-m)(n-m-1)}{2(2n-1)}\cos^{n-m-2}\varphi + \right. \\ \left. + \frac{(n-m)(n-m-1)(n-m-2)(n-m-3)}{2.4(2n-1)(2n-3)}\cos^{n-m-4}\varphi - ....\right\} \tag{B.7}$$

From $P_{n,m}(\cos\varphi)$ the orthogonal functions $P_n^m(\cos\varphi)$ (numerical multiples of $P_{n,m}$) are defined as:

$$\begin{aligned} P_n^m(\cos\varphi) &= P_{n,m}(\cos\varphi) && m=0 \\ P_n^m(\cos\varphi) &= \left\{2\frac{(n-m)!}{(n+m)!}\right\}^{\frac{1}{2}} P_{n,m}(\cos\varphi) && m>0 \end{aligned} \tag{B.8}$$

Developing $a_m(\varphi)$ and $b_m(\varphi)$ in terms of $P_n^m(\cos\varphi)$ for various values of n, formula B.1 becomes:

$$f(\varphi,\phi) = \sum_{n=0}^{\infty}\left\{\sum_{m=0}^{n}[A_{n,m}\cos(m\phi)+B_{n,m}\sin(m\phi)]P_n^m(\cos\varphi)\right\} \tag{B.9}$$

where $A_{n,m}$ and $B_{n,m}$ are coefficients of the $P_n^m(\cos m\phi)$ and $P_n^m(\sin m\phi)$ terms.

In discussing particular problems, especially in geophysics, the spherical harmonic function of degree n is introduced. This function is defined as:

$$F(\varphi,\phi) = r^n f(\varphi,\phi) = \sum_{n=0}^{\infty} r^n\left\{\sum_{m=0}^{n}[A_{n,m}\cos(m\phi)+B_{n,m}\sin(m\phi)]P_n^m(\cos\varphi)\right\} \tag{B.10}$$

where r is the radius of the sphere. If n=-1, $F(\varphi,\phi)$ is called a potential function.

A field in which spherical harmonic analysis is applied is terrestrial magnetism. In terrestrial magnetism the earth magnetic potential V is represented as a series of spherical harmonics.

From this potential the magnetic field components X, Y, Z of the earth's magnetic field as used in the Bent Ionospheric Model [24] can be derived.

The potential V at point (r,φ,λ) can be expressed as a sum of orthogonal functions [25]:

$$V = a\sum_{n=0}^{\infty}\sum_{m=0}^{n} P_n^m(\cos\varphi)\left[\left\{c_n^m\left(\frac{r}{a}\right)^n + (1-c_n^m)\left(\frac{a}{r}\right)^{n+1}\right\}A_n^m\cos m\lambda + \left\{s_n^m\left(\frac{r}{a}\right)^n + (1-s_n^m)\left(\frac{a}{r}\right)^{n+1}\right\}B_n^m\sin m\lambda\right] \quad \text{(B.11)}$$

where a is the radius of the earth. The terms with r/a indicate the origin of the magnetic potential to be of magnetic matter within the sphere of radius a ($r<a$); the terms with a/r indicates the origin of the magnetic potential to be of magnetic matter outside the sphere of radius a ($r>a$). The factors c_n^m and s_n^m are numbers lying between 0 and 1 representing the fractions of the harmonic terms $P_n^m\cos(m\phi)$ and $P_n^m\sin(m\phi)$ in V which, at $r=a$, are due to matter outside the sphere.

Using Gauss coefficients g_n^m and h_n^m formula B.11 is written as:

$$V = a\sum_{n=1}^{\infty}\left\{\left(\frac{r}{a}\right)^n T_n^e + \left(\frac{a}{r}\right)^{n+1} T_n^i\right\} \quad \text{(B.12)}$$

and

$$T_n = \sum_{m=0}^{n}\left\{g_n^m\cos(m\lambda) + h_n^m\sin(m\lambda)\right\}P_n^m\cos(\varphi) \quad \text{(B.13)}$$

with e and i indicating the external and internal origin of magnetic matter. The Gauss coefficients are determined by measurements of the magnetic field strength, magnetic inclination and declination.

In [25] it is shown that the earth's field is mainly of internal cause and B.12-B.13 can be reduced to:

$$V = a\sum_{n=0}^{\infty}\sum_{m=0}^{n}\left(\frac{a}{r}\right)^{n+1} P_n^m(\cos\varphi)\left[g_n^m\cos m\lambda + h_n^m\sin m\lambda\right] \qquad (B.14)$$

The X, Y and Z components of the magnetic field can be obtained by partial derivation of V:

$$X = \left(\frac{1}{r}\frac{\delta V}{\delta\varphi}\right) = \sum_{n=0}^{\infty}\left\{\left(\frac{a}{r}\right)^{n+2}\sum_{m=0}^{n}\frac{d}{d\varphi}P_n^m\cos(\varphi)\left[g_n^m\cos(m\lambda) + h_n^m\sin(m\lambda)\right]\right\} \qquad (B.15)$$

$$Y = \left(\frac{-1}{r\sin\theta}\frac{\delta V}{\delta\varphi}\right) = \frac{1}{\sin\theta}\sum_{n=0}^{\infty}\left\{\left(\frac{a}{r}\right)^{n+2}\sum_{m=0}^{n}P_n^m\cos(\varphi)\left[m g_n^m\sin(m\lambda) - m h_n^m\cos(m\lambda)\right]\right\} \qquad (B.16)$$

$$Z = \left(\frac{\delta V}{\delta r}\right) = -\sum_{n=0}^{\infty}\left\{(n+1)\left(\frac{a}{r}\right)^{n+2}\sum_{m=0}^{n}P_n^m(\cos\varphi)\left[g_n^m\cos(m\lambda) + h_n^m\sin(m\lambda)\right]\right\} \qquad (B.17)$$

B.2 Introduction to the technique of numerical mapping

The term "numerical map" is used to denote a function, $\Omega(\theta,\lambda,T)$, of three variables (latitude θ, longitude λ and time T) which represents the world-wide geographic and diurnal variations of an ionospheric characteristic. The method of numerical mapping used in the Bent Ionospheric Model has been developed by Jones and Gallet [27, 28]. This section only gives a short introduction. For the more mathematical description is referred to [27, 28].

The method of numerical mapping starts with Fourier analysis of the 24 hourly medians of ionospheric data. Fourier analysis is the most natural method for representing the diurnal variation, since ionospheric characteristics are periodic functions of time. The ionospheric data has been obtained at ionospheric stations (irregularly positioned on earth) at local time. This local time is corrected to universal time (UT) by a shift of the phase angles, determined by the difference between the actual station longitude and the reference longitude (Greenwich). The diurnal variation at each station is decomposed into 11 harmonics:

$$a_j \cos jt + b_j \sin jt = c_j \cos(jt - \Psi_j) \qquad j = 1,2,...,11 \tag{B.18}$$

each determined by an amplitude c_j ($= \sqrt{(a_j^2 + b_j^2)}$) and a phase Ψ_j ($= \arctan(b_j/a_j)$ or, equivalently, by a cosine and a sine coefficient. Then harmonics representing mainly real physical variation are separated from those produced mostly by noise, and the latter are truncated.

The world-wide geographic variation of each of the retained Fourier coefficients a_j and b_j (corrected to UT) is represented by a series of functions of latitude ϕ and longitude λ:

$$\sum_{k=0}^{K} D_k G_k(\phi, \lambda) \tag{B.19}$$

where the functions $G_k(\phi,\lambda)$ are called geographic functions (table B.1) and D_k are numerical coefficients.

As an end product of the analysis, the diurnal and world-wide geographic variations of the ionospheric characteristic are represented in the general form of a Fourier time series

$$\Omega(\phi, \lambda, T) = a_0(\phi,\lambda) + \sum_{j=1}^{H} [a_j(\phi, \lambda)\cos jT + b_j(\phi, \lambda)\sin jT] \tag{B.20}$$

where:

- ϕ: geographic latitude ($-90° \le \phi \le 90°$)
- λ: geographic longitude ($0° \le \lambda \le 360°$)
- T: universal time (UTC) expressed as an angle ($-180° \le T \le 180°$)
- H: the maximum number of harmonics used to represent the diurnal variation

Table B.1 Geographic coordinate functions $G_k(\lambda, \theta)$

	k	$G_k(\lambda,\theta)$
Main latitude variation	0	1
	1	sin X
	2	$\sin^2$ X
	...	...
	k_0	$\sin^{q0}$ X
First order longitude	k_0+1	cos λ cos θ
	k_0+2	cos λ sin θ
	k_0+3	sin X cos λ cos θ
	k_0+4	sin X cos λ sin θ
	⋮	⋮
	k_1-1	$\sin^{q1}$ X cos λ cos θ
	k_1	$\sin^{q1}$ X cos λ sin θ
Second order longitude	k_1+1	$\cos^2$ λ cos 2θ
	k_1+2	$\cos^2$ λ sin 2θ
	k_1+3	sin X $\cos^2$ λ cos 2θ
	k_1+4	sin X $\cos^2$ λ sin 2θ
	⋮	⋮
	k_2-1	$\sin^{q2}$ X $\cos^2$ λ cos 2θ
	k_2	$\sin^{q2}$ X $\cos^2$ λ sin 2θ
⋮	⋮	⋮
mth order longitude	$k_{m-1}+1$	$\cos^m$ λ cos mθ
	$k_{m-1}+2$	$\cos^m$ λ sin mθ
	$k_{m-1}+3$	sin X $\cos^m$ λ cos mθ
	$k_{m-1}+4$	sin X $\cos^m$ λ sin mθ
	⋮	⋮
	k_m-1	$\sin^{qm}$ X $\cos^m$ λ cos mθ
	k_m	$\sin^{qm}$ X $\cos^m$ λ sin mθ

Appendix C: Bent Ionospheric Model interpolation tables

This appendix lists the interpolation tables used in the Bent Ionospheric Model [24].

Table C.1 The Gauss coefficient g_n^m (year 1960)

g_n^m	m						
n	**1**	**2**	**3**	**4**	**5**	**6**	**7**
1	0	0.304112	0.024035	-0.031518	-0.041794	0.016256	-0.019523
2	0	-0.013381	-0.024898	-0.062130	-0.045298	-0.034407	-0.004853
3	0	0	-0.013381	-0.024898	-0.021795	-0.019447	0.003212
4	0	0	0	-0.006496	0.007008	-0.000608	0.021413
5	0	0	0	0	-0.002044	0.002775	0.001051
6	0	0	0	0	0	0.000697	0.000227
7	0	0	0	0	0	0	0.001115

Table C.2 The Gauss coefficient h_n^m (year 1960)

h_n^m	m						
n	**1**	**2**	**3**	**4**	**5**	**6**	**7**
1	0	0	0	0	0	0	0
2	0	-0.057989	0.033124	0.014870	-0.011825	-0.000796	-0.005758
3	0	0	-0.001579	-0.004075	0.010006	-0.002000	-0.008735
4	0	0	0	0.000210	0.000430	0.004597	-0.003406
5	0	0	0	0	0.001385	0.002421	-0.000118
6	0	0	0	0	0	-0.001218	-0.001116
7	0	0	0	0	0	0	-0.000325

Table C.3 Half thickness y_m at local time t_{loc} and critical frequency f_0F2

	t_{loc}											
f_0F2	**0**	**2**	**4**	**6**	**8**	**10**	**12**	**14**	**16**	**18**	**20**	**22**
2	87.7	93.0	97.8	102.0	102.3	99.4	95.1	91.3	88.0	86.8	86.0	85.2
3	96.2	98.0	103.8	109.5	112.5	112.5	107.5	101.2	96.2	95.4	97.0	98.1
4	107.6	117.7	140.1	150.4	153.3	154.0	150.0	140.2	127.1	115.5	109.2	106.5
5	114.4	125.5	144.2	162.7	175.6	180.6	174.8	157.5	134.7	115.0	110.1	110.0
6	113.3	120.7	134.9	158.2	181.6	190.5	177.0	152.5	123.0	113.4	111.5	110.3
7	113.5	125.4	139.0	158.6	199.5	188.3	183.3	166.8	136.9	119.9	111.9	108.0
8	114.0	118.2	125.6	157.0	211.4	232.3	211.2	188.3	142.5	124.8	116.8	112.5
9	122.7	132.0	143.3	158.3	187.1	214.4	196.8	185.5	152.5	130.0	120.7	117.8
10	140.8	147.5	155.0	167.8	200.0	195.6	187.0	168.3	144.4	138.7	137.7	137.5

Table C.4 Seasonal adjustment factors for y_m

		$\Delta\chi$ (degrees)						
	t_{loc} (hours)	24	16	8	0	-8	-16	-24
$\lvert\phi_m\rvert \geq 15°$	5.5	1.25	1.12	1.04	0.95	0.92	0.92	0.92
	11.5	11.1	1.06	0.99	0.88	0.78	0.73	0.7
	17.5	1.3	1.21	1.02	0.88	0.81	0.78	0.78
	24.5	21.09	1.04	1.01	0.98	0.98	0.99	1.0
$\lvert\phi_m\rvert \leq 5°$	3	0.95	0.96	0.97	1.0	1.04	1.09	1.13
	15	31.24	1.24	1.24	1.24	1.33	1.53	1.64

Table C.5 The slopes S_i ($\times 10^{-8}$) at geomagnetic latitude ϕ_m and critical frequency f_0F2

		f_0F2 (MHz)			
decay constant	**geomagnetic latitude ϕ_m (°)**	2	5	8	11
k_1	15	-7.5	-3.6	-9.0	-9.0
	45	-3.1	-3.6	-1.0	-1.8
	75	4.5	-1.6	-3.5	-2.8
k_2	15	-3.4	-0.4	-1.2	-1.2
	45	3.0	1.2	0.6	1.4
	75	2.5	1.3	1.3	1.7
k_3	15	-0.9	-0.6	-0.7	-0.7
	45	1.5	1.1	1.7	1.0
	75	1.0	0.8	1.6	1.5

Table C.6 The slopes C_i ($\times 10^{-6}$) at geomagnetic latitude ϕ_m and critical frequency f_0F2

		f_0F2 (MHz)			
decay constant	**geomagnetic latitude ϕ_m (°)**	2	5	8	11
k_1	15	12.2	8.73	15.45	15.45
	45	8.88	10.38	9.0	10.94
	75	2.3	9.58	11.9	12.8
k_2	15	7.62	4.67	5.86	5.86
	45	1.1	3.34	4.42	3.98
	75	0.8	3.16	4.41	4.54
k_3	15	3.92	3.58	4.06	4.06
	45	0.65	1.52	1.44	1.95
	75	0.5	2.74	1.22	1.55

Appendix D: Matlab listing of GLONASS ionospheric simulation model

Main program: Elevinf.m

```
global IYR IDAY MON TIME IMODY
        % Time information
        % IYR   = year
        % IDAY  = day
        % MON   = month
        % TIME  = time (UTC)
        % IMODY = Day of the month (see :
                  refrac.m)

global no ID Eccentricity Time_of_Applicability
       Orbital_Inclination
global Rate_of_Right_Ascen SQRT_A
       Argument_of_Perigee Mean_Anom
global Right_Ascen_at_TOA top
        % GLONASS Almanac parameters used in the
        % position calculation algorithm. The
        % format of the data is the same as the
        % GPS format
        % Used in: glopos2.m

global  FS HS
        % FS    = Satellite transmission
        %         frequency
        % HS    = Satellite height
        % See   : refrac.m

global um um1 wcoef U
        % Solar input coefficients
        % See   : coefdata.m/refrac.m

global SIF SIS
        % SIF   = 12-month running average of
        %         solar flux
        % SIS   = 12-month running average of
        %         sunspot number
        % See   : refrac.m

global FLAT FLON ELEV AZ
        % FLAT  = Latitude of station
        % FLON  = Longitude of station
        % ELEV  = Elevation to satellite
        % AZ    = Azimuth to satellite

global OLAT OLON HLAT HM
        % OLON  = Longitude of the ionospheric
        %         point
        % OLAT  = Latitude of the ionospheric
        %         point
        % HLAT  = Magnetic latitude of
        %         ionospheric point
        % HM    = Height at the maximum electron
        %         density hm
        % See: profl1.m

global YM YT XK RRM XNTNM foF2
        % YM    = Half thickness of the bottom
        %         bi-parabolic layer
        % YT    = Half thickness of the topside
        %         parabolic layer
        % XK    = Decay constants for lower,
        %         middle and upper section of
        %         the topside exponential layer
        % RRM   = Multiplier of the hdot term in
        %         the range rate formula
        % XNTNM = Ratio of the total vertical
        %         electron content to the
        %         electron density
        % foF2  = Critical frequency of the F2
        %         layer
        % See   : profl2.m

global TOTN TOTNA
        % TOTN  = vertical electron content
        % TOTNA = angular electron content
        % See   : refrac.m

global DRANG DRATE DELEV
        % Ionospheric range, range rate and
        % elevation correction
        % See   : refrac.m

global EDOT HDOT
        % EDOT  = Elevation rate
        % HDOT  = Altitude rate
        % Used for range rate computations
        % See   : refrac.m

global IOPT IDEL IDRD
        % See   : refrac.m

global no count
        % no    = Satellite to be used
        % count   = counting variable

count = 0;

%** Constants
Re      = 6371.2;
Q0      = 0;
Q1000   = 1000;
Q3600   = 3600;
DR      = .0174532925;
HR      = .2617993875;

PI2     = 6.2831853072;
LYRMO   = 0;
IDRD    = 0;
IORT    = 1;

IOPT    = 4;
IDEL    = 1;
IDRD    = 0;

EDOT    = 0;
```

```
HDOT    = 0;
day     = 1;

%** Load GLONASS almanac data
week793;
freqchan;

f0      = 1602;
pival   = 3.1415926536;

%** Time Information

IYR     = 95;
MON = 3;
IDAY = 23;
weekday = 5;

%** Station Information
% Latitude and longitude

FLAT    = input('Latitude: ');
FLON    = input('Longitude: ');
HEIGHT  = 0;

% Conversion of latitude and longitude (degrees
% to radians)

FLAT    = FLAT*DR;
FLON    = FLON*DR;

% Conversion of station longitude and latitude
% to ECEF coordinates

spos = statpos(FLAT,FLON,HEIGHT);

for no = 1:16,

  SIS     = 150;
  SIF     = 63.75 + 0.728*SIS + 0.00089*SIS^2;
        % Determine solar flux and sunspot
        % number

  FS      = (f0 + freq_channel(no)*0.5625);

  start = weekday*24;
  stop  = (weekday+1)*24;
  duration = .1;

  for TIME = start:duration:stop,
        % Calculation taking time steps of
        % length duration

      count     = count + 1;
      top       = TIME*3600;

      Satpos  = glopos2;
        % Calculate satellite position

      Rsat    = (sqrt(Satpos(1)^2+Satpos(2)^2+
                Satpos(3)^2))/1000;
      HS      = Rsat - Re;
        % Determination of satellite height

      [ELEV, AZ]=elaz(Satpos,spos,FLAT,FLON);
        % Elevation and azimuth calculation

      HS      = HS*Q1000;
      TIME    = TIME*HR;
        % Conversion of HS and TIME for
        % ionospheric correction calculations

      if ELEV >= (5*DR),
        refrac;
      elseif ELEV < (5*DR),
        DRANG = 0;
        TOTN = 0;
        TOTNA = 0;
        ELEV = 0;
        AZ   = 0;
      end
        % Calculates ionospheric corrections by
        % using refrac
        % Only carry out calculations if
        % elevation angle is > 5 degrees

      timevec(no, count)= top;
      totel(no, count) = TOTN;
      angulartotel(no, count) = TOTNA;
      elevat(no, count) = ELEV;
      azimuth(no, count) = AZ;
      rangeerror(no, count) = DRANG;

  end

  count = 0;

end
```

function REFRAC

```
%
% The function REFRAC prepares the coefficient
% and solar input data, it obtains the
% ionospheric profile parameters via PROFL1 and
% PROFL2 and computes the ionospheric refraction
% corrections DRANG for range, DRATE for
% instantaneous range rate and obtains the
% refraction correction DELEV for the elevation
% angle via BETA.
%
% The update option as used in the Bent
% Ionospheric Model is not implemented.
%
% Input parameters:
%
% FS    = Transmission frequency (MHz)
% FLAT  = Latitude of station (radians)
% FLON  = Longitude of station (radians)
% ELEV  = Elevation to satellite (radians)
% AZ    = Azimuth to satellite (radians)
% HS    = Height of satellite (m)
% EDOT  = Elevation rate (radians/sec)
% HDOT  = Altitude rate (m/sec)
% TIME  = Universal time (radians)
% FLXD  = Daily solar flux
% SIS   = 12-month running average of sunspot
%         number
% SIF   = 12-month running average of solar flux
% IYR   = Year (last 2 digits)
% MON   = Month (= 1 through 12)
% IDAY  = Day (= 1 through 31)
% IOPT  = Control constant for optional
%         computations:
%            1: Compute foF2 and hm
%            2: Also compute the remaining
%               profile parameters and electron
%               content
%            3: Compute deltaR in addition
%            4: Compute deltaRdot
% IDEL  = Control constant to compute deltaE
%         besides profile parameters and
%         electron content:
```

```
%            0: compute
%            1: not compute
% IDRD  = Flag to eliminate unnecessary
%         computations during calculation of the
%         second range correction used in the
%         differencing for the range rate
%         correction:
%            0: first calculation
%            1: second calculation
%
% Output parameters:
%
% DRANG = Range correction (m)
% DRATE = Range rate correction (m/sec)
% DELEV = Elevation angle correction (radians)
% foF2  = Critical frequency (MHz)
% HM    = Height at maximum electron density
%         (meters)
% YM    = Half thickness of the bottomside
%         biparabolic layer (meters)
% XK    = Decay constants of lower, middle and
%         upper section of the
%         exponential topside layer (1/meter)
% TOTN  = Total vertical electron content (e/m^2
%         column)
% TOTNA = Total angular electron content (e/m^2
%          column)

%** Constants
MONDY   = 0;
MOND    = 10000;
LYRMO   = 0;
R       = 6371.2e3;
TOL     = 1e-6;
Q0      = 0;
Q1      = 1;
Q100    = 100;
Q130    = 130;
QP1     = .1;
QNM     = 1.24e10;
RN3     = .49972;
PI      = 3.1415926536;
PI2     = 6.2831853072;

%** Initializing
DELEV   = Q0;
DRANG   = Q0;
TOTN    = Q0;
TOTNA   = Q0;
IYRMO   = IYR*100+MON;
IMODY   = MON*100+IDAY;

% Read coefficient datafile and form coefficient
% arrays. There are 36 sets of coefficient data,
% covering a whole year. The coefficients set to
% be used depends on the day of the month
% (IMODY). The right file is determined in
% coefdata.m. The datafile contains lond, londy,
% wcoef, um, um1

if ~(IMODY <= MONDY & IMODY >= MOND),
  coefdata;
end

um = um';
um1=um1';
wcoef=wcoef';

for J = 1:49,
  for I = 1:9,
    um(I,J)  =  um(I,J) + (um1(I,J) -
                um(I,J))*SIS/Q100;
  end
end

for J = 1:76,
  for I = 1:13,
    U(I,J) = wcoef((3*I-2),J)+(wcoef((3*I-1),J)+
             wcoef(I*3,J)*SIF)*SIF;
  end
end

%** Prepare solar data
% Only solar data concerning the 12-month
% running average of sunspot number and 12-month
% running average of solar flux is used in this
% model (In the original model also daily solar
% flux data can be used).

FLUX = SIF;

DFLUX   = FLUX - SIF;

if FLUX > Q130;
  FLUX = 130;
end;

%** Compute first part of profile
% The first part of the profile is calculated
% with the function PROFL1. Input data for this
% function are the globals: FLAT, FLON, ELEV,
% AZ, TIME,
% U and um. The function returns the globals:
% OLAT, OLON, foF2, HM and HLAT.

PROFL1(DFLUX);

if IOPT ~= 1,

%** Compute second part of profile
% The second part of the profile is calculated
% with the function PROFL2.Input data for this
% function are the globals: OLAT, OLON, HS,
% TIME, IDAY, MON, foF2, HM and HLAT. The
% function returns the globals: YM, YT, XK, RRM
% and XNTNM.

  PROFL2(FLUX);

  if XNTNM > Q0,

%** Compute elevation angle correction DELEV
% The elevation angle correction DELEV is
% calculated in function BETA.
% Input data for the this function is:
% FRAT = square ratio of critical frequency to
%        the transmission frequency
% SE   = sine of the elevation angle
% CE   = cosine of the elevation angle
% and the globals: FRAT, XNTNM, HS, HM and YM.
% The function returns: DELEV.

    FRAT= (foF2/FS)^2;
    SE  = sin(ELEV);
    CE  = cos(ELEV);

    if (IDEL == 0 | IDRD ~= 1),
      BETA(FRAT, SE, CE);
    end

%** Compute vertical and angular electron
%** content TOTN, TOTNA
```

```
%** Compute range correction DRANG

    RAT         = (R/(R+HM))^2;
    DEN2        = Q1-RAT*CE^2;
    DEN         = sqrt(DEN2);
    TOTN        = XNTNM*QNM*foF2^2;
    TOTNA       = TOTN/DEN;

    if IOPT > 3,
      DRANG     = FRAT*RN3*XNTNM/DEN;
    end

%** Compute range rate correction DRATE

    if (IOPT == 4 | IDRD == 0),
      DRATE  = DRANG*EDOT*RAT*SE*CE/DEN2;
      DRATE  = DRATE-FRAT*RN3*HDOT*RRM/DEN;
    end

  end

end
```

```
function PROFL1(DFLUX)

% The function PROFL1 the ionospheric
% characteristics foF2 and M(3000)F2 following
% the analysis of Jones, Graham and Leftin (see
% 'Documentation and Description of Bent
% Ionospheric Model').
%
% Input parameters
% FLAT  = Station latitude (radians)
% FLON  = Station longitude (radians)
% ELEV  = Elevation angle to satellite (radians)
% AZ    = Azimuth angle to satellite (radians)
% TIME  = Universal time (radians)
% U     = Array containing coefficients used for
%         the foF2 computation
% um    = Array containing coefficients used for
%         the M(3000)F2 computation
%
% Output parameters
%
% OLAT  = Latitude of the ionospheric point
%         (radians)
% OLON  = Longitude of the ionospheric point
%         (radians)
% foF2  = Critical frequency foF2 (Mhz)
% HM    = Height at the maximum electron density
%         hs (meters)
% HLAT  = Magnetic latitude of the ionospheric
%         point (radians)
%

K       = [11 35 53 63 67 69 71 73 75 6];
KM10    = 4;
KN      = [1 7 13 28 37 48 55 60 65 72];
NFF     = 76;
NMF     = 49;
Q1      = 1;
Q1000   = 1000;
Q3T5    = 300000;
D180    = 3.1415926536;
DG      = [1.02974426 .48869219 -.57595865];
R       = 6371.2e3;
SPLAT   = .9799246;
CPLAT   = .1993684;
PLON    = 5.078908;
H1      = 1346.92;
H2      = 526.4;
H3      = 59.825;
PER     = .00133;
CENT    = [1.035 .957 .9];
HM      = 0;

P(3)      = Q3T5;

SLAT    = sin(FLAT);
CLAT    = cos(FLAT);
SEL     = sin(ELEV);
CEL     = cos(ELEV);
SAZ     = sin(AZ);
CAZ     = cos(AZ);

%** Compute time dependent functions for foF2
%   and M3000

T       = TIME-D180;
SiCo    = SICOJT(6, T);

SIT     = SiCo(1,1:6);
COT     = SiCo(2,1:6);

DF      = DKSICO(NFF, K(10), U, SIT, COT);
DM      = DKSICO(NMF, KM10, um, SIT, COT);


%** Compute latitude, longitude of ionospheric
%   point OLAT, OLON

while (abs(P(3))-HM >= Q1000),

  if HM~=0,
    P(3) = HM;
  end

  SF      = R*CEL/(R+P(3));
  CF      = sqrt(Q1-SF*SF);
  SA      = CEL*CF-SEL*SF;
  CA      = SEL*CF+CEL*SF;
  SNLAT   = SLAT*CA+CLAT*SA*CAZ;
  CNLAT   = sqrt(Q1-SNLAT*SNLAT);
  OLAT    = atan(SNLAT/CNLAT);
  SDLON   = SAZ*SA/CNLAT;
  CDLON   = sqrt(Q1-SDLON*SDLON);
  OLON    = FLON + atan(SDLON/CDLON);

%** Compute position dependent functions for
%   foF2 and M3000

  P(1)    = OLAT;
  P(2)    = OLON;

  COM     = MAGFIN(P);

  TMP     = COM(2)*COM(2)+COM(3)*COM(3);
  C(2)    = P(2);
  C(3)    = P(1);
  C(1)    = atan( atan(-COM(1)/sqrt(TMP))/
            sqrt(CNLAT));

  G       = GK(K,C);

  KK      = 0;

  for II  = 1:2:10,
    I1    = KN(II);
    I2    = KN(II+1);

    for J = I1:I2,
```

```
      KK  = KK + 1;
      GM(KK)= G(J);
    end
  end

%** Compute H3000 and height of max. electron
%   density HM

  H3000   = DKGK(NMF, GM, DM);
  HM      = (H1-H2*H3000+H3*H3000*H3000)*Q1000;

end

%** Compute foF2 and adjust foF2 for daily
%   variation with flux

foF2    = DKGK(NFF, G, DF);
SML     = SNLAT + SPLAT +
          CNLAT*CPLAT*cos(OLON-PLON);
CML     = sqrt(Q1-SML*SML);
HLAT    = atan(SML/CML);
LAT1    = 1;
LAT2    = 1;

if HLAT < DG(LAT2),
  LAT2 = 2;

  if HLAT <= DG(LAT2),
    LAT1 = 2;
  elseif HLAT > DG(LAT2),
    break;
  end

  if HLAT ~= DG(LAT2),
    LAT2 = 3;
  elseif HLAT == DG(LAT2),
    break;
  end

  if HLAT <= DG(LAT2),
    LAT1 = 3;
  elseif HLAT > DG(LAT2),
    break
  end

end

CNT     = CENT(LAT1);

if LAT1 ~= LAT2,
  CNT = CNT + (CENT(LAT2)-CENT(LAT1))*
        (DG(LAT1)-HLAT)/(DG(LAT1)-DG(LAT2));
end

foF2    = foF2 * (PER*DFLUX + CNT);
```

function PROFL2(FLUX)

```
% The function PROFL2 computes the following
% ionospheric parameters:
% - the values of the half thickness ym, yt for
%   the bottomside bi-parabola and the topside
%   parabola respectively
% - the decay of values k1, k2, k3 for the
%   topside exponential layers
% - the ratio Nt/Nm of the total content to the
%   maximum electron density
% - the multiplier m for use in the range rate
%   computation
%
% Input parameters
%
% OLAT  = Latitude of the ionospheric point
%         (radians)
% OLON  = Longitude of the ionospheric point
%         (radians)
% HS    = Height of the satellite above earth's
%         surface (meters)
% TIME  = Universal Time (radians)
% IDAY  = Day (=1 through 31)
% MON   = Month (=1 through 12)
% FLUX  = Daily solar flux value
% foF2  = Critical frequency (MHz)
% HM    = Height at maximum electron content
%         density (meters)
% HLAT  = Magnetic latitude of ionospheric point
%         (radians)
%
% Output parameters
%
% YM    = Half thickness of the bottom
%         bi-parabolic layer (meters)
% YT    = Half thickness of the topside
%         parabolic layer (meters)
% XK    = Decay constants for lower, middle and
%         upper section of the topside
%         exponential layer (1/meter)
% RRM   = Multiplier of the hdot term in the
%         range rate formula (dimensionless)
% XNTNM = Ratio of total vertical electron
%         content to the electron density
%         (meters)

Q0      = 0;
Q1      = 1;
Q2      = 2;
Q3      = 3;
Q4      = 4;
Q5      = 5;
Q6      = 6;
Q8      = 8;
Q24     = 24;
Q37     = 37;
Q1000   = 1000;
QP05    = .5;
QP1333  = .133333;
QP95    = .95;
Q2P5    = 2.5;
Q10P5   = 10.5;
Q8O15   = .533333333;

D5      = .0872664625;
D7P5    = .13089969375;
D8      = .13962634;
D10     = .174532925;
D16     = .27925268;
D30     = .523598775;
D135    = 2.35619449;
D180    = 3.1415926536;
PIH     = 1.5707963268;
PI2     = 6.2831853072;
DEG     = [1.3089969375 .7853981625
           .2617993875];

SO1     = .4091749893;
SO2     = .0172142063;
RN4     = .9375;
H1012   = 1012000;

CEPT=[
 12.20e-6  8.88e-6  2.30e-6 7.62e-6 1.10e-6
           0.80e-6 3.92e-6 0.65e-6 0.50e-6;
```

```
  8.73e-6 10.38e-6  9.58e-6 4.67e-6 3.34e-6
            3.16e-6 3.58e-6 1.52e-6 2.74e-6;
 15.45e-6  9.00e-6 11.90e-6 5.86e-6 4.42e-6
            4.41e-6 4.06e-6 1.44e-6 1.22e-6;
 15.45e-6 10.94e-6 12.84e-6 5.86e-6 3.98e-6
            4.54e-6 4.06e-6 1.95e-6 1.55e-6];

SLOP=[-7.5e-8 -3.1e-8  4.5e-8 -3.4e-8 3.0e-8
               2.5e-8 -0.9e-8 1.5e-8 1.0e-8;
      -3.6e-8 -3.6e-8 -1.6e-8 -0.4e-8 1.2e-8
               1.3e-8 -0.6e-8 1.1e-8 0.8e-8;
      -9.0e-8 -1.0e-8 -3.5e-8 -1.2e-8 0.6e-8
               1.3e-8 -0.7e-8 1.7e-8 1.6e-8;
      -9.0e-8 -1.8e-8 -2.8e-8 -1.2e-8 1.4e-8
               1.7e-8 -0.7e-8 1.0e-8 1.5e-8];

RATK=[  .82  .86  .88   .94   .95  .94  1.125
                 .99  .985 .925 1.025 .945;
        .95  .85  .975 1.1    .97  .985 1.11
                 1.175 .9  1.055 1.09  .885;
       1.07  .9  1.05  1.115  .96  .975 1.085
                 1.08  .86  .97  1.055 .83;
       1.14 1.05 1.125 1.115 1.04 1.005 1.065
                 .94  .995 .94   .93  .84];

YMTAB=[ 87.7  96.2 107.6 114.4 113.3 113.5 114.0
                                   122.7 140.8;
        93.0  98.0 117.7 125.5 120.7 125.4 118.2
                                   132.0 147.5;
        97.8 103.8 140.1 144.2 134.9 139.0 125.6
                                   143.3 155.0;
       102.0 109.5 150.4 162.7 158.2 158.6 157.0
                                   158.3 167.8;
       102.3 112.5 153.3 175.6 181.6 199.5 211.4
                                   187.1 200.0;
        99.4 112.5 154.0 180.6 190.5 188.3 232.3
                                   214.4 195.6;
        95.1 107.5 150.0 174.8 177.0 183.3 211.2
                                   196.8 187.0;
        91.3 101.2 140.2 157.5 152.5 166.8 188.3
                                   185.5 168.3;
        88.0  96.2 127.1 134.7 123.0 136.9 142.5
                                   152.5 144.4;
        86.8  95.4 115.5 115.0 113.4 119.9 124.8
                                   130.0 138.7;
        86.0  97.0 109.2 110.1 111.5 111.9 116.8
                                   120.7 137.7;
        85.2  98.1 106.5 110.0 110.3 108.0 112.5
                                  117.8 137.5];

YRAT=[1.25 11.1  1.3  21.09  .95 31.24;
      1.12  1.06 1.21  1.04  .96  1.24;
      1.04   .99 1.02  1.01  .97  1.24;
       .95   .88  .88   .98 1     1.24;
       .92   .78  .81   .98 1.04  1.33;
       .92   .73  .78   .99 1.09  1.53;
       .92   .7   .78  1    1.13  1.64];

HLAT    = abs(HLAT);
TLOC    = TIME+OLON+PI2;
TLOC    = rem(TLOC,PI2);

%** Compute half thickness YM

T12     = TLOC/D30;
LT1     = fix(T12);
T1      = LT1;
LT2     = LT1+1;

if LT1 == 12,
  LT2 = LT1;
end

if LT1 < 1,
  LT1 = 12;
end

T1      = T12-T1;
IF1     = fix(foF2-QP95);
IF2     = fix(foF2-QP05);

if IF1 < 1,
  IF1 = 1;
end

if IF1 > 9,
  IF1 = 9;
end

if IF2 < 1,
  IF2 = 1;
end

if IF2 > 9,
  IF2 = 9;
end

YM=(YMTAB(LT1,IF1)+(YMTAB(LT2,IF1)-
    YMTAB(LT1,IF1))*T1)*Q1000;

if IF1 ~= IF2,
  YM2   = (YMTAB(LT1,IF2)+(YMTAB(LT2,IF2)-
           YMTAB(LT1,IF2))*T1)*Q1000;
  F1    = IF1;
  YM    = YM + (YM2-YM)*(foF2-F1-Q1);
end

%** Compute difference between aver. and daily
%   solar zenith angle DSZA

DAY     = (MON-1)*30+IDAY-80;
DSZA    = SO1*sin(SO2*DAY);

if abs(OLAT) >= SO1,

  if OLAT < Q0,
    DSZA = -DSZA;
  end

elseif abs(OLAT) < SO1,

  SANG  = OLAT/SO1;
  CANG  = sqrt(Q1-abs(SANG*SANG));
  DANG  = atan(SANG/CANG);
  ASZA  = SO1*(CANG+SANG*DANG)/PIH;
  DSZA  = ASZA-abs(OLAT-DSZA);

end

%** Apply seasonal effect of DSZA to half
%   thickness YM

S12     = Q4-DSZA/D8;
IF1     = fix(S12);
S1      = IF1;
S1      = S12-S1;
IF2     = IF1+1;
RAT     = Q0;

if HLAT > D5,
  T12   = (TLOC+D7P5)/PIH;
  LT1   = fix(T12);
```

```
  T1     = LT1;
  LT2    = LT1+1;

  if LT2 > 4,
    LT2 = 1;
  end

  if LT1 < 1.
    LT1 = 4;
  end

  RAT1   = YRAT(IF1,LT1)+(YRAT(IF2,LT1)-
           YRAT(IF1,LT1))*S1;
  RAT2   = YRAT(IF1,LT2)+(YRAT(IF2,LT2)-
           YRAT(IF1,LT2))*S1;
  RAT    = RAT1+(RAT2-RAT1)*(T12-T1);

end

if HLAT <= D5 | HLAT < DEG(3),

  T12      = (TLOC+D135)/D180-Q1;

  if T12  > Q1,
    T12    = Q2-T12;
  end

  if T12 < Q0,
    T12    =-T12;
  end

  RAT1     = YRAT(IF1,5)+(YRAT(IF2,5)-
             YRAT(IF1,5))*S1;
  RAT2     = YRAT(IF1,6)+(YRAT(IF2,6)-
             YRAT(IF1,6))*S1;
  RATM     = RAT1+(RAT2-RAT1)*T12;
  RAT      = RATM+(RAT-RATM)*(HLAT-D5)/D10;

  if HLAT <= D5,
    RAT    = RATM;
  end

end

YM       = YM + RAT;

%** Compute k-parameters XK

fqF2     = RN4*foF2;
I1       = 2;
I2       = 2;

if HLAT < DEG(2),
  I1     = 3;
   if HLAT <= DEG(3),
     I2     = 3;
   end
end

if HLAT > DEG(2),
  I2     = 1;
  if HLAT >= DEG(1),
    I1   = 1;
  end
end

J        = fix((fqF2+Q1)/Q3);
XF       = Q0;

if J >= 1,
  if J < 4,
    F1     = J;
    XF     = (fqF2+Q1)/Q3-F1;
  elseif J >= 4,
    J=4;
  end

elseif J<1,

  J = 1;

end

for M = 1:3,

  if J == 4,
    SLP = SLOP(J,I1+3*(M-1));
    CPT = CEPT(J,I1+3*(M-1));
  elseif J ~= 4,

    SLP    = (SLOP(J+1,I1+3*(M-1))-
             SLOP(J,I1+3*(M-1)))*XF+
             SLOP(J,I1+3*(M-1));
    CPT    = (CEPT(J+1,I1+3*(M-1))-
             CEPT(J,I1+3*(M-1)))*XF+
             CEPT(J,I1+3*(M-1));
  end

  if I1 ~= I2,
    DEL = (HLAT-DEG(I1))/(DEG(I2)-DEG(I1));

    if J == 4,
      SLP = SLP + (SLOP(J,I2+3*(M-1)) -
            SLP)*DEL;
      CPT = CPT + (CEPT(J,I2+3*(M-1)) -
            CPT)*DEL;
   elseif J ~= 4,
      SLP = SLP+((SLOP(J+1,I2+3*(M-1))-
            SLOP(J,I2+3*(M-1)))*XF+
            SLOP(J,I2+3*(M-1))-SLP)*DEL;
      CPT = CPT+((CEPT(J+1,I2+3*(M-1))-
            CEPT(J,I2+3*(M-1)))*XF+
            CEPT(J,I2+3*(M-1))-CPT)*DEL;
    end
  end

XK(M)    = SLP*FLUX+CPT;

end

%** Apply seasonal effect of DSZA to decay
%   constants XK

T12      = TLOC/DEG(3)-Q8;

if T12 < Q0,
  T12    = T12+Q24;
end

T12      = T12/Q6+Q1;

LT1      = fix(T12);
T1       = LT1;
LT2      = LT1+1;

if LT2 > 4,
  LT2 = 1;
end

S12      = Q2P5-DSZA/D16;
IF1      = fix(S12);
```

```
S1      = IF1;
S1      = S12-S1;
IF2     = IF1+1;

for M = 1:3,
  RAT1  = RATK(IF1,LT1+3*(M-1))+
          (RATK(IF2,LT1+3*(M-1))-
          RATK(IF1,LT1+3*(M-1)))*S1;
  RAT2  = RATK(IF1,LT2+3*(M-1))+
          (RATK(IF2,LT2+3*(M-1))-
          RATK(IF1,LT2+3*(M-1)))*S1;
  RAT   = RAT1+(RAT2-RAT1)*(T12-T1);
  XK(M) = XK(M)*RAT;
end

%** Compute half thickness of topside parabola
%   YT

CONV = Q1;

if foF2 > Q10P5,
  CONV  = QP1333*(foF2-Q10P5)+Q1;
end

YT      = CONV*YM;

%** Compute HDOT multiplier for range rate
%   computation RRM
%** Compute total electron content/electron
%   density XNTNM

XNTNM   = Q0;
RRM     = Q0;
D       = -(Q1 - sqrt(Q1 + (XK(1)*YT)^2))/XK(1);

H(1)    = HM+D;

if HS > H(1),

  RRM   = Q1;
  DELH  = (H1012-H(1))/Q3;
  H(2)  = H(1)+DELH;
  H(3)  = H(2)+DELH;
  H(4)  = HS;
  M     = 3;

  while M > 1,
    if HS <= H(M),
      H(M)= H(M+1);
      M=M-1;
    elseif HS > H(M),
      break;
    end
  end

  while M > 0,

    DH(M) = H(M+1)-H(M);
    RK    = Q1/XK(M);
    EX    = Q0;

    ARG   = XK(M)*DH(M);

    if ARG < Q37,
      EX  = exp(-ARG);
    end

    RRM   = RRM*EX;
    XNTNM = RK+EX*(XNTNM-RK);
    M=M-1;
  end

  TEMP  = Q8O15*YM+D-D^3/(Q3*YT*YT);
  TEMP1 = Q1-(D/YT)^2;
  RRM   = RRM*TEMP1;
  XNTNM = TEMP1*XNTNM+TEMP;

elseif  HS <= H(1),
  if HS > (HM-YM),
    DIST = HM-HS;
    if HS >= HM,
      XNTNM = Q8O15*YM-DIST+DIST^3/(Q3*YT*YT);
      RRM   = Q1-((HM-HS)/YT)^2;
    elseif HS < HM,
      XNTNM = Q8O15*YM-DIST+Q2*DIST^3/(Q3*YM^2)-
              DIST^5/(Q5*YM^4);
      RRM   = (Q1-((HM_HS)/YM)^2)^2;
    end
  end
end
```

```
function DELEV=BETA(FRAT , SinEl, CosEl)

% The function BETA computes the angular
% refraction correction to the elevation
% angle. Using the results of Maliphant's work,
% the deviation angle alpha is expressed as the
% angle between the true ray path above the
% ionosphere and the apparent ray path.
%
% Input parameters:
% FRAT  = Square ratio of critical frequency to
%         the transmission frequency
% XNTNM = Ratio of total electron content to the
%         electron density (meter)
% HS    = Height of the satellite above the
%         earth's surface (meters)
% hm    = Height of the maximum electron density
%         (meters)
% ym    = Half thickness of the bottom layer of
%         the ionosphere (meters)
% SinEl = Sine function of the elevation angle
% CosEl = Cosine of the elevation angle
%
% Output parameter:
% DELEV = Ionospheric refraction correction to
%         the elevation angle (radians)

Re      = 6371.2e3;
XAX     = [0 .2   .4   .6 .81 ];
YAX     = [1 .924 .824 .7 .553];

Rs      = HS+Re;

%** Compute squared deviation factor xcom

ROM     = Re+HM;
SFIM    = Re*CosEl/ROM;
CFIM    = sqrt(1-SFIM^2);
XCOM    = FRAT/CFIM^2;

%** Interpolate tabulated values yax to get ycom

for I = 1:5,

  if XCOM < XAX(I),
     YCOM = YAX(I)+(YAX(I-1)-YAX(I))*
          (XCOM-XAX(I))/(XAX(I-1)-XAX(I));
     break
  end
```

```
  if XCOM == XAX(I),
     YCOM =  YAX(I);
     break
  end

end

if (XCOM > XAX(5) & I==5),
     DELEV = 0;
end

if (XCOM < XAX(5) & I<=5),
   YCOM = 1/YCOM;

%** Compute deviation angle alpha
   ROO      = ROM + .5333*YM;
   SFIO     = Re*CosEl/ROO;
   CFIO     = sqrt(1-SFIO^2);
   ALPHA    =
FRAT*YCOM*XNTNM*SFIO/(2*ROO*CFIO*3);

%** Compute elevation angle correction
   CA       = cos(ALPHA);
   SA       = sin(ALPHA);
   X3       = Re*CosEl*SA/(1+CA);
   X2       = Re*SinEl-X3;
   X1       = sqrt(Rs^2-Re^2*CosEl^2)+X3;
   CTE      = (X1*CA-X2)/
              sqrt(X1^2+X2^2-2*X1*X2*CA);
   STE      = sqrt(abs(1-CTE^2));
   DELEV    = atan(STE/CTE);

end
```

function SiCo=SICOJT(L,T)

```
% The function SICOJT computes the trigonometric
% functions for multiples of the angle. It forms
% sin(jT), cos(jT) for j=1...L by computing
% sinT, cosT for the single angle T, and by
% using for multiple angles recursive equations

C(1) = cos(T);
S(1) = sin(T);

for I = 2:L,

  C(I) = C(1)*C(I-1)-S(1)*S(I-1);
  S(I) = C(1)*S(I-1)+S(1)*C(I-1);

  SiCo = [S;C];

end
```

function DK=DKSICO(MX, LH, D, SITIME, COTIME)

```
% The function DKSICO calculates the time
% dependent coefficients which are required for
% the computation of critical frequency and
% associated height.
%
% Input parameters:
%
% MX     = Cutoff index = cutoff point of series
%                         +1
% LH     = Number of harmonics retained in
%          Fourier series representation of Dk
% D      = Predicted coefficient array Ui,k for
%          foF2 or for M(3000)F2
% SITIME= Array of values sin(jT)
% COTIME= Array of values cos(jT)
%
% Output parameters:
% DK     = Array of coefficients Dk at fixed time
%          T, k=0....K

LMAX     = LH*2+1;
LK       = 1-LMAX;

for K = 1:MX,
  LK = LK+LMAX;
  DK(K) = D(LK);
    for L = 1:LH,
      NK     = LK+L*2;
      DK(K) = DK(K)+D(NK-1)*
              SITIME(L)+D(NK)*COTIME(L);
    end
end
```

function UNE=MAGFIN(POS)

```
% The function MAGFIN computes the earth's
% magnetic field components at a desired
% location following the spherical harmonic
% analysis of the magnetic field by Chapman and
% Bartels and using the coefficients given by
% Jensen and Cain for Epoch 1960 (see
% 'Documentation and Description of Bent
% Ionospheric% Model').
%
% Input parameters:
%
% POS    = Array containing latitude, longitude
%          and height (radians and meters)
%
% Output parameters:
%
% UNE    = Array with Z (vertical up), X (north),
%          and Y (east) components of magnetic
%          field (gauss) at the location %
%          specified by POS

CT       = [0 0 .33333333 .26666667 .25714286
                          .25396825 .25252525;
             0 0      0     .20000000 .22857142
                          .23809523 .24242424;
             0 0      0         0     .14285714
                          .19047619 .21212121;
             0 0      0         0         0
                          .11111111 .16161616;
             0 0      0         0         0
                          0     .09090909;
             0 0      0         0         0
                          0         0     ;
             0 0      0         0         0
                      0         0     ];

G        = [0 .304112  .024035 -.031518 -.041794
                                .016256 -.019523;
             0 .021474 -.051253  .062130 -.045298
                               -.034407 -.004853;
             0      0  -.013381 -.024898 -.021795
                               -.019447  .003212;
             0      0       0   -.006496  .007008
                               -.000608  .021413;
             0      0       0         0  -.002044
                                .002775  .001051;
```

```
          0     0       0         0       0
                                .000697  .000227;
          0     0       0         0       0
                                  0     .001115];

H       = [0     0       0         0       0
                                  0         0  ;
            0 -.057989 .033124  .014870 -.011825
                               -.000796 -.005758;
            0     0   -.001579 -.004075  .010006
                               -.002000 -.008735;
            0     0       0     .000210  .000430
                               .004597 -.003406;
            0     0       0       0     .001385
                               .002421 -.000118;
            0     0       0       0       0
                               -.001218 -.001116;
            0     0       0       0       0

                                  0   -.000325];


P(1,1)  = 1;
DP(1,1) = 0;
SP(1)   = 0;
CP(1)   = 1;

RE      = 6371200;
Q0      = 0;
R899    = 1.569050998;

P2      = POS(2);
P1      = POS(1);

if abs(P1) > R899,
  P1      = abs(R899)*SIGN(P1);
  P2      = Q0;
end

AR      = RE/(RE + POS(3));
C       = sin(P1);
S       = sqrt( CP(1)-C*C );
AOR(1)  = AR*AR;

%** Compute sin, cos for multiple longitude
%   angle

SiCo    = SICOJT(6,P2);
CP      = [CP(1) SiCo(2,1:6)];
SP      = [SP(1) SiCo(1,1:6)];

for M = 2:7,
  AOR(M)  = AR*AOR(M-1);
end;

%** Clear outer sums and set up loop

BV      = Q0;
BN      = Q0;
BPHI    = Q0;

for N = 2:7,
  FN = N;

%** Clear innner sums and set up loop

  SUMR    = Q0;
  SUMT    = Q0;
  SUMP    = Q0;

  for M   = 1:N,

%** Compute functions and derivatives of mult.
%   ass. Legendre function
%** Is this last contribution to inner sum

    if M ~= N,
      if N~=2,
        P(N,M) = C*P(N-1,M)-CT(N,M)*P(N-2,M);
        DP(N,M)= C*DP(N-1,M)-S*P(N-1,M)-
                 CT(N,M)*DP(N-2,M);
      elseif N==2,
        P(2,1) = C;
        DP(2,1)=-S;
      end
    elseif M==N,
      P(N,N) = S*P(N-1,N-1);
      DP(N,N)= S*DP(N-1,N-1);
    end

    FM    = M - 1;
    TS    = G(N,M)*CP(M)+H(N,M)*SP(M);

%** Sum into inner sums for z, y, x

    SUMR  = SUMR + P(N,M)*TS;
    SUMT  = SUMT + DP(N,M)*TS;
    SUMP  = SUMP + FM*P(N,M)*(-G(N,M)*SP(M)+
            H(N,M)*CP(M));


  end

%** Sum into outer sums for z, y, x

  BV      = BV + AOR(N)*FN*SUMR;
  BN      = BN - AOR(N)*SUMT;
  BPHI    = BPHI - AOR(N)*SUMP;

end

%** Set magnetic field components Z-vertical up,
%   X-north, Y-east

UNE(1)  = -BV;
UNE(2)  = BN;
UNE(3)  = -BPHI/S;
```

---

function G=GK(K,C)

```
% The function GK computes the geographic
% coordinate functions Gk as function of
% latitude phi, longitude lambda, and modified
% magnetic dip x=x(phi,lambda), which itself is
% dependent of the geographic position.
%
% Input parameters:
% K     = Integer index array containing (m_j-1)
% C     = Array containing modified magnetic
%         dip, geographic latitude and longitude
%         (radians)
%
% Output parameters:
%
% G     = Array with geographic functions Gk,
%         k=0,...,75

Q1      = 1;
N       = 8;

X       = C(1);
Y       = C(2);
Z       = C(3);
```

```
KO      = K(1);
SX      = sin(X);

%** Set terms due to main latitudinal variation

G(2)    = SX;
G(1)    = Q1;

for I = 2:KO,
  G(I+1)= SX*G(I);
end

KDIF    = K(2)-KO;
J       = 1;
CX1     = cos(Z);
CX      = CX1;
T       = Y;

while (KDIF ~= 0 | J ~= N),

  KC    = K(J) + 4;

%** Compute first 2 terms of j-th longitudinal
%   variation

  G(KC-2) = CX*cos(T);
  G(KC-1) = CX*sin(T);

%** Are only 2 terms to be computed for this
%   order longitude

  if KDIF ~= 2,

    KN=K(J+1);

%** Compute remaining terms of j-th order
%   longitude

    for I = KC:2:KN,
      G(I)        = SX*G(I-2);
      G(I+1)      = SX*G(I-1);
    end

  end

%** Are terms for maximum order longitude
%   computed

  if J == N,
    break
  end

%** Prepare for next order longitude
%   computations

  KDIF  = K(J+2)-K(J+1);

  if KDIF == 0,
    break
  end

  CX = CX*CX1;
  J=J+1;
  FJ=J;
  T=FJ*Y;

end
```

---

function OMEGA=DKGK(MX, G, DKSTAR)

```
% The function DKGK computes the ionospheric
% characteristic OMEGA, by forming a series of
% products of time dependent coefficients Dk and
% position dependent geographic functions G.
%
% Input parameters:
% MX    = Cutoff index = cutoff point K of
          series +1
% G     = Array of geographic functions Gk,
          k=0,...,K
% DKSTAR= Array of coefficients Dk, k=0,...,K
%
% Output parameters:
% OMEGA = Ionospheric characteristic foF2(MHz)
          or M(3000)F2 (dimensionless)

OMEGA   = G(1)*DKSTAR(1);

for K   = 2:MX,
  OMEGA = OMEGA+DKSTAR(K)*G(K);
end
```

---

function [el, az] = elaz(Xglo, Xstat, phi, lambda)

```
% This function calculates the elevation and
% azimuth.
%
% Input parameters:
% Xglo  = position of satellite in ECEF
%         coordinates
% Xstat = position of station in ECEF
%         coordinates
% phi   = latitude of station
% lambda= longitude of station
%
% Output parameters:
% el    = elevation to satellite (range 0 -
%         .5*pi)
% az    = azimuth to satellite   (range 0 -
%         2*pi)

X = Xglo(1)-Xstat(1);
Y = Xglo(2)-Xstat(2);
Z = Xglo(3)-Xstat(3);
R = sqrt(X^2 + Y^2 + Z^2);

sinel= (X*cos(phi)*cos(lambda) +
        Y*cos(phi)*sin(lambda) + Z*sin(phi) )/R;
el = asin(sinel);
cosaz = ( Z/R - sin(el)*sin(phi) ) /
        (cos(el)*cos(phi));
az = acos(cosaz);

if (Y*cos(lambda) - X*sin(lambda)) < 0,
  az = 2*pi - az;
end
```

---

function [satpos]=glopos2

```
% This function calculates the GLONASS satellite
% position in SGS85 ECEF coordinates. Input is
% almanac data provided by the MIT GLONASS page
% on WWW
% This almanac is in the so called YUMA format
% (The MIT has converted GLONASS
% almanac data to the YUMA format). The YUMA
% format is the format in which GPS almanac is
```

```
% transmitted.

omegaearth      = 0.7292115e-4;
   %Earth rotation velocity
mu              = 3.9860044e14;
   %Earth gravitational constant
pi_SGS          = 3.1415926536;

sqrtA           = SQRT_A(no);
toa             = Time_of_Applicability(no);
ma              = Mean_Anom(no);
e               = Eccentricity(no);
omega           = Argument_of_Perigee(no);
omega0          = Right_Ascen_at_TOA(no);
omegadot        = Rate_of_Right_Ascen(no);
incl            = Orbital_Inclination(no);

axis            = sqrtA^2;
n               = sqrt(mu/axis)/axis;
time_k          = top-toa;

if time_k>302400,
   time_k=time_k-604800;
end

if time_k<-302400,
    time_k=time_k+604800;
end

Mk              = ma+n*time_k;
Ek              = ecceanom(Mk,e);

vkNominator   = sqrt(1-e^2)*sin(Ek);
vkDenominator = cos(Ek)-e;

if vkDenominator==0,
  if vkNominator>=0,
     vk=pi_SGS/2;
  else
     vk=pi_SGS*1.5;
  end

else
  vk=atan(vkNominator/vkDenominator);
  if vkDenominator<0,
    vk=vk+pi_SGS;
  end
  if vkDenominator>0 & vkNominator<0,
    vk=vk+2*pi_SGS;
  end
end

latitude = vk+omega;
radius = axis*(1-e*cos(Ek));

xposorbit=radius*cos(latitude);
yposorbit=radius*sin(latitude);

corrOmega=omega0+(omegadot-omegaearth)*time_k-
                 (omegaearth*toa);

satpos(1)=xposorbit*cos(corrOmega)
          -yposorbit*cos(incl)*sin(corrOmega);
satpos(2) = xposorbit*sin(corrOmega)
           +yposorbit*cos(incl)*cos(corrOmega);
satpos(3) = yposorbit*sin(incl);
```

```
function [Ek]=ecceanom(Mk,e);

eps=1e-8;
MaxIterations=25;
delta_Ek = 10;
NumIter=0;

Ek_loc=Mk+e*sin(Mk);
while abs(delta_Ek)>eps & NumIter<MaxIterations,
   delta_Ek = (Mk-Ek_loc+e*sin(Ek_loc))/
                      (-1+e*cos(Ek_loc));
   Ek_loc = Ek_loc-delta_Ek;
   NumIter = NumIter+1;
end

Ek = Ek_loc;
```

```
function [spos] = statpos(phi,lambda,h)

% This function calculates the position of a
% station on earth in ECEF coordinates from the
% longitude and latitude.
% Input : latitude (phi), longitude (lambda) and
%         height (h) above ellipsoid
% Output: ECEF coordinates

a_e     = 6378136;
e2      = 0.006694366;

NA      = a_e/sqrt( 1 - e2*sin(phi)^2 );

spos(1)  = (NA+h) * cos(phi) * cos(lambda);
spos(2)  = (NA+h) * cos(phi) * sin(lambda);
spos(3)  = (NA * (1-e2) + h) * sin(phi);
```

---

coefdat.m

```
%**Selection of 1 of the 36 sets of
%  coefficients
% Each out??? datafile consists of the
% coefficients:
% lond  = (month*100+day), first date for which
%         coefficients are valid
% londy = (month*100+day), last date for which
%         coefficients are valid
% wcoef = generalized foF2 coefficients valid
%         for the time interval londy-lond
%         In the Bent Model wcoef is an array of
%         dimension 3*13*76. This array is
%         converted to a matrix of 39*76
%         elements since MATLAB requires n*m
%         matrices. The elements are arranged as
%         follows:
%         wcoef = [wcoef(1,i,k) wcoef(2,i,k)
%                  wcoef(3,i,k).....]
%         i = 1,....,13 and k = 1,....,76
% um    = M(3000)F2 coefficients valid for a
%         12-month running average of the
%         sunspot number = 0, and to be used for
%         the time interval londy-lond um is a
%         matrix of 9*49 elements
% um1   = M(3000)F2 coefficients valid for a
%         12-month running average of the
%         sunspot number = 100, and to be used
%         for the time interval londy- lond.
%         um1 is a matrix of 9*49 elements

if      (IMODY >= 101 & IMODY <= 110),
        out101;
elseif  (IMODY >= 111 & IMODY <= 120),
        out111;
```

```
elseif  (IMODY >= 121 & IMODY <= 131),
        out121;
elseif  (IMODY >= 201 & IMODY <= 210),
        out201;
elseif  (IMODY >= 211 & IMODY <= 220),
        out211;
elseif  (IMODY >= 221 & IMODY <= 231),
        out221;
elseif  (IMODY >= 301 & IMODY <= 310),
        out301;
elseif  (IMODY >= 311 & IMODY <= 320),
        out311;
elseif  (IMODY >= 321 & IMODY <= 331),
        out321;
elseif  (IMODY >= 401 & IMODY <= 410),
        out401;
elseif  (IMODY >= 411 & IMODY <= 420),
        out411;
elseif  (IMODY >= 421 & IMODY <= 431),
        out421;
elseif  (IMODY >= 501 & IMODY <= 510),
        out501;
elseif  (IMODY >= 511 & IMODY <= 520),
        out511;
elseif  (IMODY >= 521 & IMODY <= 531),
        out521;
elseif  (IMODY >= 601 & IMODY <= 610),
        out601;
elseif  (IMODY >= 611 & IMODY <= 620),
        out611;
elseif  (IMODY >= 621 & IMODY <= 631),
        out621;
elseif  (IMODY >= 701 & IMODY <= 710),
        out701;
elseif  (IMODY >= 711 & IMODY <= 720),
        out711;
elseif  (IMODY >= 721 & IMODY <= 731),
        out721;
elseif  (IMODY >= 801 & IMODY <= 810),
        out801;
elseif  (IMODY >= 811 & IMODY <= 820),
        out811;
elseif  (IMODY >= 821 & IMODY <= 831),
        out821;
elseif  (IMODY >= 901 & IMODY <= 910),
        out901;
elseif  (IMODY >= 911 & IMODY <= 920),
        out911;
elseif  (IMODY >= 921 & IMODY <= 931),
        out921;
elseif  (IMODY >= 1001 & IMODY <= 1010),
        out1001;
elseif  (IMODY >= 1011 & IMODY <= 1020),
        out1011;
elseif  (IMODY >= 1021 & IMODY <= 1031),
        out1021;
elseif  (IMODY >= 1101 & IMODY <= 1110),
        out1101;
elseif  (IMODY >= 1111 & IMODY <= 1120),
        out1111;
elseif  (IMODY >= 1121 & IMODY <= 1131),
        out1121;
elseif  (IMODY >= 1201 & IMODY <= 1210),
        out1201;
elseif  (IMODY >= 1211 & IMODY <= 1220),
        out1211;
elseif  (IMODY >= 1221 & IMODY <= 1231),
        out1221;
end
```

The input datafiles out???.m, freqchan.m and week793.m are not listed in this appendix. These files are provided on disk.

Appendix E: GLONASS almanac data

This appendix contains the GLONASS almanac data, obtained from the MIT Lincoln Laboratory (in GPS format), of week number 793 used with the simulations. On March 23rd 1995 (the date for which the simulations were carried out), 16 satellites were operational (table E.1)

Table E.1 Operational satellites on March 23rd 1995

GLONASS No.	Kosmos No.	Plane	Slot	Frequency Channel	Launch date
249	2111	1	5	23	08-12-1990
769	2178	1	8	2	30-01-1992
771	2179	1	1	23	30-01-1992
756	2204	3	21	24	30-07-1992
774	2206	3	24	1	30-07-1992
759	2235	1	7	21	17-02-1993
757	2236	1	2	5	17-02-1993
758	2275	3	18	10	11-04-1994
760	2276	3	17	24	11-04-1994
761	2277	3	23	3	11-04-1994
767	2287	2	12	22	11-08-1994
770	2288	2	14	9	11-08-1994
775	2289	2	16	22	11-08-1994
762	2294	1	4	12	20-11-1994
763	2295	1	3	21	20-11-1994
764	2296	1	6	13	20-11-1994

The almanac parameters for the 16 operational satellites are given in table E.2 (week number 793).

Table E.2 GLONASS almanac data (week number 793)

ID	ϵ ($\times 10^{-4}$)	$T_{applicability}$ (s) ($\times 10^{4}$)	i (rad)	$\dot{\Omega}$ (rad/s) ($\times 10^{-9}$)	$\sqrt{A}$ ($m^{1/2}$) ($\times 10^{3}$)	Ω (rad)	ω (rad)	M_0 (rad)
0123	6.208419800	8.079062500	1.133655545	-7.084000000	5.050549615	4.951471153	-2.729718812	2.729221520
0205	5.865097046	8.566300000	1.133790367	-7.084000000	5.050546939	4.949101190	-2.907756457	2.907484539
0321	29.01077271	9.078790625	1.132678830	-7.084000000	5.05054637	4.950528339	-2.971416660	2.970431920
0412	3.080368042	9.586178125	1.132301327	-7.084000000	5.050550426	4.950466294	-0.8672743880	0.8668046598
0523	8.850097656	10.25140000	1.134548369	-7.084000000	5.050572810	4.957059644	-1.363325425	1.361593601
0613	13.56124878	10.59413750	1.132469106	-7.084000000	5.050547182	4.950717135	-0.5691068723	0.5676465468
0721	9.622573853	11.10310938	1.134200872	-7.084000000	5.050544911	4.948574693	-3.048019826	3.047839877
0802	17.24243164	11.58741875	1.133679513	-7.084000000	5.050538018	4.951128217	0.2988386322	5.985360692
1222	9.222030640	9.419256250	1.131333601	-7.084000000	5.050551237	0.7563105622	2.171925048	4.112781932
1409	2.889633179	10.43058438	1.131231735	-7.084000000	5.050549940	0.7565881330	0.8302671014	5.453344718
1622	15.42091370	11.44280938	1.131120881	-7.084000000	5.050549210	0.7567916737	0.003834951970	6.279362169
1724	4.444122314	7.723034375	1.130836256	-7.084000000	5.050548480	2.857384068	2.632886275	3.650732058
1810	13.30375671	8.230859375	1.130530658	-7.084000000	5.050552129	2.857572144	0.7259564079	5.558993924
2124	7.963180542	9.762943750	1.133041353	-7.084000000	5.050551643	2.850198137	-0.2223313404	0.2219803620
2303	26.34048462	10.76424688	1.130683457	-7.084000000	5.050547669	2.857183909	-2.800281928	2.798515290
2401	2.918243408	11.26891250	1.132831629	-7.084000000	5.050547344	2.849711183	-0.6956602873	0.6952862941

This table contains the following parameters:

- ID : Satellite identifier consisting of satellite and slot number
- ϵ : Eccentricity
- $T_{applicability}$: Time of Applicability
- $\dot{i}$: Orbital Inclination
- $\dot{\Omega}$: Rate of Right Ascension
- $\sqrt{A}$: Square Root of the Semi Major Axis
- Ω : Right Ascension at Time of Applicability

- ω : Argument of Perigee
- M_0 : Mean Anomaly

The clock correction terms: Af0 (s) and Af1(s/s) are not listed in table E.1 as these parameters are always zero (see chapter 9, section 9.2). All satellites were indicated healthy (Health = 000).